This is to certify that the

thesis entitled

A Computer Aided Modeling and Performance Analysis of a Variable Eccentricity Tree Shaker Mechanism

presented by

Farzin Khorasanizadeh

has been accepted towards fulfillment of the requirements for

Masters degree in Agricultural Engineering

Gary B. Van Ee
Major professor

Date July 14, 1988

A COMPUTER AIDED MODELING AND PERFORMANCE ANALYSIS OF A VARIABLE ECCENTRICITY TREE SHAKER MECHANISM

By

Farzin Khorasanizadeh

A THESIS

Submitted to
Michigan State University
in partial fulfillment of the requirements
for the degree of

MASTER OF SCIENCE

in
Agricultural Engineering
Department of Agricultural Engineering

1988

ABSTRACT

A COMPUTER AIDED MODELING AND PERFORMANCE ANALYSIS OF A VARIABLE ECCENTRICITY TREE SHAKER MECHANISM

By

Farzin Khorasanizadeh

Shake and catch harvesting of tree crops in commercial orchards is now practiced on a world wide basis to meet today's high volume market demand for these products with more efficiency in fruit removal and less cost. Recent study results on Michigan's mechanical cherry harvesting operations have emphasized the need for development of improved machinery to reduce mechanical damage to trees, and increase efficiency in fruit removal. A new inertia type shaker concept has been developed with strong potentials to reduce tree damage by means of variable eccentricity and increase shake transfer ability by means of a sliding tail weight, for better fruit removal. A dynamic analysis of this shaker was needed to find sensitive parameters effecting its operation and the nature of such effects.

The operating conditions of the shaker were simulated by modeling a rigid body version of the mechanism using ADAMS, an advanced mechanism analysis program. The simulated tree displacements were analyzed for variations in several model parameters. Critical parameters effecting overall shaker performance were found to be: shaker weight and the location of its center of

mass, eccentric mass housing position, tail weight and its location. The graphic simulations of the shaker mechanism gave excellent insights to the general behavior of individual shaker parts under dynamic conditions. Performance trends of the shaker have also been established under varying parameter conditions. The results and the existing model can assist in further design optimization of the shaker mechanism.

Dedication

To my father, Mohammad Ali Khorasanizadeh, my mother, Fatemeh Sadeghi, and my youngest sister, Sadaf, who are so far away but closer than ever in my heart.

Acknowledgments

I thank my father, Mohammad Ali Khorasanizadeh, my mother, Fatemeh Sadeghi, my sisters, Firuzeh, Sepideh, Sadaf, and my brother-in-law, Dr. Kourosh Danai for providing me with an abundance of unconditional love, support, and encouragement at all times.

I would like to take this opportunity to express my special gratitude to Dr. Gary R. Van Ee, my major professor, for his professional guidance, constructive comments for the preparation of this work, and his personal concern and advise.

I wish to thank Dr. Thomas A. Esch (former Agricultural Engineering graduate student) for his cooperation and assistance throughout this study.

I would also like to thank Dr. Larry J. Segerlind (professor Department of Agricultural Engineering) and Dr. Joseph E. Whitesell (Associate professor Department of Mechanical Engineering) for serving on my graduate committee and for their constructive comments and suggestions for the completion of this work.

Table of Contents

List of Figures

Figure	Page

Figure Page

List of Tables

Chapter 1

Introduction

Mechanical shaking of several orchard fruit and nut trees has proven to be the most efficient and economical method of harvesting, mainly because it exhibits a very high ratio of output to input when conducted properly. *Shake-and-catch* harvesting systems have now become a necessity for growers in order to reduce the high cost of manual labor while meeting today's high volume market. Although a large variety of fruits are presently mechanically harvested throughout the world, cherry production has perhaps benefited the most from the introduction of this method because of the relatively higher number of fruit (cherries) per tree. Michigan cherry growers, the leading producers of tart cherries in the United States, adopted the shakers in the late 1960's and now use them annually to harvest over 95% of the state's tart and sweet cherries (Brown *et al.*, 1982 and 1987). As a result of the extensive use of these machines, mechanical damage has prevailed as a major threat to the productivity and health of the bearing cherry trees. Mechanical damage is now the major cause of tree decline (loss of vigor and yield, resulting in earlier replacement of the orchard) in orchards of all ages throughout the state. Damage is caused by excessive static and dynamic pressures applied to the tree when clamping to the trunk and during the actual shaking operation.

Injury due to clamping has been extensively studied and safe pressure ranges have been recommended to eliminate overclamping (Brown *et al.*, 1984). Clamp pads have also been improved to limit shear and compressive stresses, decreasing the amount of damage to the tree bark.

Excessive dynamic forces during tree vibration, however, are due to the design nature of the existing shaker models. Recent experiments on the dynamic response of a typical shaker, commonly used in Michigan for harvesting cherries, have shown that the shaker experiences a magnification of shake amplitude, referred to as *gallop*, for a short period (approximately 1 to 2 seconds) during "start-up" and "shut-down" (Affeldt *et al.*, 1987). The steady state shake occurs between these periods and delivers desired stroke for fruit detachment. Shaker gallop creates excessive dynamic forces that exert high compressive stresses due to clamp arm movement, and shear stresses from clamp slip on the bark. Gallop is caused during the short periods when the shaker eccentric masses are brought up to desired frequency and when shut down to rest. The rotating frequency of the eccentric masses passes through the natural frequency of the shaker-tree system and creates a desirable condition for unstable, resonant amplitudes that are limited by high system damping exerted by the tree.

The Agricultural Engineering Department at Michigan State University has developed a new concept for shaker design that eliminates the gallop problem. The shaker is equipped with four eccentric masses and a rotation phasing mechanism that provide a *controlled variable eccentricity.* A heavy sliding concrete block (tail weight), placed at the tail of the shaker, also resists shaker tail movement thus reducing shear stress on the bark.

The shaker system was modeled using ADAMS (Automatic Dynamic Analysis of Mechanical Systems, version 5.2) on a VAX-11/750 computer, to analyze its dynamic response and examine parameters for design optimization. Model input variable parameters were shaker mass, tail weight, eccentric mass housing position, tail weight position, and eccentric mass rotating frequency. The simulations gave good qualitative results in predicting shaker behavior under free shake and tree shake conditions.

1.1 - Cherry Production

Cherries are generally produced in the tart and the sweet varieties, most of which are marketed for processing, with a small quantity provided for fresh market. Cherries are of high nutritional value and are ideal for processing. Processed cherries are mainly used for the production of juice, jam, jelly, ice cream, dessert toppings, and wine. Some processed cherries are marketed frozen. The United States is one of the largest producers of cherries in the world, second only by a small margin to the Federal Republic of Germany. In the U.S , Michigan is the largest producer of tart cherries with 85,000 tons of total production in 1986, and is ranked third for sweets with 20,000 tons of total production in 1986 (Figures 1.1 and 1.2)(United States Agricultural Statistics, 1987). The utilized tart and sweet cherry production in Michigan in 1985 was at its highest since 1982. The total production data refer to the quantity of fruit harvested plus quantities which would have been acceptable for fresh market or processing but were not harvested or utilized because of economic or other factors. The utilized production refers to the amount sold plus the quantities used on farms and quantities used in storage. There was a decline in production in 1986 (28% for tarts and 35% for sweets) which was mainly due to early season frosts and heavy rains at harvest. Figures 1.3 and 1.4 show the trend of cherry production in Michigan between 1982 and 1986 (Michigan Agricultural Statistics, 1987).

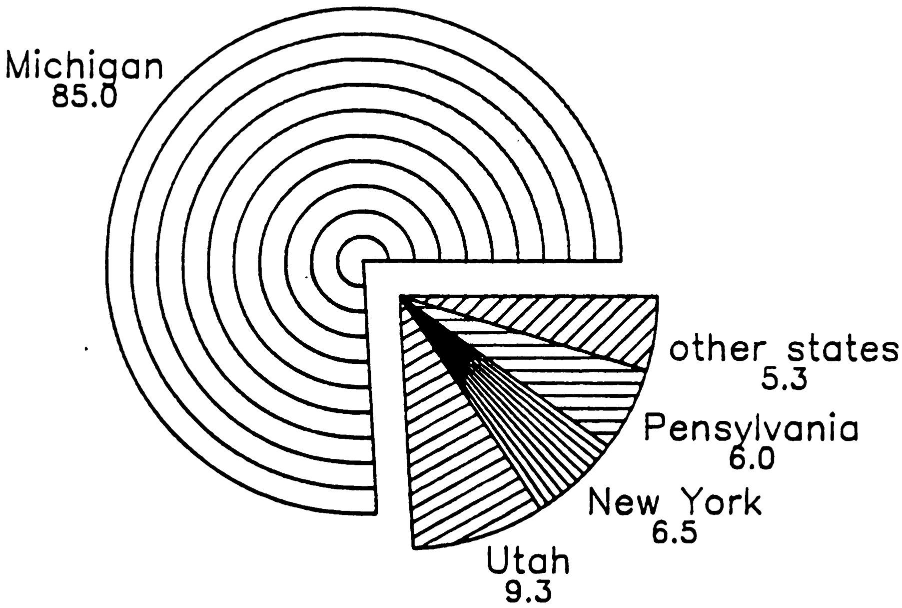

Figure 1.1-United States total tart cherry production in 1986 (thousand tons)

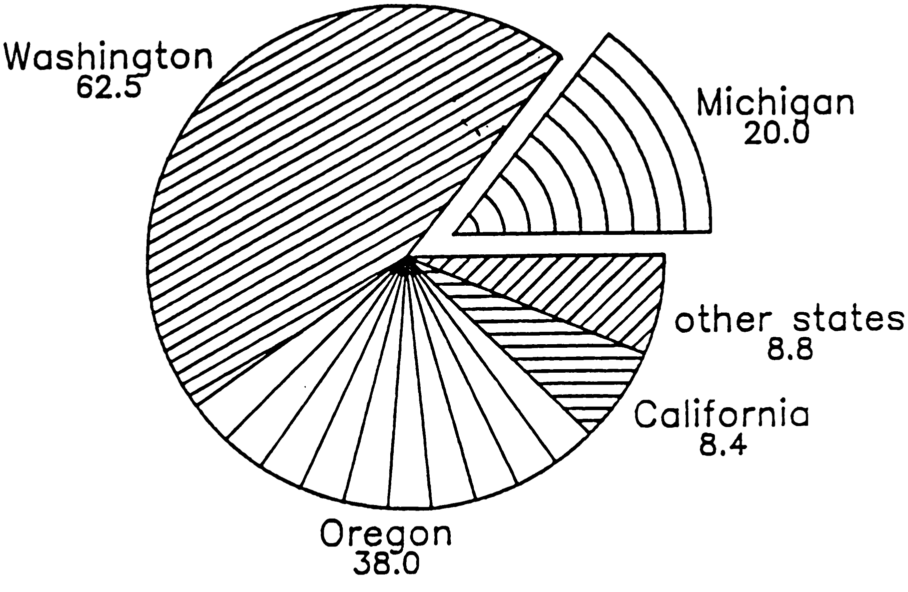

Figure 1.2-United States total sweet cherry production in 1986 (thousand tons)

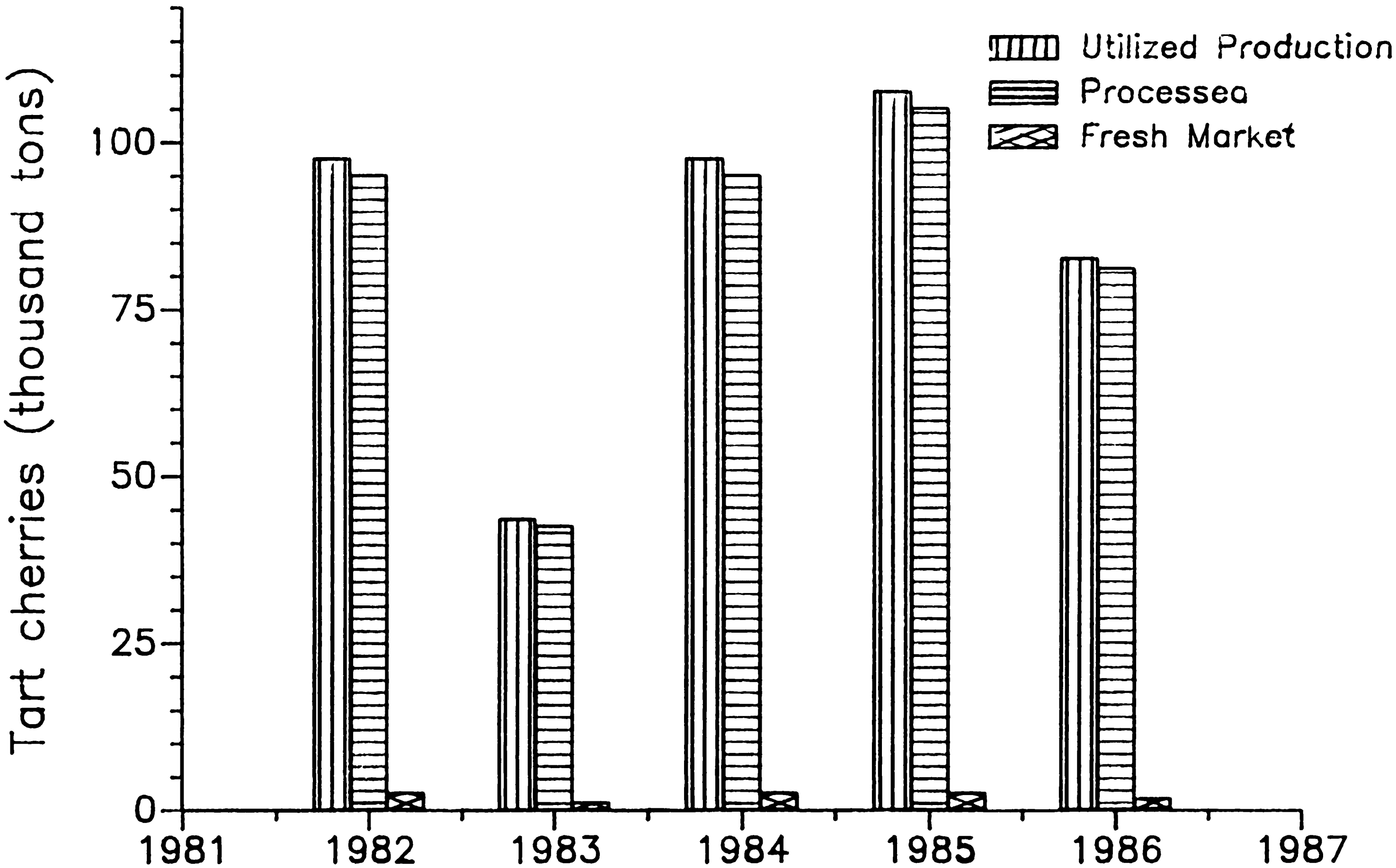

Figure 1.3 – Michigan utilized tart cherry production (1982 – 1986)

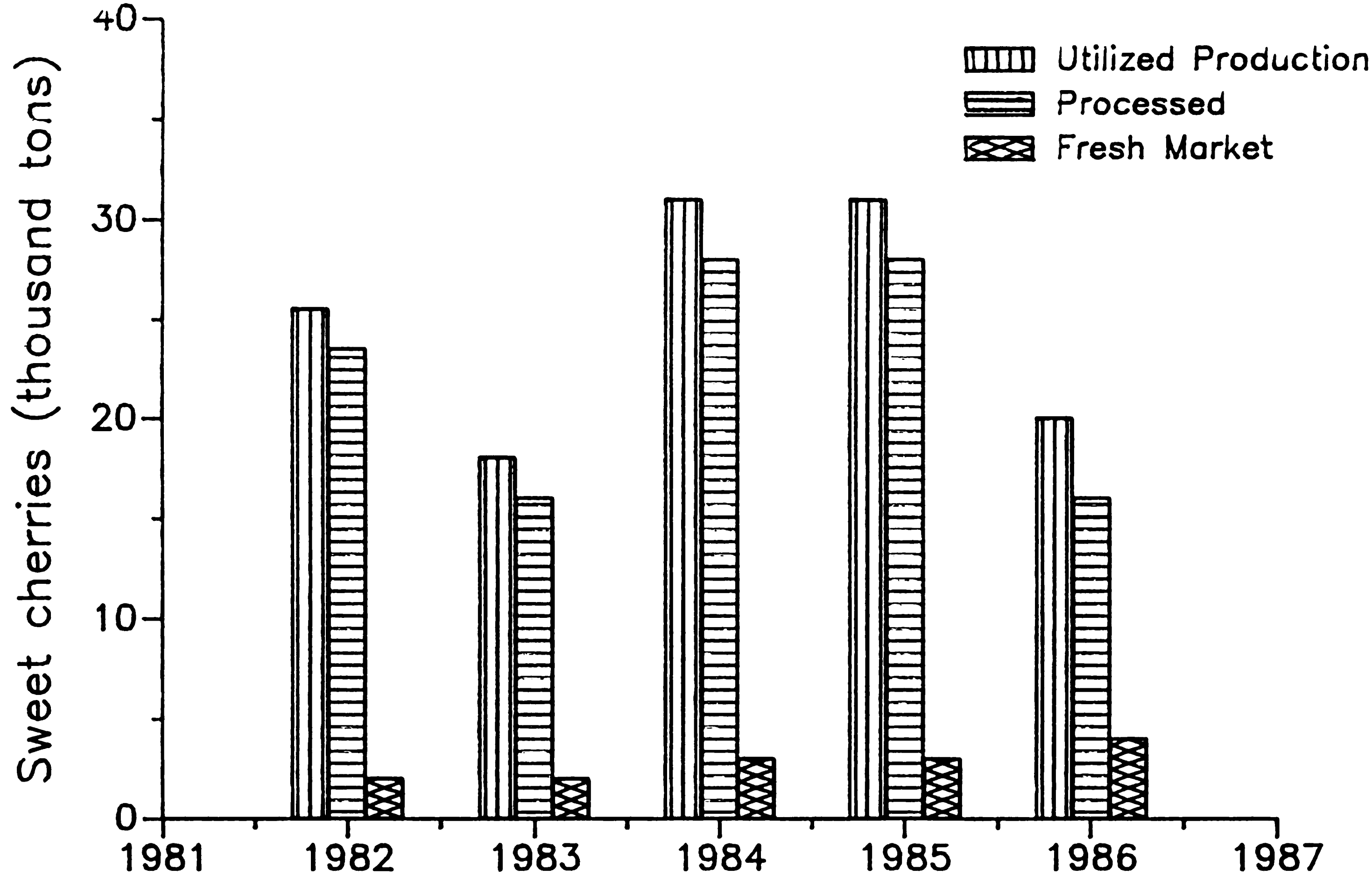

Figure 1. 4 — Michigan utilized sweet cherry production (1982 – 1986)

1.2 - Tree Damage

Tree damage due to mechanical shaking is caused by static and dynamic pressures applied to the tree by the shakers. Excessive clamping pressures and dynamic forces subject the trunk to high compressive and shear forces that result in ripping the bark or crushing of the internal cells. When the bark is damaged insects may carry fungi to the injured area, providing a favorable environment for fungus development and subsequent cankers that become parasitic and threaten the life of the tree. Internal damage, not immediately visible to the naked eye, takes place when the phloem (bark), cambium and xylem (wood) cells are crushed while leaving the bark intact. When internal cells are crushed, the flow of fluids that carry nutrients essential to the vitality of the tree is interrupted. To counteract this trauma, the tree walls off the affected areas; a defensive maneuver that draws on the energy reserves of the tree. When these stressful events are repeated for several years, a mature tree becomes weakened, resulting in reduced growth and a decline in fruit production (Burton *et al.*, 1986).

Moisture content of the tree due to irrigation or rain has a substantial effect on the strength of the tree. During wet conditions, cells in the cambial layer swell and enlarge in the radial direction. The radial walls become thinner and the cell contents seem to change from a solid to a liquid consistency. As soon as this stage is reached, the cambial walls can break easily and allow the bark to slip over the wood during shaking. Cherries, which are harvested early in mid-summer when the cambium is still highly active, are more susceptible to damage by mechanical harvesters than fruits harvested later in the season (Fridley *et al.*, 1970). Researchers, who studied the relation of bark strength to its moisture content, have recommended that farmers stop irrigation at least two weeks prior to harvest (Brown *et al.*, 1987).

1.3 - Computer Modeling

Computer based analysis techniques are playing a major role in the engineering research and design. The availability of increasingly powerful hardware is allowing timely, cost effective, detailed analyses aiding in the study of more complex, and efficient machines. Accurate analysis of a mechanism requires careful mathematical formulation of all possible motion and forces of its components. Numerical techniques (numerical integration, linear equations solution, etc.) must also be employed to solve the mathematical model. Although some recurring analysis problems (such as, Four bar or Slider crank mechanisms) lend themselves to existing special programs, the majority of dynamic problems have some unique characteristics or are much more complex that require specific treatment. As a result, the mathematical formulation becomes highly time consuming and often requires special expertise in analytical techniques. The problem is compounded if there are several alternate designs, each requiring a separate analysis.

The development of sophisticated general purpose dynamic simulation software combined with today's effective computer graphics has made the process of applying dynamic analysis in the design cycle both practical and effective. ADAMS (Automatic Dynamic Analysis of Mechanical Systems) is one of the more capable and developed of the few available mechanism analysis programs. It performs dynamic analysis of both planar and spatial mechanisms utilizing the rigid body theory for setting up the characteristic system equations. ADAMS was chosen for the shaker dynamic analysis because of its availability, suitability, and research preference due to past experience.

1.4 - Objectives of this study

The main objective of this study was to develop a computer model of the controllable variable eccentricity shaker, developed by Esch (1988), possessing the actual physical characteristics of the shaker and to be able to simulate it under dynamic conditions. Two machinery simulation programs, ADAMS (Automatic Dynamic Analysis of Mechanical Systems) and IMP (Integrated Machinery Design), were considered for the study. After some preliminary tests and evaluations, ADAMS was chosen as a more suitable program for this specific application. The model was written in the program's code and simulated. The results were satisfactory since they followed the actual shaker's behavior closely. Five parameters were then chosen as model variables. These parameters were

1) Shaker housing mass
2) Rotating frequency of eccentric masses
3) Position of the mass housing
4) Tail weight mass
5) Position of the tail weight.

A number of simulations were conducted with a range values for the above parameters under free shake and tree shake conditions. For tree shake conditions, each simulation condition was given approximate stiffness and damping values for two different diameter trees (63mm and 165mm).

The simulation results were used to predict the variable eccentricity shaker's behavior and its sensitivity to changes in the above parameters.

Chapter 2

Review of Literature and Research

2.1 - Mechanical Harvesting Methods

Orchard fruit and nut growers had chosen tree shaking as an alternative to hand harvesting even before the development of mechanical shakers. The concept of shaking originated before the 1960's when farmers found that some tree fruits could be detached by hitting the primary scaffold limbs with a mallet or a club. The mallets were about one meter long, and had a hard rubber pad near one end that contacted the limbs. Hitting the limbs generated a low-amplitude, high frequency vibration that transmitted to the bearing branches and caused fruit detachment. However, the use of mallets was laborious, and in larger trees, workers had the difficult task of climbing up the tree in order to shake the small top limbs (O'Brien *et al.*, 1983).

Eventually, the need for more effective methods led to the design of more sophisticated, mechanically powered devices. Among the first was the *cable shaker* developed by J.P. Fairbanks (1946) to harvest walnuts. The device consisted of a cable with a hook at one end attached to an eccentric on a tractor.

The cable would be hooked onto a limb while the tractor backed up to tighten it. The eccentric would then be activated to impart a shaking motion to the limb, thus detaching the nuts. Because only a tension force could be exerted by the cable, the rate at which the limbs returned toward their static position was determined by their fundamental natural frequency; therefore, the shaking frequency was limited by the resonant frequency of the limbs. Also, care had to be taken to avoid too great an initial cable tension, to avoid limb breakage. Shortly after, *boom shakers* were developed by replacing the cable with a rigid boom. The advantages were the elimination of the second man on the tree to hook the cable and an easier positioning of the shaker relative to the limb. Two types of boom shakers were developed. The more effective type had a hydraulically actuated clamp fastened to the boom to enable the grabbing of the limb and thus applying sustained vibration. By clamping to the tree, the frequency of the shake was no longer limited by the natural frequency of the limb, but rather could be varied as desired by adjusting the eccentric. The eccentric was rigidly supported on the tractor so that, for practical purposes, the stroke delivered to the limb was equivalent to the stroke of the eccentric. The other type of boom shaker was equipped with a hard rubber pad instead of a clamp at the end of the boom. Commonly known as a *knocker*, it was operated by placing the pad against a limb and activating the eccentric, thus delivering a series of pulses to the limb.

Through the years, a variety of new harvesting concepts have been developed in an attempt to minimize damage to the tree and fruit while maintaining effective fruit removal rates. Among these are: using pulsating air blasts on the tree utilizing large, high powered fans; using vibrating multi-layered combing devices to intrude the periphery of the tree and remove the fruit by shaking the bushes; and the use of optically activated robot hand pickers.

The complex design, high manufacturing, operating, and/or maintenance cost of these concepts have been primary factors in their lack of current acceptance among growers.

In the early 1960's, Adrian and Fridley developed the concept of inertia type shakers. The basic principle behind this type of shaker was that it used an unbalance inside a housing which was suspended by suspension bars from its carrier. The two kinds of inertia type mechanisms developed were (1) a pair of eccentric masses, and (2) a slider-crank mechanism with the slider fixed to the tree. These shakers soon gained considerable acceptance among the growers because of their isolation of vibration from their carriers, adaptability to catching frames, high harvest rates of up to 60 trees per hour, and better maneuverability in the orchards (O'Brien *et al.*, 1983).

The slider crank device is used on shakers intended to attach to limbs, as it can be designed in the form of a long slender boom desirable for reaching primary limbs over the catching surface. It is commonly referred to as the *limb shaker* and is ideal for older orchards having larger trees with heavy, willowy branches which require separate limb shaking. Limb shakers are still being used in some of Michigan's older orchards on large sweet cherry trees.

Rotating masses are primarily for shakers designed to attach to tree trunks and are commonly referred to as *trunk shakers.* They usually consist of two eccentric masses set to counter-rotate at slightly different speeds when clamped to the tree trunk. The speed difference of the masses creates a multi-directional shake perpendicular to the main axis of the tree. Trunk shakers are ideal for shaking stiff, smaller trees with three or four scaffolds, because of better vibration transfer from the trunk to the fruit. Early research on trunk shakers showed direct clamping to the trunk to be the most efficient method of attaching the harvester to the tree, mainly because a single attachment is sufficient for

shaking the whole tree, thus increasing harvest rates (Adrian and Fridley, 1963). Trunk shakers have gained popular acceptance among most of Michigan's commercial cherry growers since the early 1960's, and are annually used on over 95% of the tart and sweet cherry trees harvested for processing in this state (Brown *et al.*, 1982). Today, trunk shakers are also used for harvesting many other tree crops such as, apples, citrus, peaches, apricots, pears, plums, olives, nuts, and coffee (Cook and Rand, 1969).

There are many types of catching frames that accompany mechanical shakers, for collection of the fruit. Four general designs have been used for catching frames. The simplest configuration is an improvement on canvas laid on the ground and is commonly called the *canvas roll-out.* Canvas roll-out frames are part of a general category of extension-type catching frames. The second configuration consists of *two unit machines.* The two units move straight down the row in unison, one on each side of the tree row. The third is an *inverted umbrella* concept, which has a catching surface that is wrapped around each tree. The fourth is an *over-the-row* framework, which provides a single machine while achieving down-the-row movement of a two unit machine (O'Brien *et al.*, 1983). The catching frames are usually sloped in one direction with a conveyor at the bottom of the slope to carry the fruit to the carrying pallets.

2.2 - Tree Damage

The adoption of mechanical shakers as a major harvesting practice has shown a few disadvantages in the past. Tree injury, root damage, improper design and operation of the machines have caused a considerable amount of tree decline. Growers' concern for better crop yields and healthier orchards has prompted researchers and shaker manufacturers to study mechanical harvesting methods and equipment in order to better understand their impact on yield and tree life.

Tree damage was perhaps first investigated in California where almond growers used mallets or clubs to knock almonds to the ground (DeVay *et al.*, 1960). Beating trees with mallets caused a certain amount of bark and wood injury including crushing and splitting of the bark tissue. Injured portions of the bark provided entry points and a favorable nutrient medium for certain fungi elements known as *Ceratocystic fambria* and *Cytospora rubescens.* These fungi, although commonly present in almond orchards, were found to become parasitic and cause cankers when in contact with injured bark tissues. The cankers expand rapidly and kill major limbs within three or four years. *Ceratocystic fambria* was later found to cause similar canker diseases in mechanically harvested peach, apricot, prune, and nut trees (DeVay *et al.*, 1965). Later studies showed that tree bark strength during harvest plays a major role in bark damage.

Adrian *et al.* (1965) found that tree barks are at their weakest during the early months of summer when moisture and cell growth conditions in the cambial zone increase, and regain strength shortly after July reaching full strength by the end of September (Fridley *et al.*, 1970). It is for this reason that mechanical harvesting poses a greater threat to cherry trees. Cherries are among the few tree crops which must be harvested in the early months of summer when cambial activity is high, unlike other crops such as apples and nuts which are usually not ready for harvest until early fall.

Tree damage in general takes on three different forms (Cargill *et al.*, 1982)

1) Damage to the bark at the point of attachment of the shaker clamp.

2) Breakage of large stiff limbs (usually in older orchards previously harvested with a limb shaker).

3) Breakage of small branches, leaves, and other new growth.

Recent orchard management techniques, such as reducing the number of tree scaffolds to three or four, removing or cutting back of low hanging branches, stubbing of the willowy branches, and trunk shaking instead of limb shaking have reduced damage to the upper part of the trees, but bark injury to the trunk at the point of clamp attachment still remains to be a major problem.

Bark damage is caused by excessive shear or compressive stress or strain during clamping and shaking of the tree. Fridley *et al.* (1970) developed a hydraulic, padded bark tester to apply radial (compressive) and shear stresses to determine critical bark strengths. Test results indicated that the bark can withstand about three or four times as much stress applied radially as when applied tangentially to the limb. They also found that bark moisture content has a substantial effect on the force required to shear a fruit tree limb. High moisture content was shown to be associated with low shear strength, and low moistures with high shear strengths. For high moisture conditions of the bark, shear strength decreased with increase in radial pressure, while at low moisture, shear strength increased with increase in radial stress. They suggested that proper scheduling of irrigation prior to harvest may increase bark strength and therefore decrease the probability of damage. Seasonal tests also indicated that bark strength is directly related to the cessation of cambial activity and the associated shrinkage of cambial cells which takes place as the tree gets ready for colder weather toward the end of the summer.

In a more recent study, Brown *et al.* (1982) developed another bark tester to apply both clamping pressure (compressive) and shear stress to cherry trunks. The tester was equipped with electrical transducers to provide force and displacement signals and a magnetic tape recorder to record signals for later analysis. Obvious bark injury occurred for clamping pressures exceeding 1,034 kpa (150 psi) for sweet cherry barks and 2,412 kpa (350 psi) for tart cherry barks during the pressure tests, under stable moisture conditions. Shear tests also agreed with these pressure limits.

Proper selection of clamp pads also has a great effect on the amount of damage subjected to the bark. Shaker manufacturers have redesigned their clamp pads to increase the contact surface during clamping for a better distribution of clamp and shake forces. Today, common pad systems consist of two molded cylindrical rubber pads, each covered by two layers of belting. Each pad is wrapped with one layer of belting to form a sling that holds the pad in place. The second layer or flap is usually placed over the sling and contacts the tree. A lubricant is applied between the two pads to reduce shear forces transmitted to the bark by the shaker.

Frahm *et al.* (1983) evaluated mechanical properties of four different varieties of clamp systems commonly used in Michigan and measured peak contact pressures under the pads to determine their relationship to bark damage. Contact pressure was measured by a miniature pressure transducer that was sequentially moved on a grid pattern across the pad contact areas while clamped on steel pipes, to simulate pressures in the bark due to clamping. A computer program normally used to draw topographic maps was then used to plot pressure contours under the pad. An average peak contact pressure of 2,067 kpa (300 psi) was chosen from previous research (Brown *et al.*, 1982) as a criterion for pad evaluation. Manufacturer's recommended clamping forces were used for each pad. The pressure contour maps showed that peak pressures on all pads exceed the contact pressure limit of 2067 kpa. Two of the pads exceeded the value on approximately 35% to 50% of the contact area, while the other two exceeded the pressure limit on only 15 to 20% of the contact area. Recommendations were made to reduce clamping forces to limit contact pressure.

For some of the pads, the suggested clamping force to limit peak pressures to 2,067 kpa were about half the manufacturer's recommended values.

Dynamic compressive and shear stresses on the bark during shaker operation was studied by (Brown *et al.*, 1984). A Friday C-clamp trunk shaker with a standard pad was used to shake instrumented steel pipes in the laboratory. Tests showed that static compressive stresses increased during the start-up and the shut-down period of the shaker. For example, a static compressive stress of 1,137 kpa (165 psi) on a 165 mm (6.5 in.) diameter pipe, resulting from a clamping force of 18,237 Newtons (4100 lbs.), increased to 1,654 to 2,067 kpa (240 to 300 psi) at start-up when the shaker operated at 900 rpm. The increase in compressive stress due to dynamic pressures suggests that it is another source of bark damage.

Timm and Brown (1985) conducted detail static dynamic friction tests to identify possible changes in flap belting and lubrication choices that would minimize shear force transmission. Two different machines were developed for estimating the relative static and dynamic forces existing between two lubricated surfaces. Static friction, the characteristic of the belting surface to resist the start of sliding, was estimated using a static friction machine. Dynamic friction, the resistance of the belting surface to slide at high velocity, was estimated using a dynamic friction machine. Three different beltings (Polymate 135 Polyurethane COS, Polymate 135 Nitrile COS, and conventional Neoprene) and five different lubricants (Modoc gear lubricant, light bearing grease, food grade grease, Crisco shortening, and Silicone spray) were tested. The results of both static and dynamic tests showed that Nitrile or Polyurethane belting with any of the lubricants had the lowest friction between smooth surfaces, and thus reduce shear force transmission to the bark better than Neoprene belting. Field observations narrowed down the lubricant choices to spray Silicone because of easy application, easy cleaning (resulting in less dirt build up), less heat build up, and longer operation hours before lubrication.

2.3 - Shaker-Tree Vibrations

An inertia type mechanical shaker basically acts as a vibrating exciter which, when attached to a tree or a limb, must transmit necessary forces to overcome its inertia. When a limb or a tree is excited, it transmits motion throughout its length and fruit is detached when its acceleration is large and/or if the fruit-stem system has gone through a sufficient number of stress cycles. Researchers have studied the dynamics of tree shaking by utilizing a number of mathematical and numerical methods to come up with a better understanding of the shaker-tree vibrational characteristics and determine optimum conditions for effective fruit removal. An optimum system has been defined as one that causes effective fruit removal in the least time, with minimum power, without developing prohibitive forces as determined by bark strengths (Adrian and Fridley, 1963).

Adrian and Fridley (1962) developed the first mathematical model of an inertia shaker-tree system. The single degree of freedom model represented the tree and the shaker as a single mass, constrained by linear stiffness and viscous damping and excited by a sinusoidally varying force. An expression for the approximation of the stroke delivered by the shaker was derived from the equation of motion to be

$$S = \frac{2mr}{M_{shaker} + M_{limb}}$$

where

S = displacement of the limb

m = mass of unbalance (eccentric)

r = eccentricity

M_{limb} = mass of limb

M_{shaker} = mass of shaker

Test results indicated that within the common frequency range, the calculated stroke from the above equation varied about 25% from the actual displacements in the field. Expressions for required power and torque were also derived, but did not correlate well with the actual values because they did not account for the torque required to overcome friction.

Halderson (1966) used the following equation for work done by a harmonically varying force upon a harmonic motion of the same frequency to approximate the work done by a mechanical harvester

$$W = \frac{\pi}{2P_o X_o \sin\phi}$$

where

W = work/cycle

P_o = maximum applied force

X_o = peak to peak displacement

ϕ = phase angle between the applied force and the resulting displacement

The maximum work occurs when the force is 90 degrees ahead of the motion, a component of force in phase with displacement does no work. Assuming that the force applied to the tree varied sinusoidally, the power applied was determined by

$$HP = \frac{WN}{33000(12)}$$

where N is the vibrating frequency. Actual phase angles were obtained by simultaneously recording force and displacement through the use of an oscillograph strain indicator. For larger power transmissions, the actual phase was found to be at or very close to 90 degrees. Theoretically, a shaking force leads the displacement by zero degrees when vibrating a pure spring, and leads it by 90 degrees when vibrating a pure dashpot, and by 180 degrees when vibrating a pure mass (Thompson, 1981). This shows that almost all the energy applied to the tree is dissipated by damping.

Lenker and Hedden (1968) used a vector method in a similar manner to the analysis of alternating-current circuits, to derive an equation for limb displacement of a limb shaker. A dimensionless form of the equation was plotted from which the effect of a change in shaker or limb properties could be determined. They concluded that a light boom weight was desirable, but that compromises must be made since the boom weight could not be made zero. An unbalance mass to boom mass, $(\frac{m_u}{m_b})$, ratio of 0.5 to 1.0 was theoretically shown to greatly increase shaker effectiveness.

Fruit-stem dynamics have also been modeled and studied to determine ideal shake frequencies for detachment. The fruit-stem system generally has three degrees of freedom, which may be described as a pendulum mode (motion of the fruit and stem about the supporting branch), a tilting mode (motion of the fruit about its own axis, perpendicular to the axis of the stem), and a twisting mode (motion of the fruit about the axis of the stem)(Diener *et al.*, 1969).

Cook and Rand (1969) formulated a linear, three degree of freedom model of the fruit-stem system. They found that maximum instability occurs when the frequency of the support (branch) motion is twice the natural frequency of the system in the planar (pendulum and tilting) modes. The natural frequency of each fruit, however, is dependent on its individual mass, radius, and stem length; which indicates that apples, for example, have a lower natural frequency than cherries because of their shorter stem length and larger mass. Therefore, a higher range of shake frequency is needed to detach cherries.

The introduction of finite element methods in the 1970's prompted researchers to use the numerical techniques to develop more complex models to study the tree and fruit vibrations. Yung and Fridley (1975) used a finite element approach to develop a computer model of a complete tree system. A complete tree system was considered as a combination of three portions: (a) a tree structure which consisted of tree trunk, limbs, secondary branches, and larger branches, (b) the fruit and stems, (c) the leaves and twigs. The finite element modeling allowed the use of six generalized coordinates (three translational and three rotational) and incorporation of elastic properties into the system. The steady state results of forced vibration of the model correlated fairly well with previous experimental test results on models made of steel bars to study vibrational behavior of branched cantilever beam systems. Upadhyaya *et al.* (1981) developed another finite element model to predict the dynamic behavior of a fruit bearing limb impacted at its base. Their model was also verified to be fairly accurate when compared with simpler tests and with experimental results.

Recent studies have concentrated more on the vibrational characteristics of existing machines through field tests. Affeldt *et al.* (1984) analyzed the dynamic displacement of an eccentric-mass trunk shaker relative to the trunk of a cherry tree and analyzed results to determine the relationship of relative displacements to bark damage. A Friday C-clamp eccentric-mass trunk shaker and a cherry tree trunk were set up with accelerometers to detect their planar xy motion. The signals from the sensors were amplified and then channeled through an analogto-digital acquisition unit. The displacement data was later plotted versus shake time. The plots showed larger than expected amplitudes during the two to three seconds of "start-up" and "shut-down" of the shaker operation. These unexpected transient amplitudes are referred to as *shaker gallop*. Gallop, which is induced by very large and complex acceleration patterns upon mass engagement, may cause potential damage to the tree in the form of tangential or longitudinal pad slip or radial impact. A probable cause of gallop was attributed to the passage of the shake frequency through the lower natural frequency of the shaker-tree system, that could cause resonance in the absence of damping. With the presence of large damping forces in trees, the passage over the natural frequency merely causes higher than steady state amplitudes.

Gallop was actually first noticed by Gould *et al.* (1971). In a patent request they reported that: "With the use of a solid mass bob of fixed inertia in an eccentric-mass trunk shaker, there is an interim period when the shaker is not up to normal operating speed which is unstable and in which the operator and the apparatus are subjected to uncomfortable asynchronous shaking motion, which is not particularly effective as a harvesting motion." To eliminate the problem, they developed a variable inertia weight bob in which the moment of inertia rapidly increased as a function of its rotating speed during its initial acceleration from rest and rapidly decreased during deceleration. The bob was a shell-like structure which contained a mass of flowable heavy matter (such as oil) and a suitable amount of metal pellets such as BB's or lead shots. By partially filling the cavity, the moment of inertia and the eccentricity at rest had relatively low values, whereas when the bob was rotated and the metal pallets moved outward, the moment of inertia and the eccentricity increased in proportion to the redistribution of mass from portions adjacent to the axis of rotation to regions more remote within the bob.

Al Soboh (1986) developed a rigid body model of a Friday C-clamp shaker using a mechanism design program called IMP (Integrated Machinery Program). Parameters such as eccentric mass acceleration, weight, and starting phase angle between masses were used as variables to determine conditions that limit gallop. Although the model was not successful in simulating clamped shaker-tree conditions, some results were obtained for free shake conditions. The simulation results indicated that for a starting phase angle of 255 degrees between the masses, "start-up" gallop was eliminated. This could be due to the fact that the rest position of the center of gravity of the shaker system with the masses at this relative angular position is closer to the dynamic center of gravity during shaker operation. Therefore, the shaker would not have to position itself about the dynamic center of gravity when started. Although this hypothesis agrees better with a 180 degree phase angle between the masses, other parameters such as the shaker housing center of mass location could count for the 255 degree phase angle simulation results. The shut down conditions could not be simulated due to model limitations.

Affeldt (1987) developed and installed a controlled eccentricity mass housing unit on a Friday C-clamp shaker to eliminate gallop. The unit consisted of a C-shaped shell filled with molten lead and a hydraulic cylinder assembled on a circular plate, mounted on a central shaft (Figure 3.3). The unit allowed achieving high rotation frequencies at zero eccentricity. Eccentricity was then created by extension of the hydraulic cylinder. The design, while correcting the gallop problem, required high speed rotation of the hydraulic cylinder in action that was complicated and required expensive components (cylinder, seals, bearings, etc.).

Chapter 3

The Variable Eccentricity Shaker And The Computer Model

3.1 - Conventional shaker design

Today's most commonly used cherry shakers are multi-directional, inertia type units that operate using two eccentric masses on a single or separate shafts driven by separate variable displacement hydraulic motors. The masses counter-rotate at slightly different speeds to create a multi directional shake pattern. The shaker body is suspended using suspension bars with bushings used at both ends to prevent vibration transfer to the support frame. The crude geometry and design of these shakers limit their performance to an extent where their desirable shake for one range of trees may not be effective for another. They also induce unacceptable damage to tree barks causing tree decline. Although experienced operators have learned to operate and modify shakers to fit their needs while reducing the damage to the trees, there are still a few problems which originate from the nature of their design and cannot be eliminated by modifications.

Major problems associated with almost all multi-directional, inertia type shakers are :

a) **Gallop** - Gallop is a term referred to higher than normal amplitudes of shake at the "Start-up" and "Shut-down" periods of operation and is considered as the major cause of tree damage in mechanical harvesting. These initial and final deviations from desired amplitudes have been observed in recent studies conducted on shakers (Affeldt *et al.*, 1984). The large forces that cause gallop result in high stresses and strains at the cambium zone of the tree. While proper pads and clamp pressures reduce the amount of injury, invisible damage in forms of internal cell crushing still occur.

Probable causes of gallop can be attributed to the following which are fixed characteristics of inertia type shakers :

1) The shaker natural frequency is low due to high mass and relatively low stiffness over the natural frequency of the shaker, or the lower natural frequency of the shaker-tree system when clamped. This causes resonant shake amplitudes at lower "start up" and "shut down" rotating frequencies of the shaker eccentric masses.

2) As the shaker shuts down, the masses stop at a random position, with an unknown phase angle in between. This results in a randomly displaced shaker center of mass at the end of each shake. As the succeeding shake starts, the masses accelerate about the previous center of mass for a short period until the steady state is reached, by which time the shake will be about the actual center of mass of the shaker. In this short period the shake center

moves a distance close to the gallop amplitude. The same action happens at shut-down as the the masses stop at random positions and the center of mass is displaced.

b) **Fixed amplitude** - The shake amplitude (stroke) of the shaker is fixed, unless the eccentric masses are replaced with heavier (for a larger stroke) or lighter (for a smaller stroke) ones. This requires the time consuming task of disassembling the shaker.

c) **Random shake pattern** - Cherry orchards are not uniform in tree shapes and sizes. This is especially true in case of older orchards or previously mechanically harvested ones. Irregular tree growth in these orchards is common and is usually caused by insect attacks, disease, and injury due to mechanical harvesting. These trees have uneven fruit yield and may require more shake time in one direction than others. Also, lateral shaking forces face reaction from stiff trees that act at the suspended shaker tail, resulting in a lower force transfer in that direction. This causes an uneven elliptic pattern with lower amplitudes in the lateral direction which results in less fruit removal from the sides of the tree. The reaction forces also cause displacements at the shaker tail, causing a radial movement about the tree which results in shear forces between the clamp and the bark surfaces.

3.2 - Single degree of freedom shaker system

In order to illustrate general vibrational behavior of a shaker, a single degree of freedom system is considered and analyzed here. The system is a spring loaded, viscously damped mass excited by a rotating machine that is unbalanced, as shown in figure 3.1 . The unbalance is represented by an eccentric mass m with eccentricity e that is rotating at an angular velocity w. Letting x be the displacement of the nonrotating mass $(M - m)$ from the static equilibrium position, the displacement of m is

$$x + e \sin \omega t$$

The equation of motion is

$$(M - m)\ddot{x} + m\frac{d^2}{dt^2}(x + e \sin \omega t) = - kx - c\dot{x}$$

which, when differentiated, can be rearranged to

$$M\ddot{x} + c\dot{x} + kx = (me\omega^2) \sin \omega t$$

The complete solution to the above differential equation is the combination of the homogeneous and the particular; or otherwise known as the transient and the steady-state solutions, respectively

$$x(t) = x_t(t) + x_{ss}(t)$$

The transient solution is given by

$$x_t(t) = X_1 e^{-\varsigma\omega_n t} \, sin(\sqrt{1 - \varsigma^2}\, \omega_n t + \phi_1)$$

where

X_1 and ϕ_1 are achieved by introducing initial conditions.

k = spring stiffness

$\omega_n = \sqrt{\dfrac{k}{m}}$ = natural frequency of the undamped oscillation

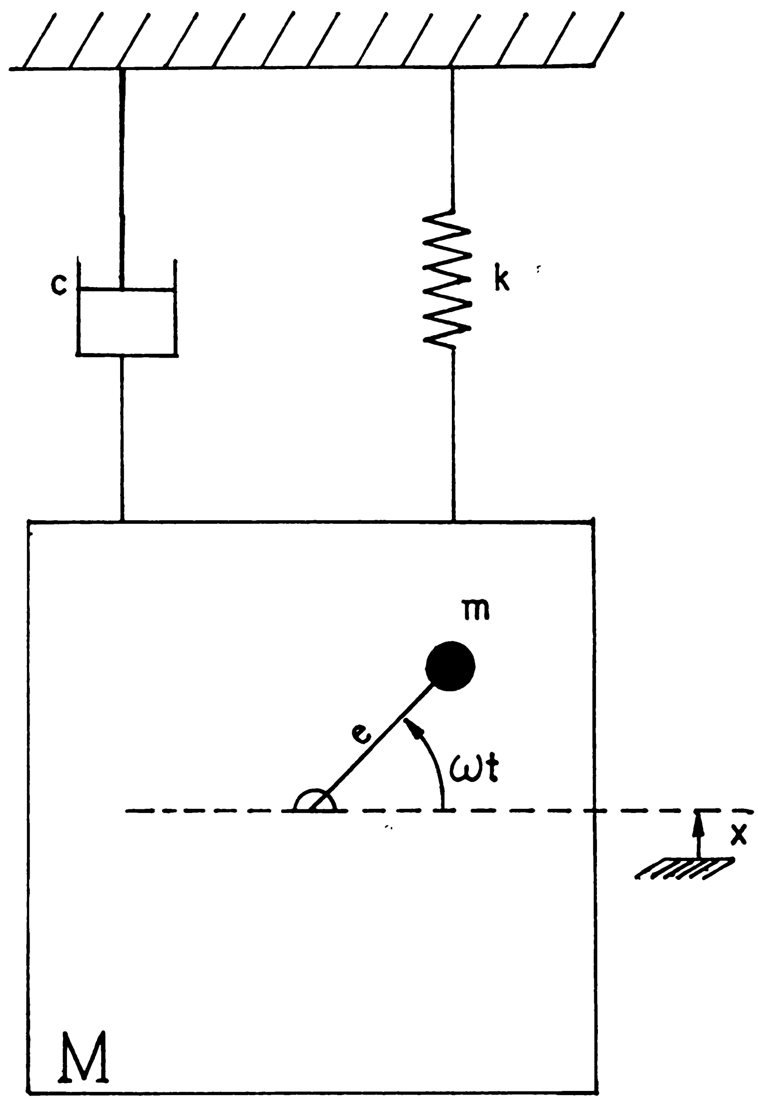

Figure 3.1 - Single degree of freedom vibrating system excited by an unbalanced rotor

$$c = \text{damping coefficient}$$

$$c_c = 2m\omega_n = \text{critical damping}$$

$$\varsigma = \frac{c}{c_c} = \text{damping ratio}$$

The steady state solution is given by

$$x_{ss}(t) = \frac{me\omega^2}{\sqrt{(k - m\omega^2)^2 + (c\omega)^2}} \sin(\omega t - \phi)$$

where

ω = frequency of the exciting force

ϕ = the phase of displacement with respect to the exciting force

$$\phi = \tan^{-1} \frac{c\omega}{k - m\omega^2}$$

When reduced to a nondimensional form, the steady state equations take the following form

$$\frac{MX}{me} = \frac{(\frac{\omega}{\omega_n})^2}{\left\{\left[1 - (\frac{\omega}{\omega_n})^2\right]^2 + \left[2\varsigma\frac{\omega}{\omega_n}\right]^2\right\}^{1/2}}$$

$$\phi = \tan^{-1} \frac{2\varsigma(\frac{\omega}{\omega_n})}{1 - (\frac{\omega}{\omega_n})^2}$$

Plots of the above equations (Figure 3.2) show that for small frequency ratios of less than 1.0 the inertia forces are small which means that the shake forces are approximately equal to the spring force and are spent in overcoming the stiffness of the system. When the frequency ratio equals 1.0, the inertia force gets larger and becomes balanced by the spring force. At this point, called resonance, the displacement amplitude of the system becomes dependent on the amount of damping present in the system. At frequency ratios of greater than 1.0, the damping has little effect on the displacement amplitude and a stable shake in achieved. A shake frequency greater than the natural frequency of the system is ideal for shaking trees because of its stability.

The equation of motion was programmed in FORTRAN using zero initial conditions for x and $\dot{x}$. The displacement results of the program were compared with identical systems programmed with ADAMS and IMP, to verify program accuracies. The program codes and results are presented in appendix C.

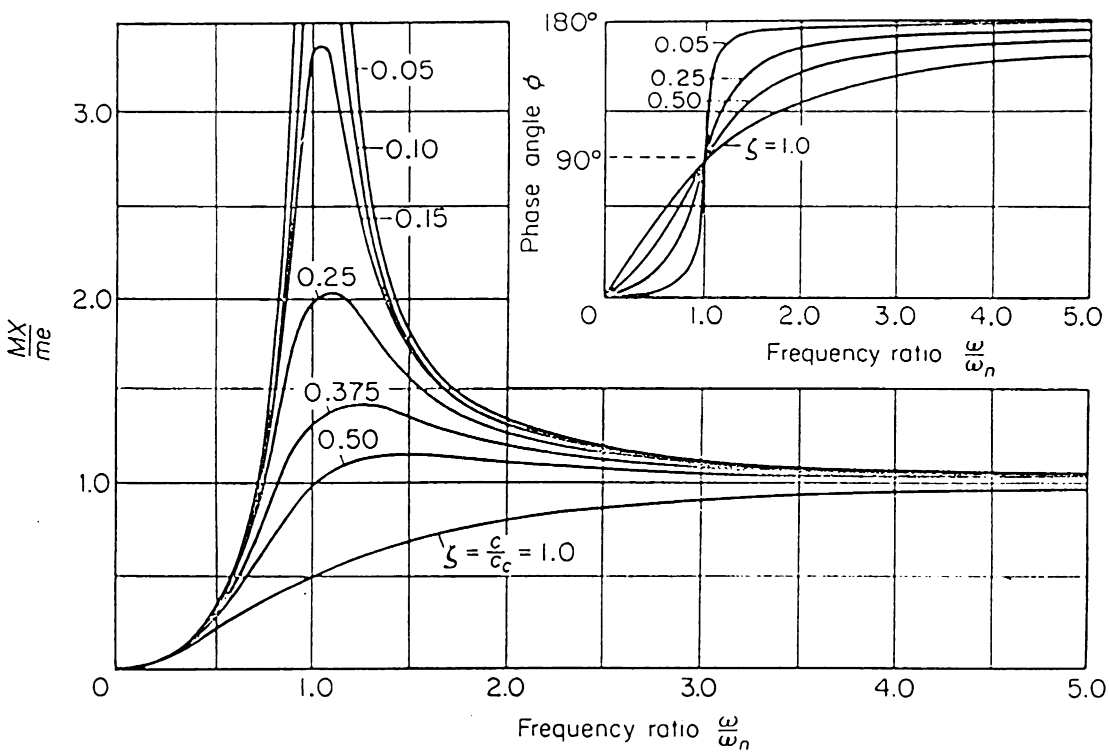

Figure 3.2 - Frequency ratio plot vs. amplitude and phase angle of a single degree of freedom vibrating system

3.3 - The Variable Eccentricity shaker

The shaker was designed and built at the department of Agricultural Engineering, Michigan State University. The following criteria were considered as objectives:

1) To eliminate gallop.
2) To have variable eccentricity for a broad range of shaking forces.
3) To transfer shake effectively in all directions.
4) To control shake direction.

The objectives were achieved by introducing the following design changes into a multi-directional, inertia type shaker concept:

1) Four eccentric masses to allow phase angle control during operation.
2) A phasing mechanism to control phase angle between masses during operation.
3) A weight at shaker tail for effective shake transfer in the lateral direction.
4) Separate drive to control shake direction.

As previously discussed, the galloping problem is attributed to: (a) The passage over the natural frequency of the system while masses speed up to shaking frequency, and (b) Random resting angular position (phase angle) of the masses. As shown in the previous section, the resultant eccentricity is one of the main parameters in control of the sinusoidal shake force. Conventional inertia type shakers develop the force by increasing frequency, from zero, to the desired value. This causes large excitations at periods when $\omega = \omega_n$. However, with variable eccentricity it is possible to achieve shaking frequency with eccentricity set to zero (zero resultant force) and then move eccentricity up to full or desired value, creating shake force. This had been proven to eliminate gallop when Affeldt (1987) installed a variable eccentricity mass housing unit on a Friday C-clamp shaker. The unit consisted of a C-shaped shell filled with molten lead, and a hydraulic cylinder assembled on a circular plate, mounted on a central shaft (Figure 3.3). The C shell is free to pivot to an open position, extending eccentricity, or to a closed position (zero eccentricity) with the motion of the hydraulic cylinder. To create a full shake period with no gallop, the cylinder is extended from a retracted to an open position after the housing is at shaking frequency. Retracting the cylinder before shutting down also eliminates end gallop.

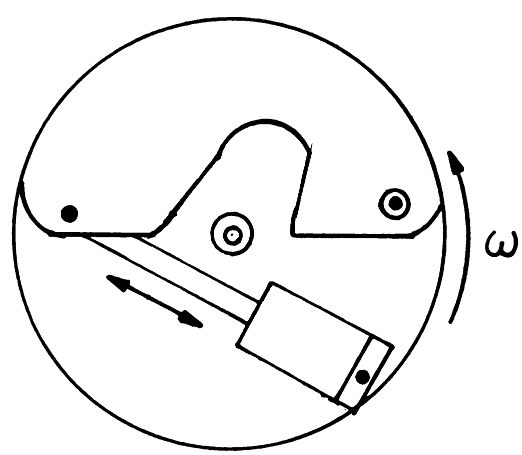

Figure 3.3 - Top view of the C shell variable eccentricity concept

A simpler alternative was implemented in the variable eccentricity shaker with the use of four eccentric masses. Figure 3.4 shows a four mass configuration with a position and angular velocity combination that results in zero force and moment about its center, providing that the rotational axes of the masses are fixed and are all symmetric relative to the center.

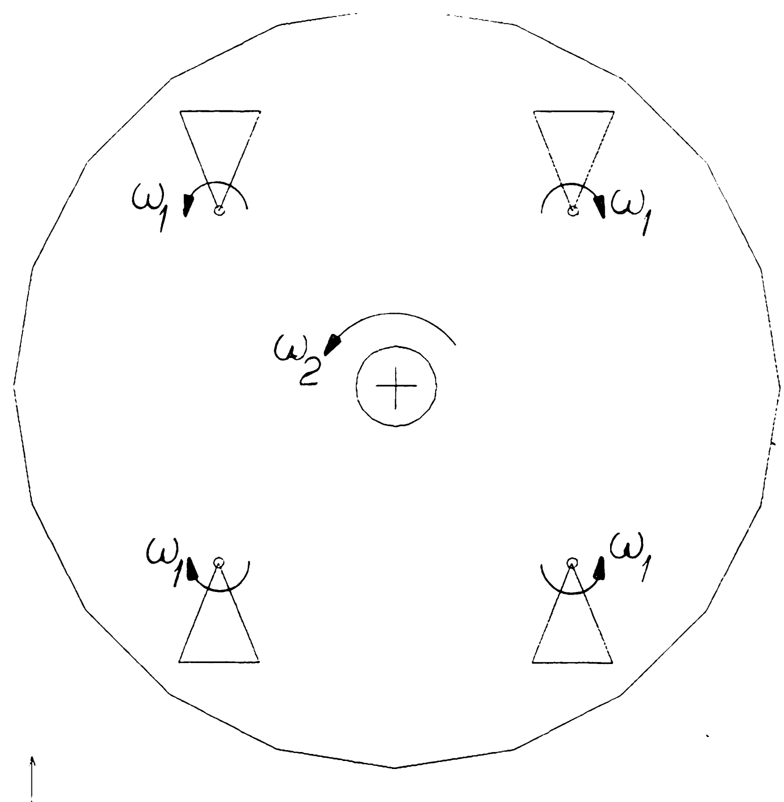

Figure 3.4 - Phase angle configuration of four eccentrics for zero resultant force.

In the position shown, the force from each counter rotating pair is equal and opposite in direction to the other. When the upper pair accelerate downward, the force created cancels with the equal force from the upward acceleration of the lower pair since the acceleration and the physical property of both pairs is the

same. In this condition, the resultant moment about the center is also zero. When the phase angle between the pairs is decreased from 180 degrees, the created force from each pair add, producing a resultant force at the center. Maximum force is achieved at a zero phase angle between the pairs which has a magnitude of $4me\omega^2$. The rotation of this configuration about the center distributes the force in all directions (Figure 3.5).

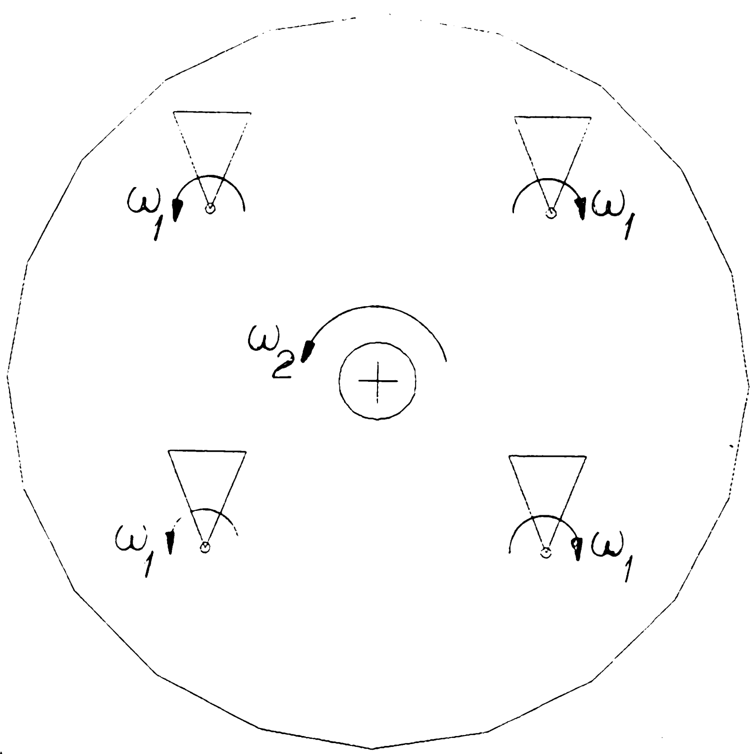

Figure 3.5 - Phase angle configuration of four eccentrics for maximum resultant force.

A mass assembly and a phasing mechanism have been developed for the shaker that permit control of the phase angle between two pair of masses. Four eccentric, pie shaped, molten lead masses on four separate shafts were fitted between two circular plates. The masses were paired. Within each pair, the masses were chained in reverse order to counter-rotate at the same speed. Both pairs were chained around a central shaft that supported the mass assembly. With the help of a phasing mechanism, placed in the chain connection of one of the masses and the drive motor, it is possible to vary the phase angle between the two pairs, when masses are engaged. A single hydraulic motor has been used to drive both pairs. The central shaft (mass housing) is belt driven by a side motor on the top of the shaker housing. The rotation of the mass housing creates a multi-directional shake.

Figure 3.6 shows a view of the variable eccentricity shaker. The block at the tail is made of poured concrete and is free to slide on the aluminum tubing. The tube is bolted to the shaker housing. The concrete block (referred to as the tail weight) acts as a reaction force when clamped to a tree and resists tail movement. It is also expected to increase shake amplitude in y direction. Conventional multi-directional shakers create a smaller shake in y direction resulting in an elliptical shake pattern instead of a circular pattern.

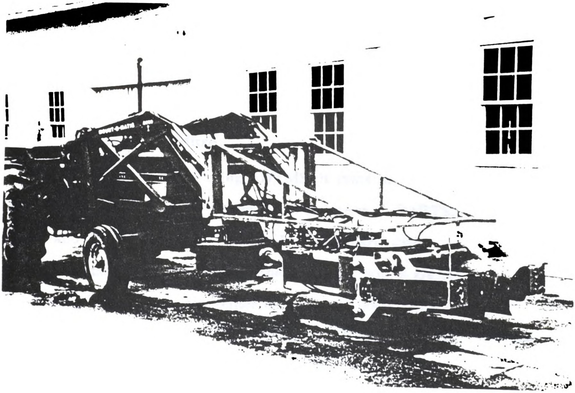

Figure 3.6 - The variable eccentricity shaker

3.4 - Computer Modeling

The variable eccentricity shaker mechanism was modeled using ADAMS. The program allows the user to design a closed or open loop mechanism and simulate its motion for a dynamic or a kinematic analysis. It employs the rigid body theory for creating the equations of motion and setting up the mechanism geometry. A brief explanation of the program's language and scope is included to familiarize reader with the modeling process.

3.4.1 - Modeling Procedure

To model a mechanism using ADAMS, it must first be "broken down" into its individual links or rigid bodies that are termed PARTS. The user must choose and locate a reference frame for each part with respect to a global reference frame. The coordinates of the parts key points are called MARKERS. These are points such as the center of mass and joint positions relative to the local reference frame. The PART statement defines the inertial properties of a part, its position, orientation, and velocity. The parts can have any shape or size and are the only model elements that can have mass, although they may be massless under certain circumstances.

MARKERS are points with fixed location and orientation with respect to the local part reference frame. They should be used to define any point that is significant to the analysis or display of the model. For example, they can be used to :

1) Designate the center of mass of a part.

2) Indicate the position and orientation of a reference frame with respect to which the moments of inertia are specified.

3) Define position and orientation of a joint.

4) Denote force action and reaction points.

5) Specify points for request, and graphics output.

6) Provide other reference frames for resolving the components of vector quantities such as velocities.

After the definition of all link characteristics, the user must define the connections between parts using the JOINT statement. The joint statement describes a combination of constraints on the motion of one part relative to the other, such as translational, revolute, cylindrical, universal, spherical, planar, rack and pinion, and screw joints. Each part must be connected to at least one other by including a marker from each, in a joint statement. Constraint combinations other than those available with joint statements can be defined using a joint primitive or a JPRIM statement. A GEAR statement is also available to simulate the constraints of a spur, helical, bevel, or a planetary gear pair. GEAR connects the motion of a pair of joints.

Mechanism motion, velocity and acceleration with respect to simulation time must be defined by the MOTION statement. The MOTION statement is user programmable and can define a set of complex translational or rotational motions within a joint. The program solves for the applied forces and torques to create the specified motions, in the execution mode. It also solves for reaction forces (between constrained markers) and inertia (or d'Alembert) forces. Other applied forces must be defined using the following statements :

FIELD, and SFORCE - Linear or non linear translational or torsional force between two markers.

BUSHING - Massless bushing with linear stiffness and damping.

SPRINGDAMPER - Massless spring and/or damper with linear properties.

ACCGRAV - Gravitational effect.

The program has three modes of simulation; Static, Kinematic, and Dynamic. Simulation time and output steps must be specified for a mechanism undergoing motion. Desired simulation results in forms of displacement, velocity, acceleration, or force, must be predefined in the code using REQUEST statements. In addition to the above statements, complex motions, forces, and requests can be defined by using FUNCTION statements, or by assigning a user written subroutine to the model code file. The output of the program is in tabular form that can also be plotted in ADAMS' postprocessor. The postprocessor is utility provided to view the requested results in a graphical form, and to graphically simulate the model with respect to time (ADAMS user's manual 5.2, 1987).

3.4.2 - Model Assumptions

The actual shaker has almost no displacements in the vertical z direction, therefore, the shaker-tree system was modeled in a two dimensional xy frame. Assumptions made for modeling and analysis were:

1) System is a combination of rigid links and joints.
2) The restoring force is proportional to displacement for both the shaker and the tree.
3) Damping is viscous (linearly proportional to velocity).

The simple pendulum theory was used to determine the shaker and the tail weight's restoring force to avoid drifting problems. The rate of the restoring force and the damping coefficient can be defined as

$$k = \frac{mg}{l}$$

and

$$c = 2\varsigma\sqrt{km}$$

where

m - total mass of the shaker or tail weight.

l - length of the hanger chains.

ς - damping ratio.

g - gravitational constant

3.4.3 - Model Definition :

The shaker was integrated into nine parts (Figure 3.7). The names and definitions are as follows:

Part 1 : Ground (global reference frame)

Part 2 : Tube - connection between shaker housing and tail weight.

Part 3 : Tail weight.

Part 4 : Shaker housing.

Part 5 : Mass housing.

Part 6 : Mass #1.

Part 7 : Mass #2.

Part 8 : Mass #3.

Part 9 : Mass #4.

Trees was modeled as a pair of springs and dampers connected to the clamp position of the shaker housing. There are seven joints linking the above parts :

JOINT/11 : PLANAR - Connects the mechanism to ground (part one) through part three. Since rigidity is assumed, one planar joint is sufficient to connect the entire system to ground.

JOINT/22 : TRANSLATIONAL - Connects parts three and two. It allows only one translational degree of freedom between parts which constrains the block for all movements relative to the shaker, but sliding along the long axis of the tube.

JOINT/33 : REVOLUTE - Connects parts four and five. It acts as the central shaft connecting the mass housing to the shaker allowing one degree of rotational freedom about a vertical axis parallel to the shaft.

JOINT/44 : REVOLUTE - connects parts six and five. It acts as a vertical shaft connecting the eccentric mass one to the mass housing.

JOINT/55 : REVOLUTE - Connects parts seven (mass two) and five (mass housing).

JOINT/66 : REVOLUTE - Connects parts eight (mass three) and five (mass housing).

JOINT/77 : REVOLUTE - Connects parts nine (mass four) and five (mass housing).

In addition to the joints, two JPRIMs rigidly connect the tube to the shaker housing.

There are five sources of motion in the mechanism. All the moving components are modeled to be driven independently :

MOTION/1 : on joint/33, Rotational. Mass housing motion.

MOTION/2 : on joint/44, Rotational. Mass one motion.

MOTION/3 : on joint/55, Rotational. Mass two motion.

MOTION/4 : on joint/66, Rotational. Mass three motion.

MOTION/5 : on joint/77, Rotational. Mass four motion.

Motions are defined by a polynomial function, using its first term to create constant velocity.

$$\text{Function} = \sum_{j=0}^{n} a_j \left(t - t_0 \right)$$

with

t = time

a_1 = speed

Function = speed * time

Mass one and mass two are in one pair and masses three and four in another. Masses are assigned to counter-rotate with the same speed within each pair. Figure 3.6 shows a simple view of the model and figure 3.7 shows a short period of simulation. ADAMS code of the model is provided in appendix A.

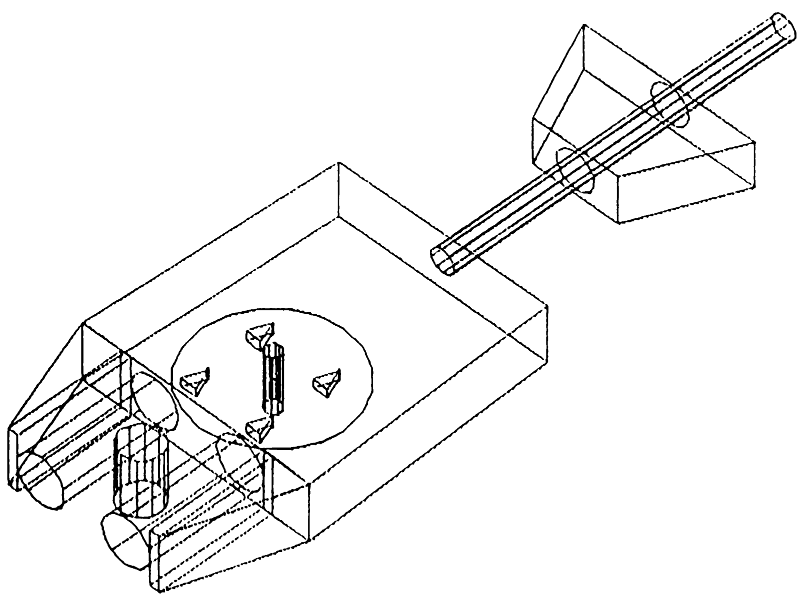

Figure 3.7 - The variable eccentricity model

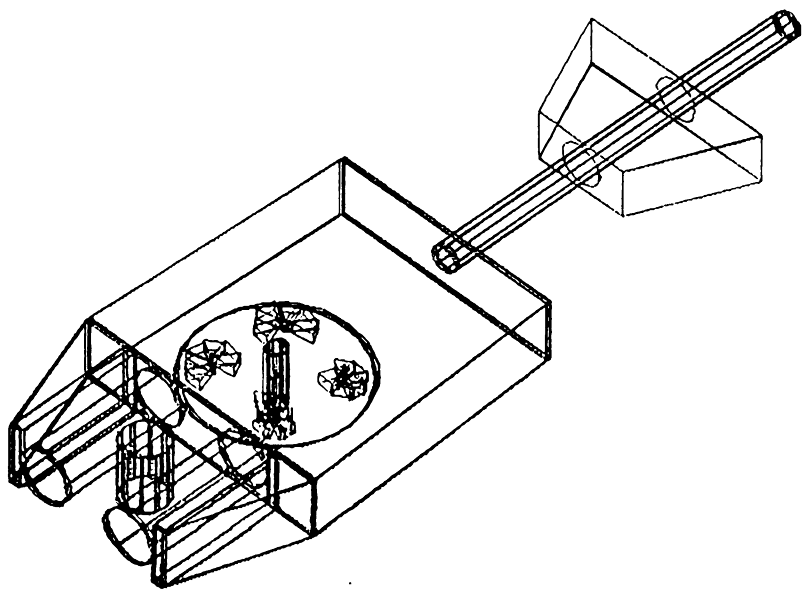

Figure 3.8 - The variable eccentricity shaker model in motion

Chapter 4

Model Response and Evaluations

4.1 - Shaker Model

An initial model of the shaker was set up with approximate physical characteristics of the shaker at a rotating mass frequency of 13.3 Hz (800 rev/min) and a mass housing speed of 50 rev/min. Each eccentric had a mass of 21.6 kg (47.6 lbs) at an eccentricity of 70 mm (2.8 in.). The model response to variations in several parameters were studied under three conditions:

1) Free shake
2) small tree shake
3) Large tree shake

Trees were modeled as pure linear stiffness and viscous damping applied at the clamp point of the shaker model. Two spring and damper sets were used for the x and y direction, which at one end connected to the clamp point and at the other end connected to points on the ground reference frame. Values for tree masses were obtained from experimental data presented by Al-Soboh (1986). The following equation, used for determining the average mass of trees, is a regression fit through a scatter plot of tart cherry tree diameters vs. their mass

$$Y = 1.055(\frac{X}{2.54})^{2.628}$$

where

Y = tree mass (kg)

X = tree diameter (cm)

Average tree stiffness and damping ratios were obtained by Esch and Affeldt (1986) by performing pull tests on a number of tart cherry trees. The static displacements for specific applied forces were recorded and used for determination of tree stiffness. Subsequent displacements, after release of the trees, were also recorded to find the displacement rate of decay for a logarithmic decrement approach to determine damping ratios for each tree. Given mass (m), stiffness (k), and damping ratio (ς), the following equation has been used to find tree damping coefficients (c) for input to the shaker model

$$c = 2\varsigma\sqrt{km}$$

Values used for tree models are presented in Table 4.1.

Table 4.1 - Tree physical characteristics for model input

Tree diameter $mm\,(in.)$	63 (2.5)	165 (6.5)
Average mass (kg)	11.5	144.0
Average stiffness $(\frac{N}{mm})$	12.7	657.9
Average damping ratio (ς)	0.1	--
Average damping coefficient	2.4	62.0 est.

Parameters assumed to have nonlinear effect on shaker displacements were chosen as model variables. These were:

1) Mass of the shaker housing

2) Rotating frequency of eccentric masses

3) Position of the eccentric mass housing

4) Tail weight mass

5) Position of the tail weight

The parameter values were varied in the neighborhood of the original values taken from the actual shaker, to determine their individual effects on shaker behavior. Requested results from the model simulations were x and y displacements of the clamp location where, in cases of tree shake, stiffness and damping was applied. The steady state portion of the outputs were used for measuring peak to peak amplitudes. Figure 4.1 shows the reference frame in which displacements were measured, and shaker orientation with respect to this reference frame. Figure 4.2 and 4.3 are x and y plots of the base model steady state response versus time, respectively. Figure 4.4 is an illustration of the x vs. y plot of the same simulation. Real plots of shaker behavior at the clamp position are actually smoother but, to reduce simulation time, a lower rate of definition (output steps) was used in running the models.

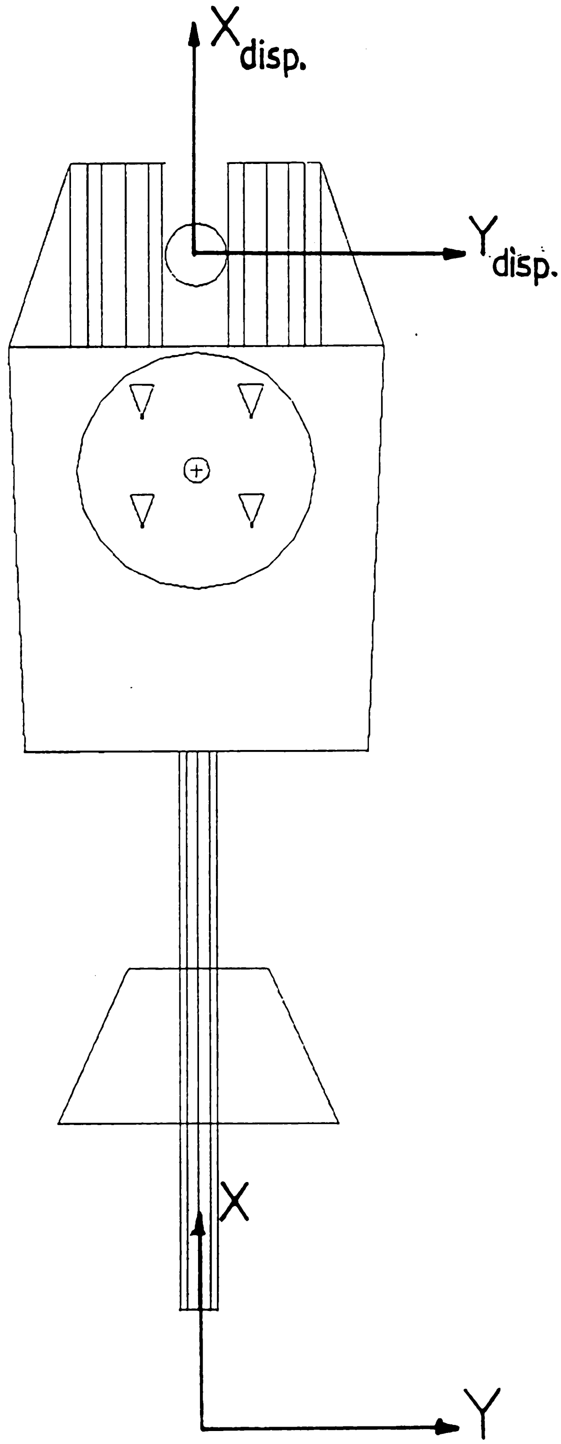

Figure 4.1 - Shaker model reference frames

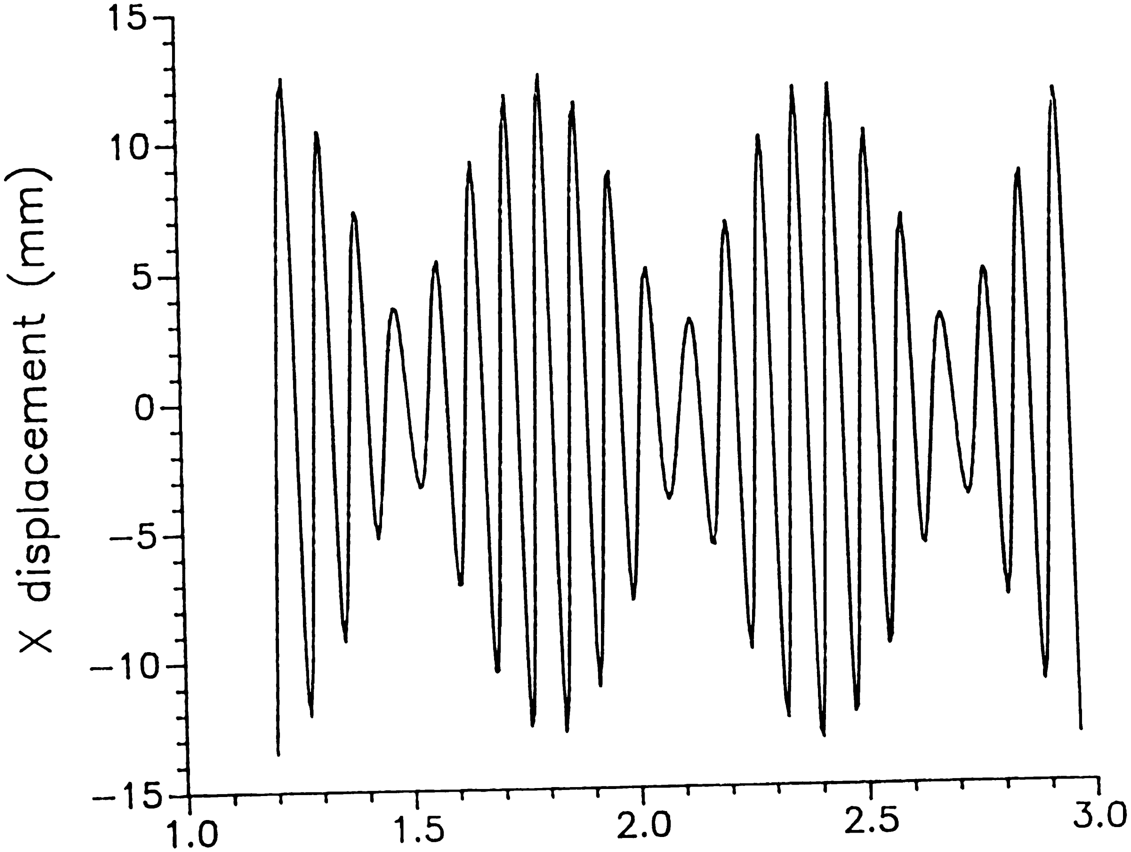

Figure 4.2 – Steady state X displacements during free shake

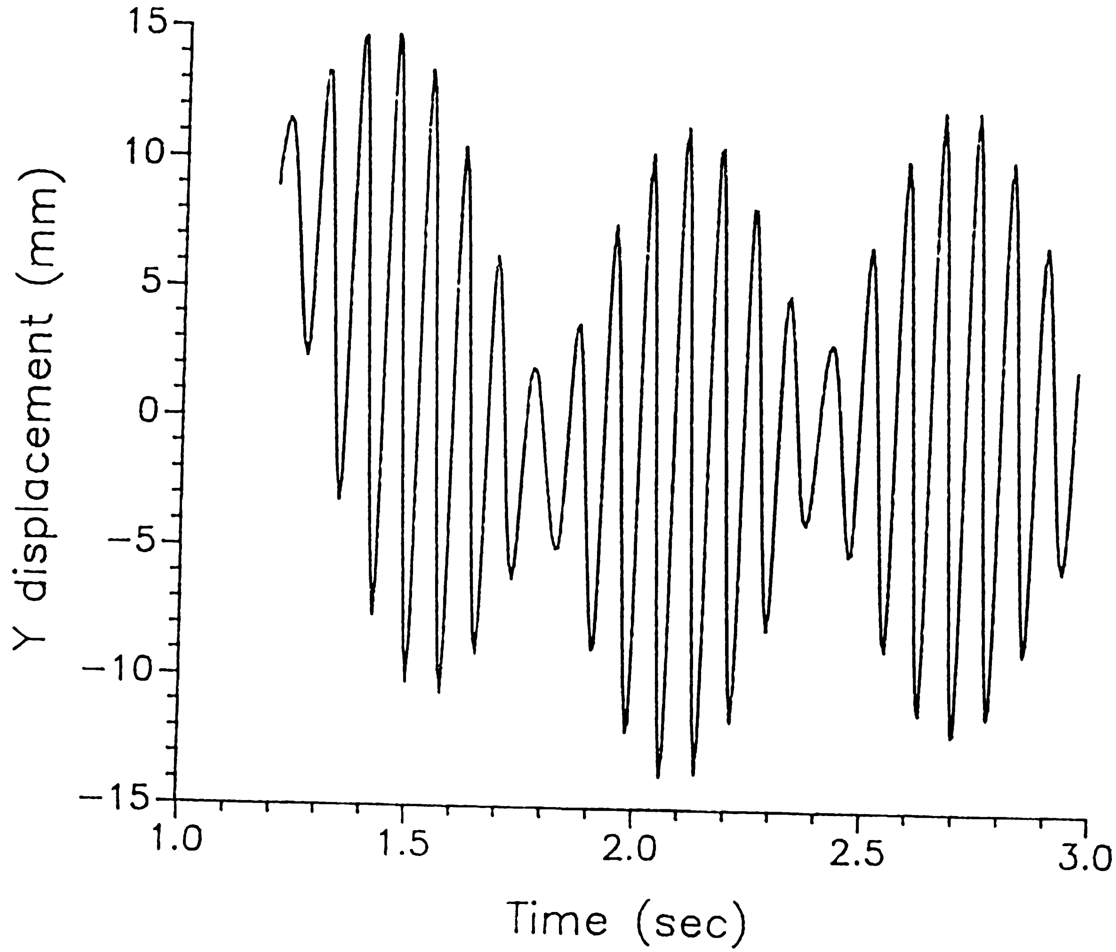

Figure 4.3 — Steady state Y displacements during free shake

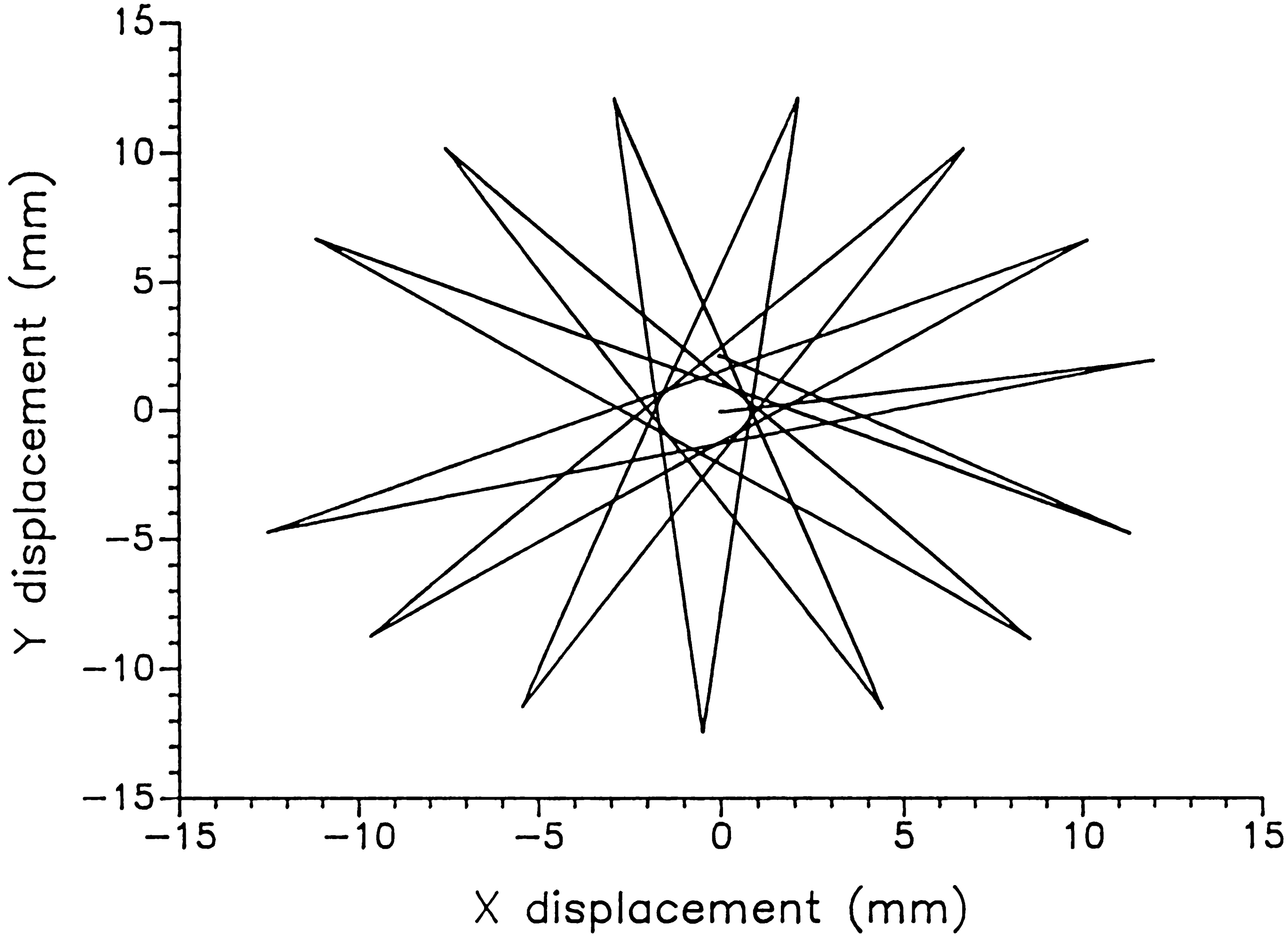

Figure 4.4 — Steady state XY displacements during free shake

4.2 - Variation of shaker housing mass

The effect of shaker housing mass on shaker displacement was investigated by performing five simulations, with a different shaker mass and moment of inertia for each run while keeping other variables constant. Exact input values for masses and moments of inertia were:

1) M = 293 kg (650 lbs) I_{xx}, I_{yy}, I_{zz} = 45.0 , 125.0 , 160.0 kg.m^2

2) M = 315 kg (700 lbs) I_{xx}, I_{yy}, I_{zz} = 48.0 , 134.0 , 173.0 kg.m^2

3) M = 337 kg (750 lbs) I_{xx}, I_{yy}, I_{zz} = 51.0 , 144.0 , 185.0 kg.m^2

4) M = 360 kg (800 lbs) I_{xx}, I_{yy}, I_{zz} = 55.0 , 154.0 , 198.0 kg.m^2

5) M = 383 kg (850 lbs) I_{xx}, I_{yy}, I_{zz} = 58.0 , 164.0 , 210.0 kg.m^2

In free shake simulations, the x and y amplitude curves were close, for practical purposes and declined in a relatively linear rate as the shaker housing mass increased (Figure 4.5). When a small tree was introduced, the amplitude curves followed approximately the same decline with increase in shaker housing mass (Figure 4.6). However, tree shake simulations resulted in smaller amplitudes in the y direction than the x direction, with the greatest difference in shaking the large tree model. Shaker housing mass variations, within the range of study, did not have as much an effect on displacement amplitudes when shaking the large tree model (Figure 4.7).

Shaker housing mass effects displacements by absorbing a portion of the force created by the masses to overcome its own inertia. A decrease in the ratio of unbalance mass to shaker mass results in a higher rate of energy spent for shaker displacement. In this study, the variation of the ratio, although not significant (0.2-0.3), indicated that a higher unbalance to shaker housing mass ratio results in a more effective transmission of shake amplitude to the tree. The weight of the hardware (that is hydraulic motors, shafts, chains, bearings, and housing structure material), however, limits the possibility of increasing the unbalance to shaker mass ratio.

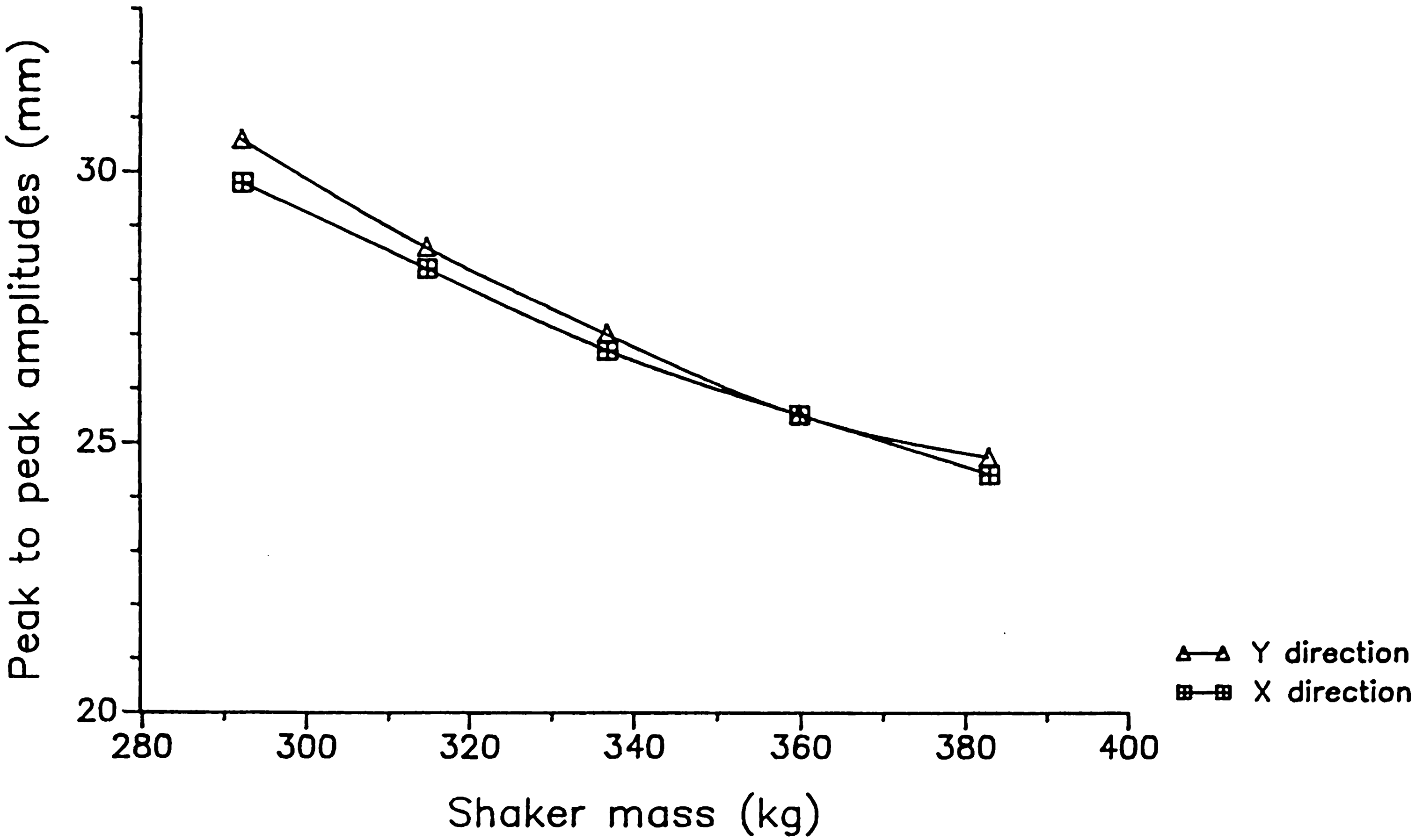

Figure 4.5 – Variation of shaker mass
Free shake

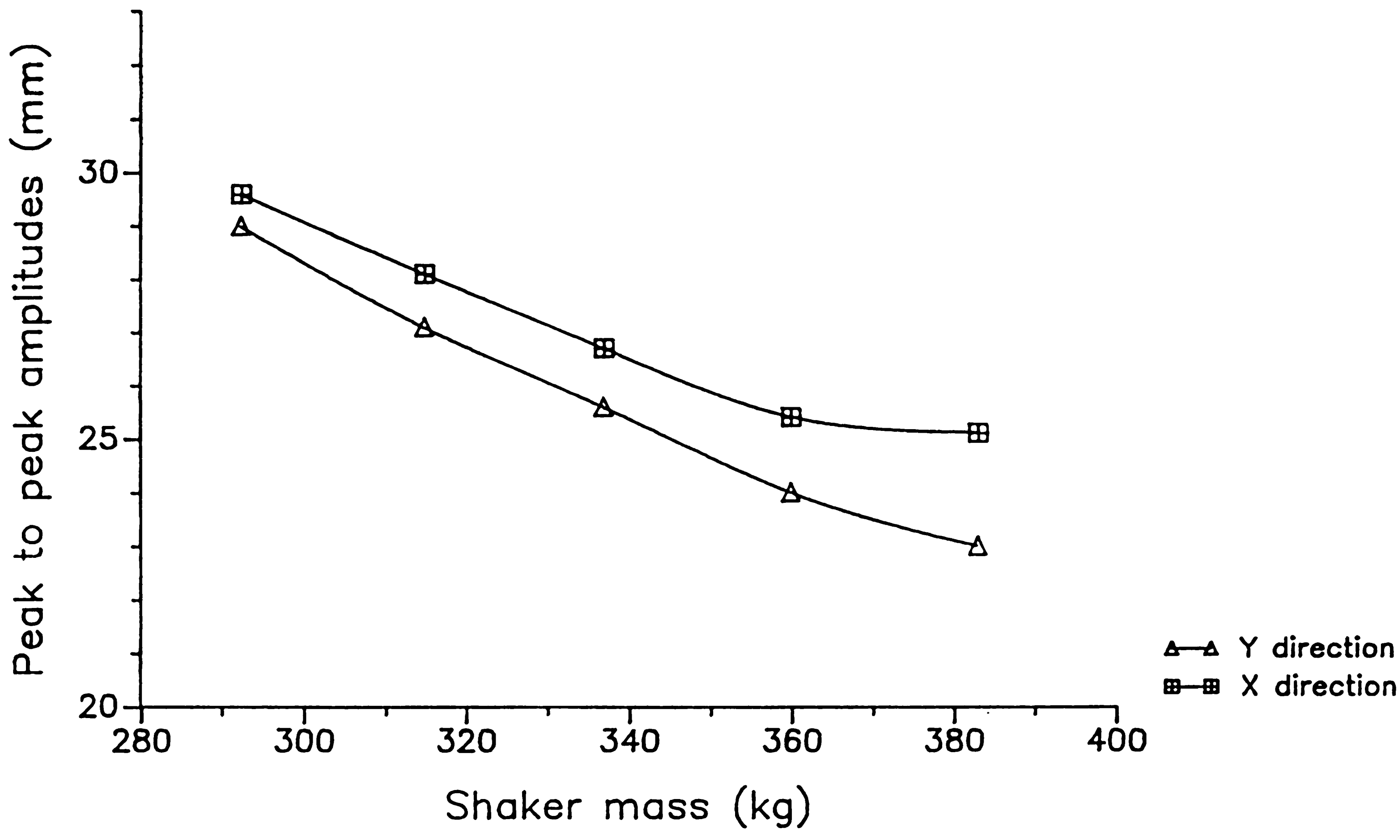

Figure 4.6 — Variation of shaker mass
Small tree shake

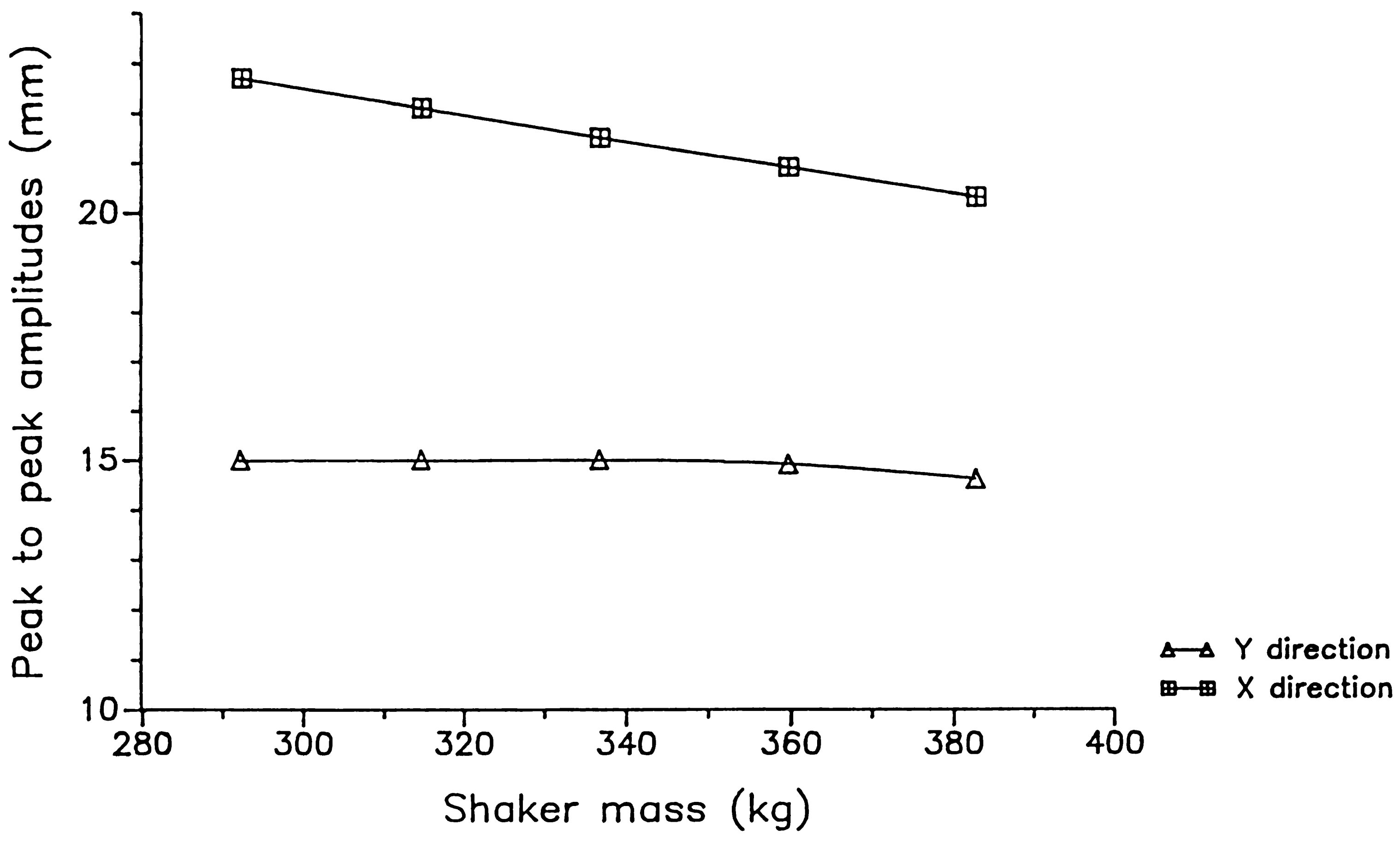

Figure 4.7 — Variation of shaker mass
Large tree shake

4.3 - Variation of eccentric mass rotating frequency

Figures 4.8, 4.9, and 4.10 illustrate the effect of change in rotating mass frequency on shake amplitudes during free shake, small tree, and large tree shakes, respectively. Five different frequencies were simulated with the following specific values:

1) 3.3 Hz (200 rev/min)
2) 6.7 Hz (400 rev/min)
3) 10 Hz (600 rev/min)
4) 13.3 Hz (800 rev/min)
5) 15 Hz (900 rev/min)

Common frequencies for effective fruit removal are between 13 and 15 Hz. The above range was specifically considered to find approximate locations where the frequency ratio is equal to one.

For free shake simulations, increase in frequency from 3.3 Hz had little effect on steady state displacement amplitudes. This is due to the low natural frequency (ω_n) of the shaker, that allows its motion to enter into the steady state phase at lower frequency ratios ($\frac{\omega}{\omega_n}$). During tree shakes, the stiffness of the tree contributes to increase the total natural frequency of the shaker-tree system. In small tree shakes, it appears that the natural frequency of the shaker-tree system model was somewhere between 6.7 and 10 Hz. The curves in Figure 4.9 show that during this period the shake frequency passed through the resonant frequency ratio, where $\frac{\omega}{\omega_n}$=1, and entered steady state motion when at 10 Hz. The high damping coefficient of trees limit resonance which might otherwise cause extreme amplitudes.

The large tree shake simulation curves show that system natural frequency is much higher than the operating frequency range of 13-15 Hz since amplitudes continue to increase within this range. This phenomena is one of the main reasons that shaker damage is usually higher in smaller trees, and is due to the fact that more resonant amplitudes are likely to be created while shaking smaller trees. The variable eccentricity shaker eliminates this problem by reaching desired shake frequency at no resultant eccentricity (therefore, no shake forces) and instantly shifting to full or desired eccentricity, "jumping over" and avoiding resonant frequencies.

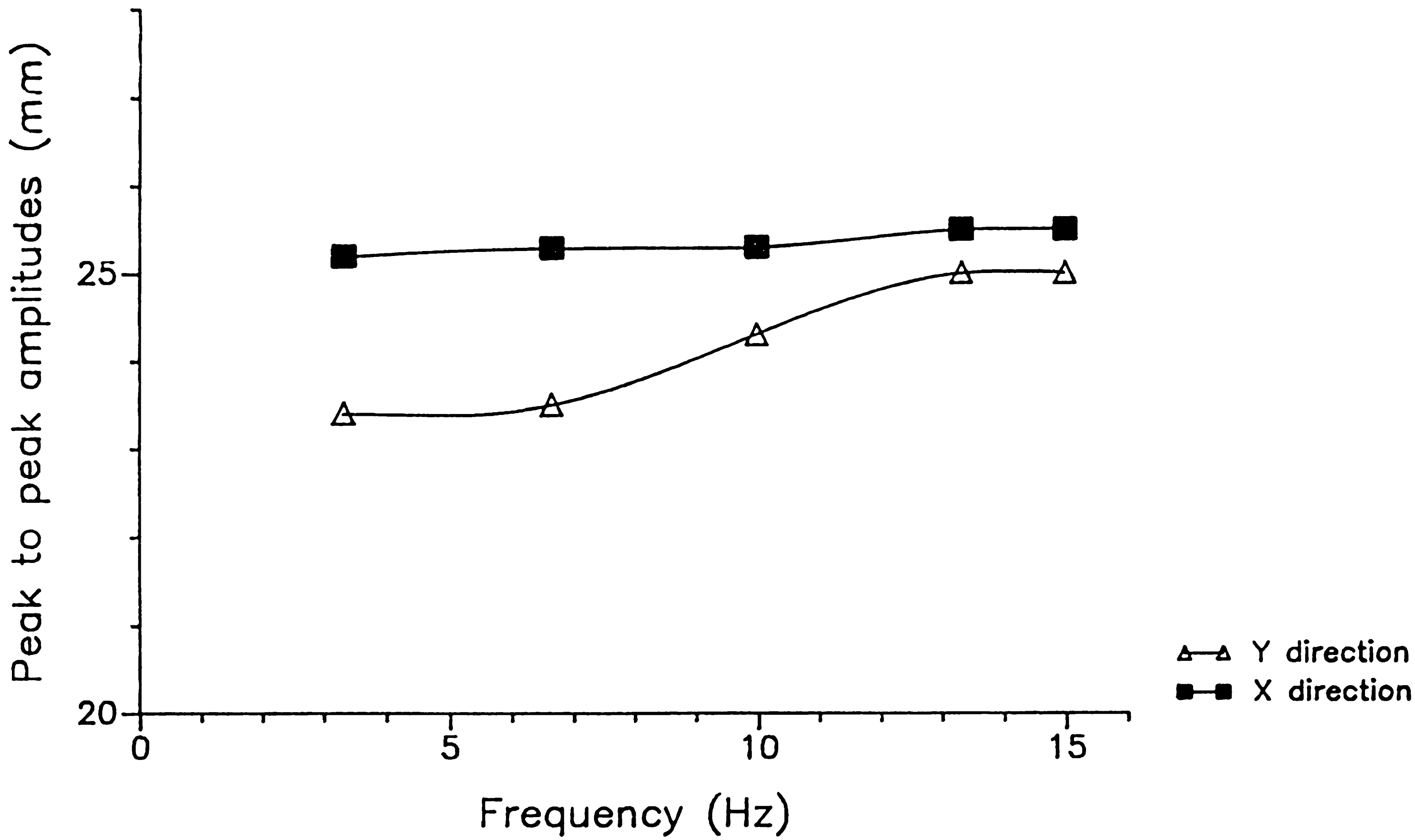

Figure 4.8 — Variation of the rotating frequency of the eccentric masses
Free shake

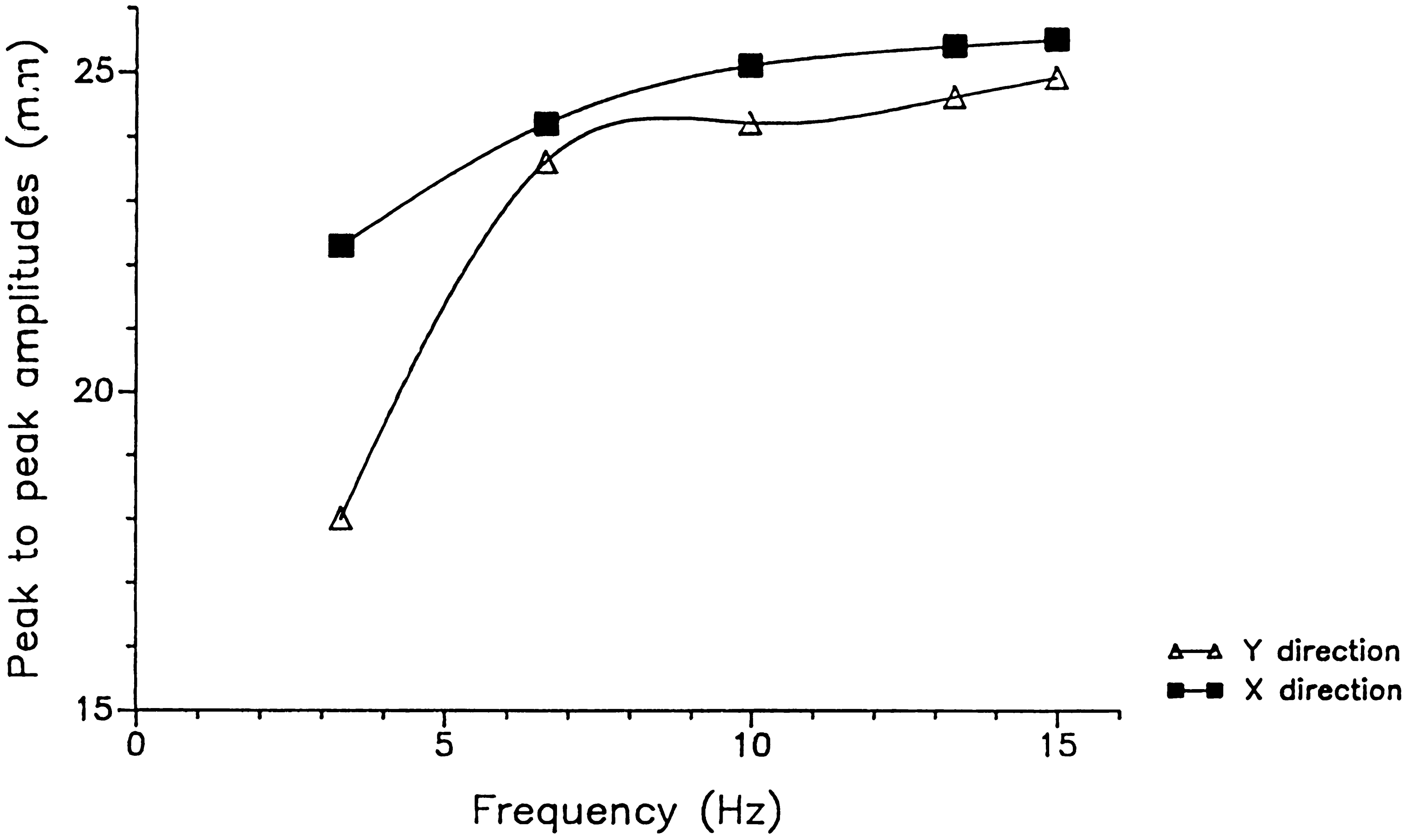

Figure 4.9 – Variation of the rotating frequency of the eccentric masses
Small tree shake

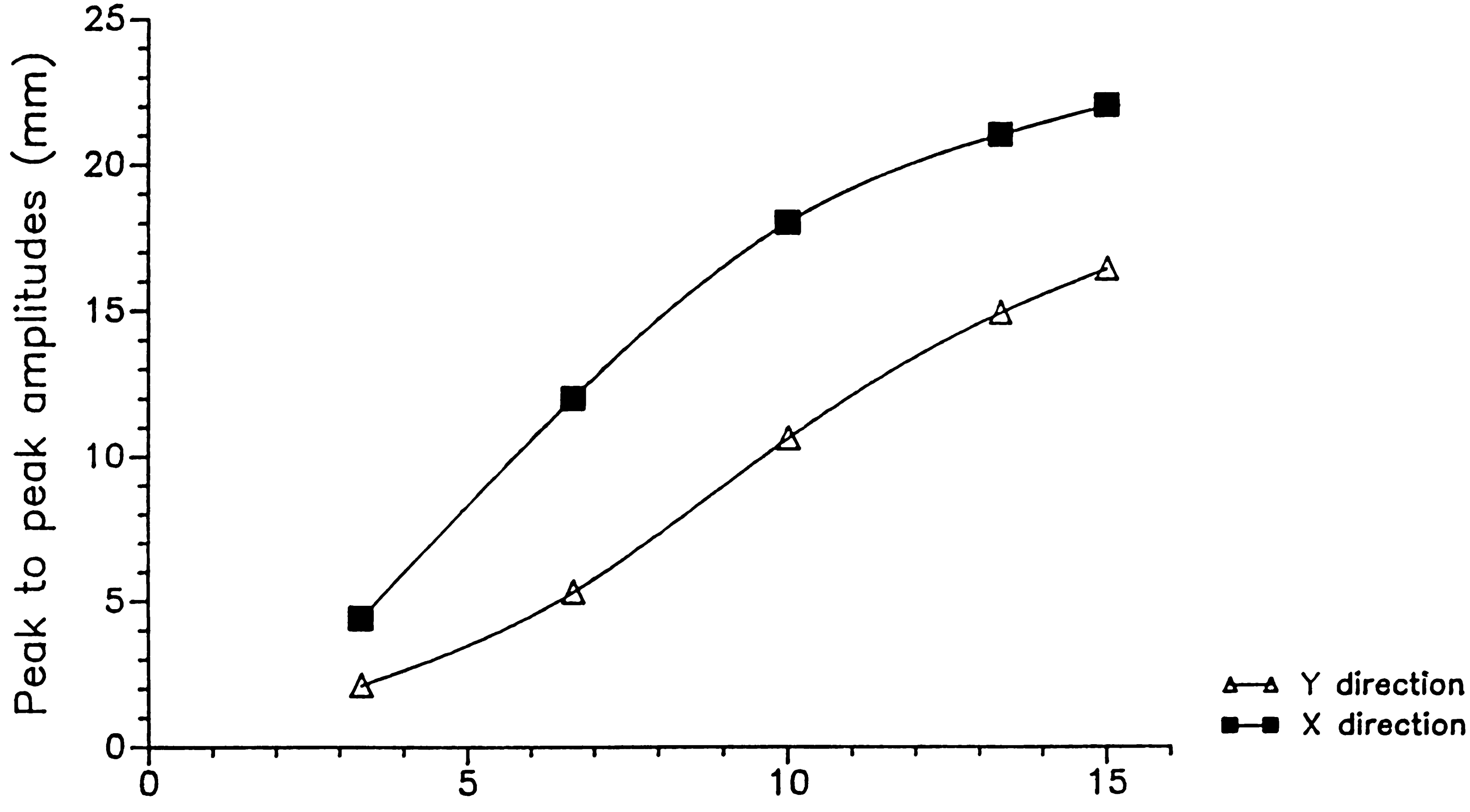

Figure 4.10— Variation of the rotating frequency of the eccentric masses
Large tree shake

4.4 - Variation of the position of the eccentric mass housing

The x distance between the mass housing (center of shake forces) and the clamp point was varied to study shake force proximity effects on displacement magnitude differences in the x and y directions. The x direction amplitudes naturally stayed the same in all simulations since the variation of the mass housing distance to the clamp, within the simulated range, should only effect the y component of the applied forces. The actual shaker mass housing is located at approximately 0.75 m (40 in.) from the clamp point. In all simulations, the shaker housing, the tail weight, and the connecting tube's center of mass were located at 0.6 m (24 in.), 2.9 m (115 in.), and 2.8 m (112 in.) from the clamp point, respectively. Therefore, the resultant x component of the shaker center of mass, excluding the eccentric masses, remained at 1.4 m (56 in.) from the clamp point.

In free shake simulations, the x and y amplitudes were approximately uniform at a mass housing distance of 1.0 m. Amplitudes in the y direction increased as the housing position moved closer toward the clamp point (Figure 4.11). In small tree shakes, the y amplitude curves followed free shake results closely, but with a lower rate of increase as the distance was reduced (Figure 4.12).

In large tree conditions, the y direction amplitudes were about 6 mm smaller than amplitudes in the x direction, at a mass housing distance of 1.0 m from the tree (Figure 4.13). Amplitudes in the y direction increased as the mass housing distance to tree was reduced, and came close to the x amplitudes at a distance of 0.4 m (8 in.).

Theoretically, the most effective location for force application is at the center of the clamp where trees are grabbed. This, however, is not totally possible with the variable eccentricity shaker due to existence of the four masses

and geometrical limitations associated with them. Therefore, the mass housing is positioned between the resultant center of mass of the shaker and the clamp, so that the total weight of the shaker can oppose the y component of the reaction forces from the tree, restricting rotational movement of the shaker about the tree's vertical axis and also result in more uniformity in the x and y amplitudes.

The simulation curves here indicate that a mass housing position suitable for causing equal x and y amplitudes in shaking small trees may not be sufficient to do the same in shaking larger trees, or vise versa. As illustrated by plots of Figure 4.12 and 4.13, a mass housing x distance from clamp of 1.0 m, for shaking the small tree model, and 0.4 m, for shaking the large tree model, are suitable for creating equal x and y amplitudes.

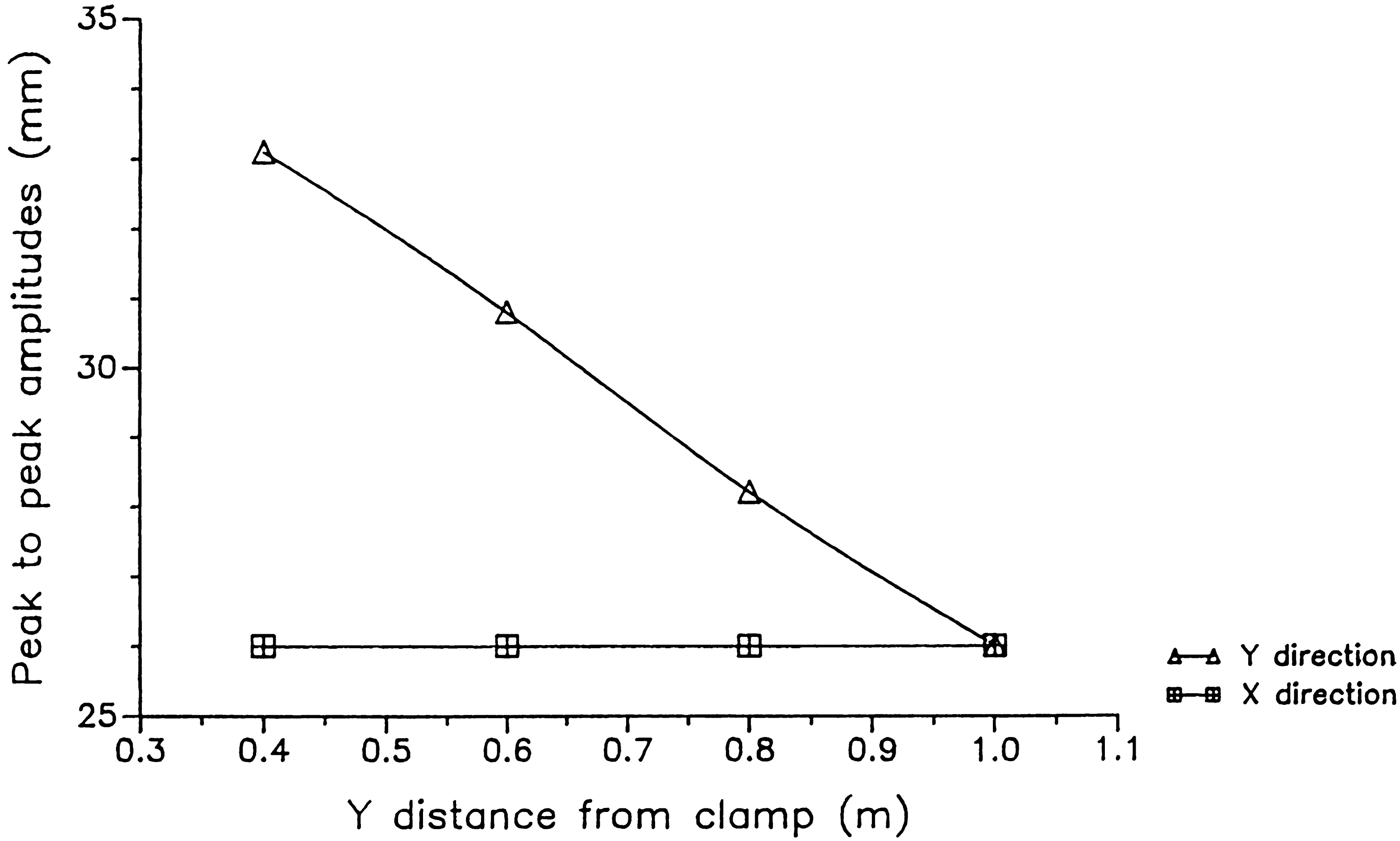

Figure 4.11– Variation of the position of the mass housing
Free shake

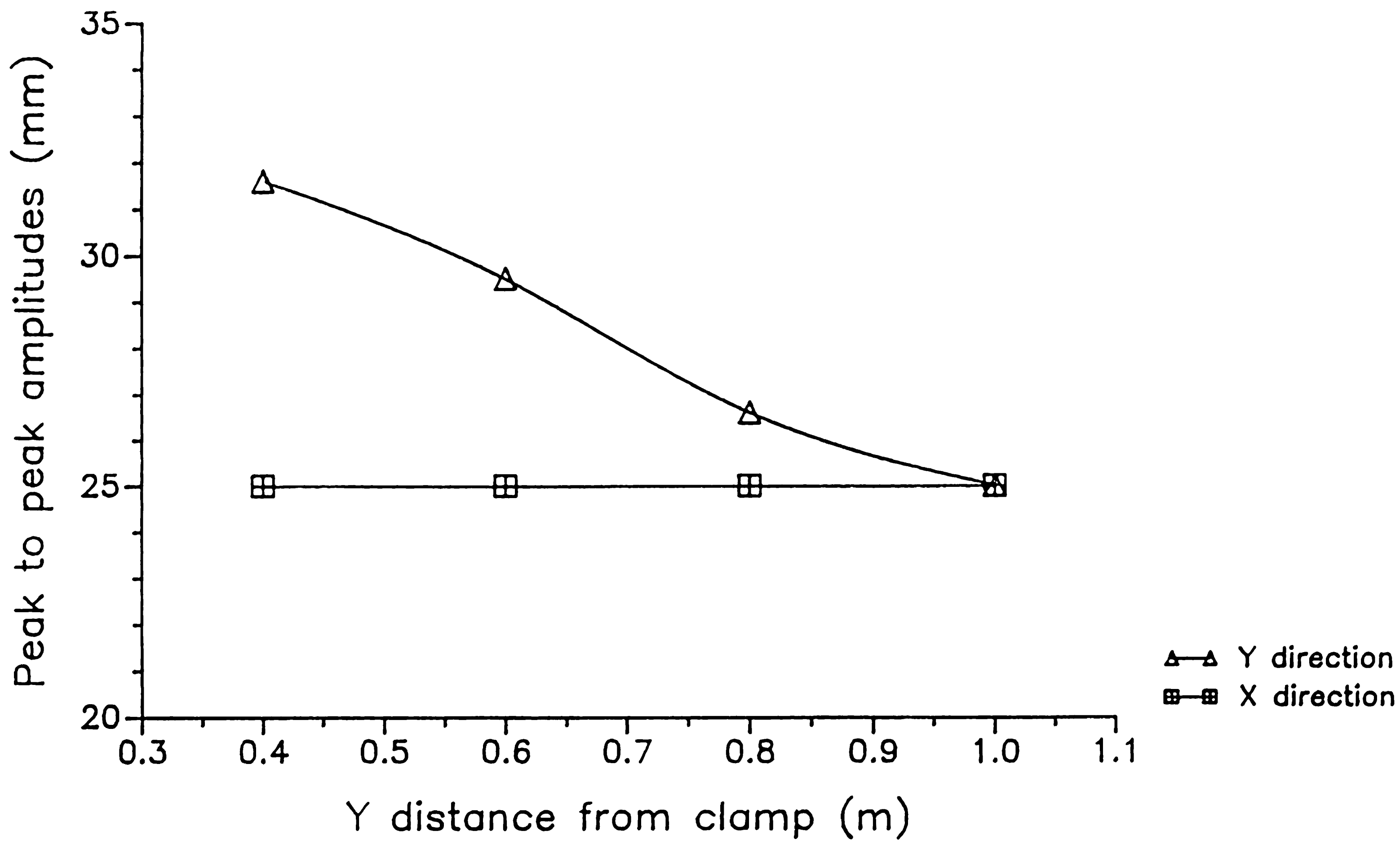

Figure 4.12— Variation of the position of the mass housing
Small tree shake

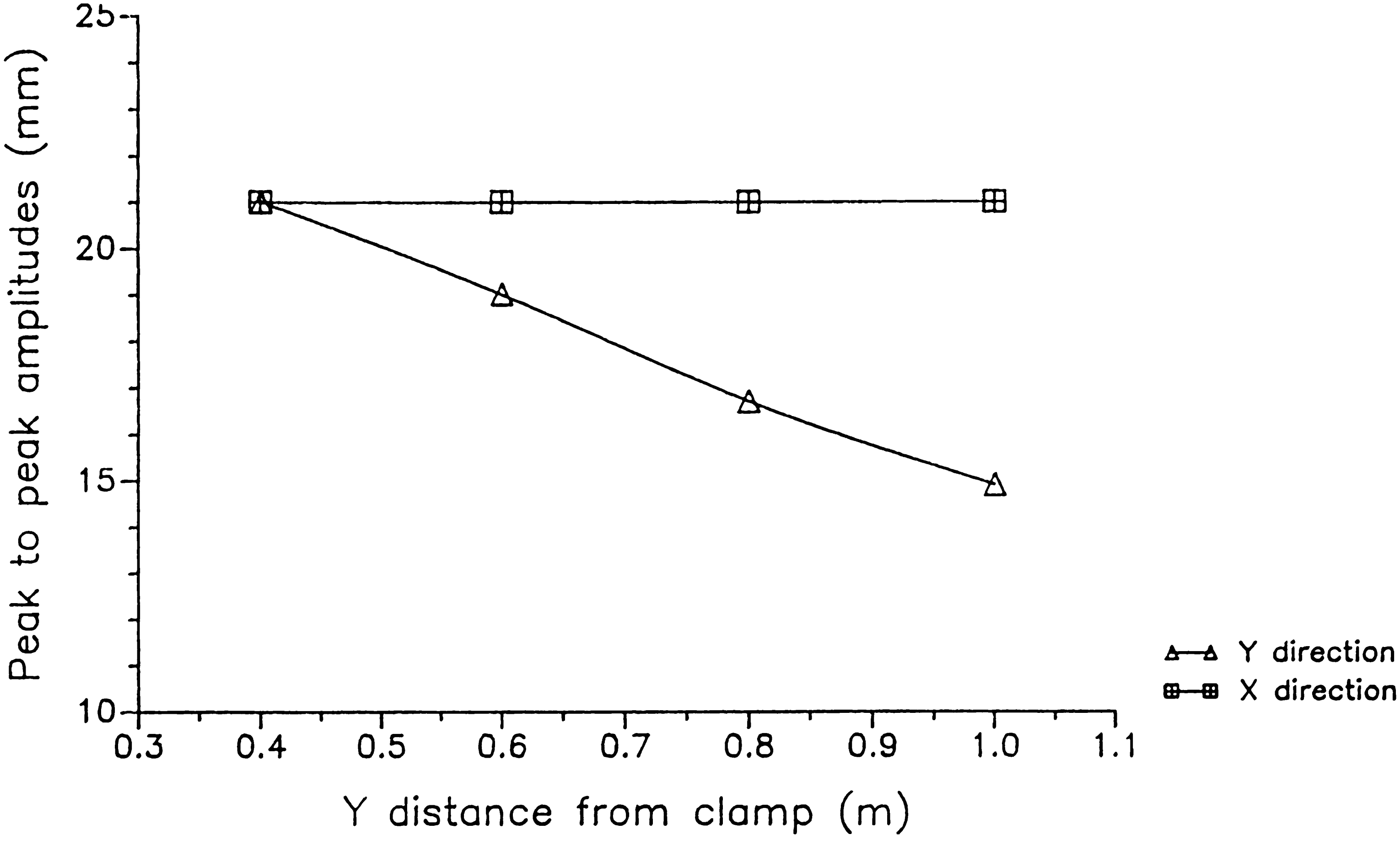

Figure 4.13– Variation of the position of the mass housing
Large tree shake

4.5 - Variation of the tail weight mass.

The mass of the tail weight is a determining factor in positioning the x component of the resultant center of mass of the shaker. Its value was varied to examine its effect on the y amplitude of the shake. Since the tail weight is free, for practical purposes, to slide on the tube in the x direction, its physical characteristics do not effect the x component of the shake amplitude. The simulated mass values for the tail weight were:

1) 90 kg (200 lbs)
2) 112 kg (250 lbs)
3) 158 kg (350 lbs)
4) 180 kg (400 lbs)

An increase in the mass value from 90 kg resulted in an increase in the y amplitude of the shake for free shake and small tree shake simulations. The x and y amplitudes became uniform within the range of 160-180 kg for the tail weight mass (Figure 4.14 and 4.15). In shaking the large tree model, a lower rate of increase in y displacements was noticed as the tail weight weight mass varied in the simulated range (Figure 4.16).

The results indicate a relatively low sensitivity of shaker displacement to the mass of the tail weight for larger trees, in a 90 kg (200 lbs) range. A mass of 160-180 kg is sufficient for uniformity in the x and y amplitudes in shaking only small trees whereas, for larger trees, a much larger mass (perhaps in the 300 kg range) is needed. A larger mass value was not simulated because, although sufficient for amplitude uniformity in both directions, it would create much higher y direction displacements in small tree shakes.

The mass of the tail weight, however, has a great effect on shaker rotational movement about the tree's vertical axis when shaking a large tree (Figure 4.17). A tail weight mass in the 160-180 kg range reduces its motion in the y direction during operation leading to less rotational shaker movement about the tree, thus decreasing shear stresses between the bark and the clamp pads.

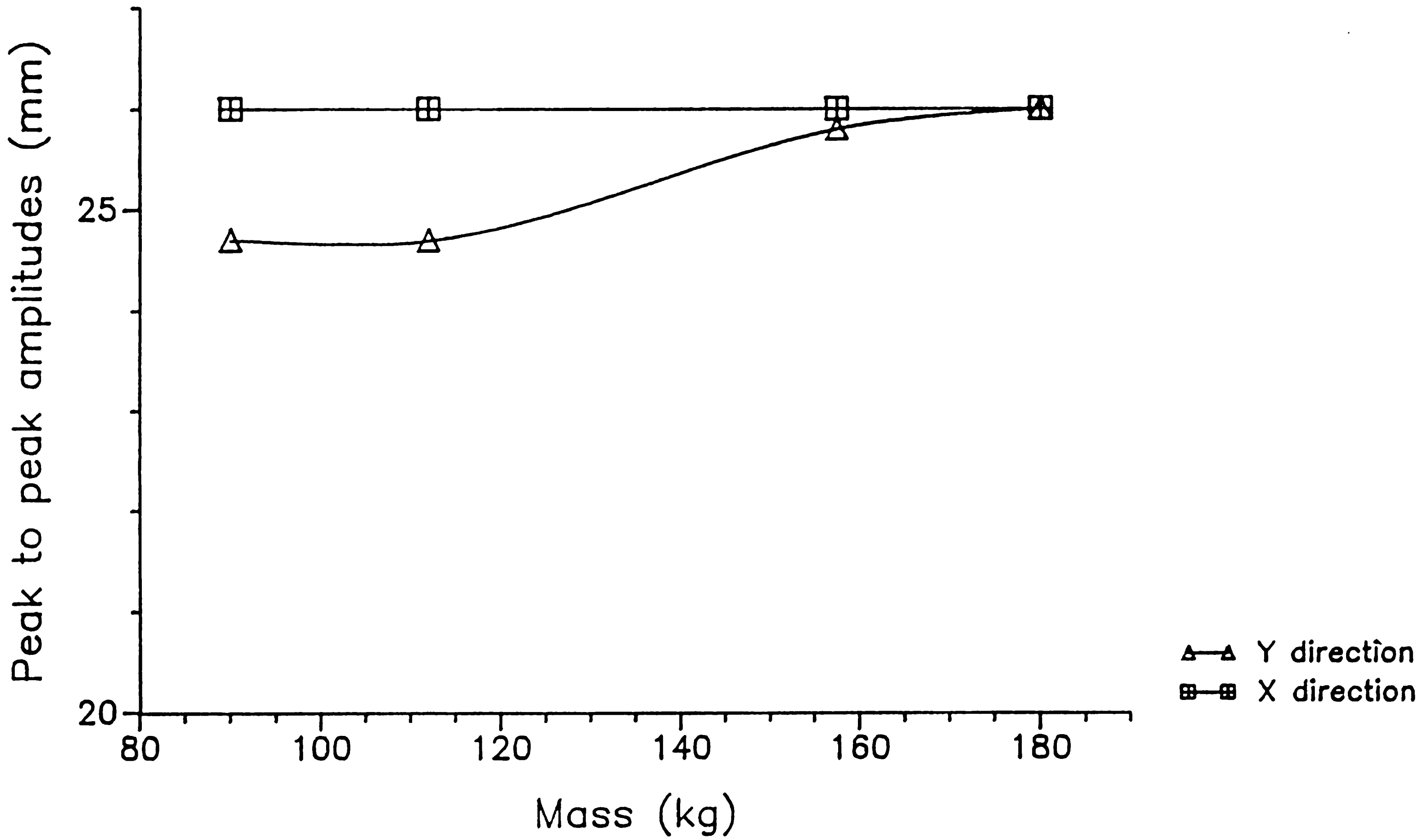

Figure 4.14— Variation of tail weight mass
Free shake

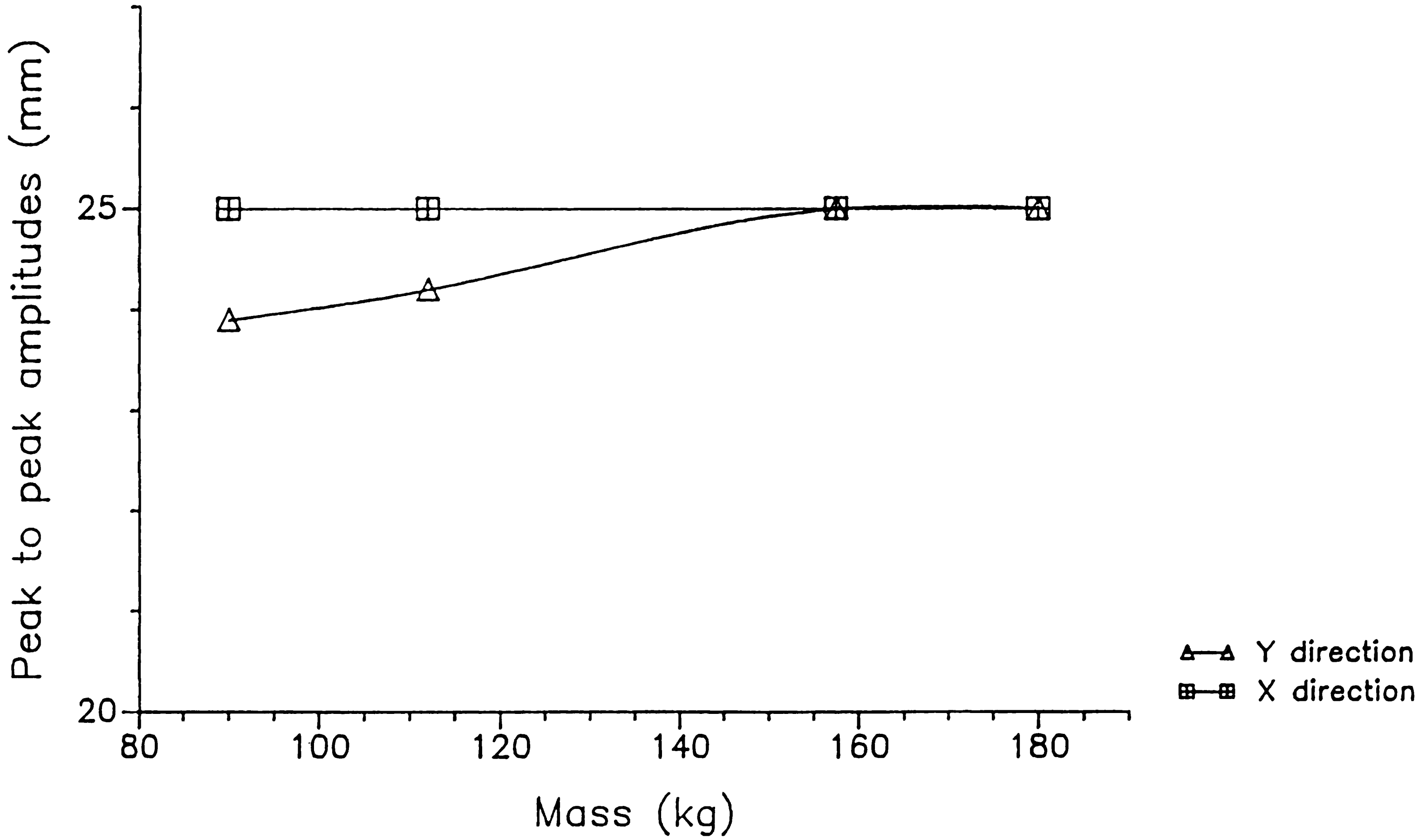

Figure 4.15— Variation of tail weight mass
Small tree shake

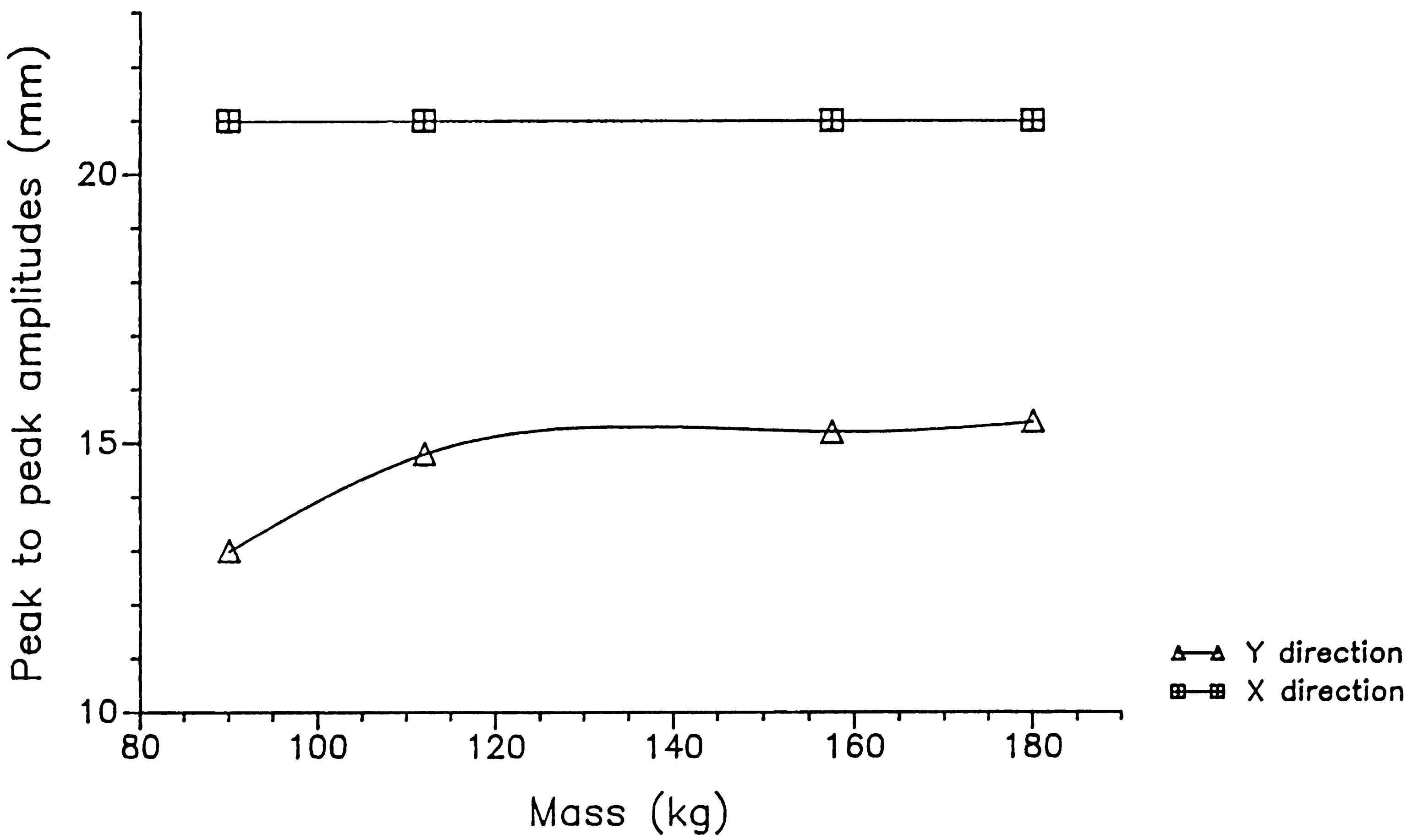

Figure 4.16– Variation of tail weight mass
Large tree shake

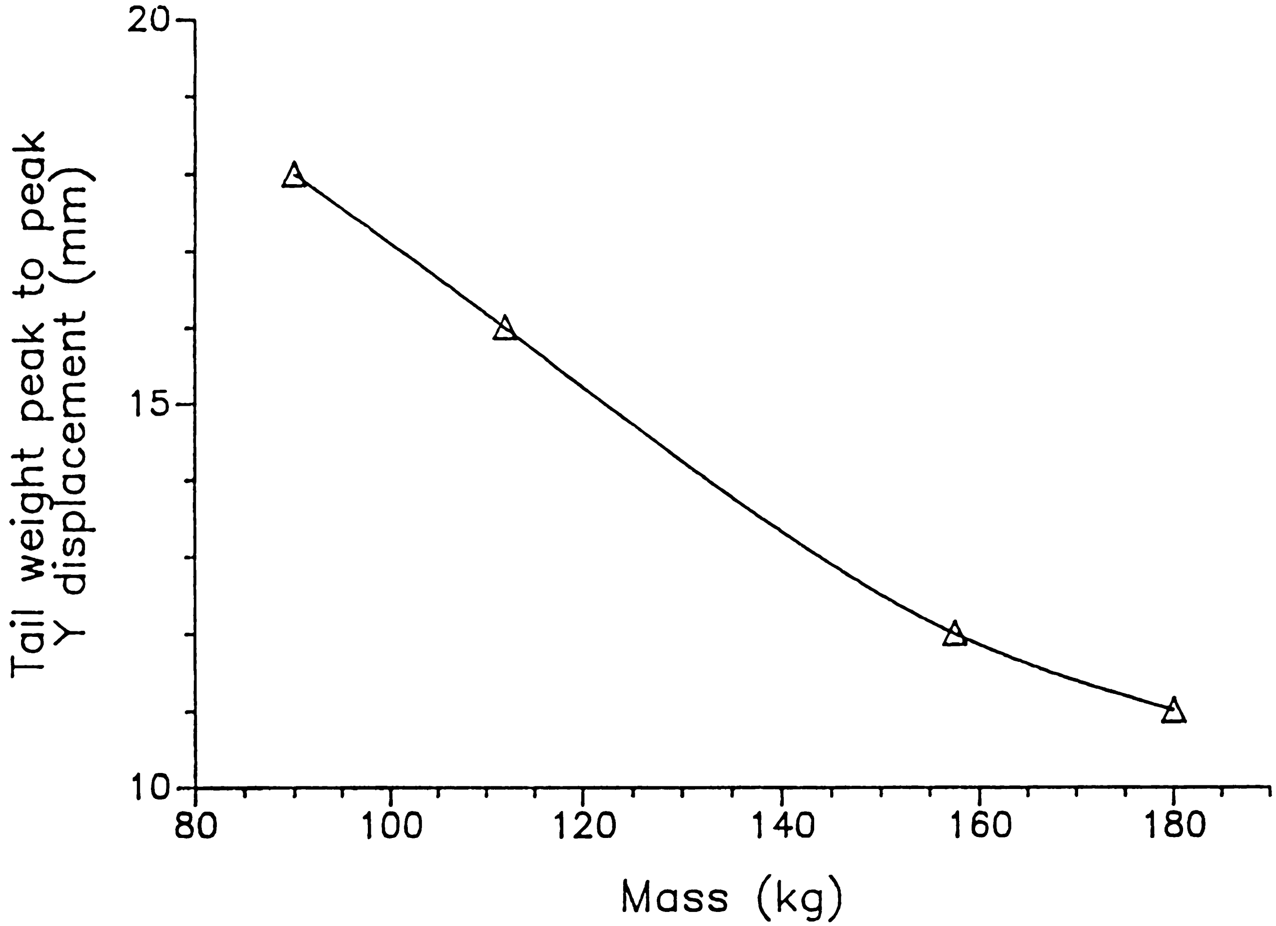

Figure 4.17– Effect of tail weight mass on its displacement
Large tree shake

4.6 - Variation of the position of the tail weight

The present position of the tail weight in the variable eccentricity shaker is approximately 2.9 m (115 in.) from the clamp point, in the x direction. During initial shaker tests, the reinforced aluminum tubing experienced resonance at operating shake frequencies of 13.3-15 Hz (800-900 rev/min) for tail weight distances higher than 2.9 m. Therefore, unless the tube is replaced by a stronger member, the tail weight cannot be positioned farther than 2.9 m from the clamp point. In the simulations, the distance between the tail weight and the clamp point was reduced to observe their respective effects on shaker displacement.

In free shake and small tree shake simulations, a tail weight position of 2.9 m from the clamp point was sufficient for uniformity in the x and y displacements (Figure 4.18 and 4.19). The y displacement amplitude curves declined as the tail weight was moved closer to the clamp point. This trend was also evident in shaking the large tree model, with the exception that a tail weight distance of higher than 2.9 m from the clamp point is needed for uniformity in the x and y shake amplitudes (Figure 4.20).

The tail weight location relative to the clamp point is another factor in positioning the resultant center of mass of the shaker. The results here indicate that a more effective shake is achieved by placing the tail weight at farther distance from the clamp for large trees, than for small trees. Orchard tree spacings, however, dictate the allowable shaker length. A larger shaker length also limits its own maneuverability between trees. Therefore, compromises have to be made, based on experimental tests, between the mass of the tail and its distance from clamp for a more uniform shake in both x and y directions and better shaker maneuverability.

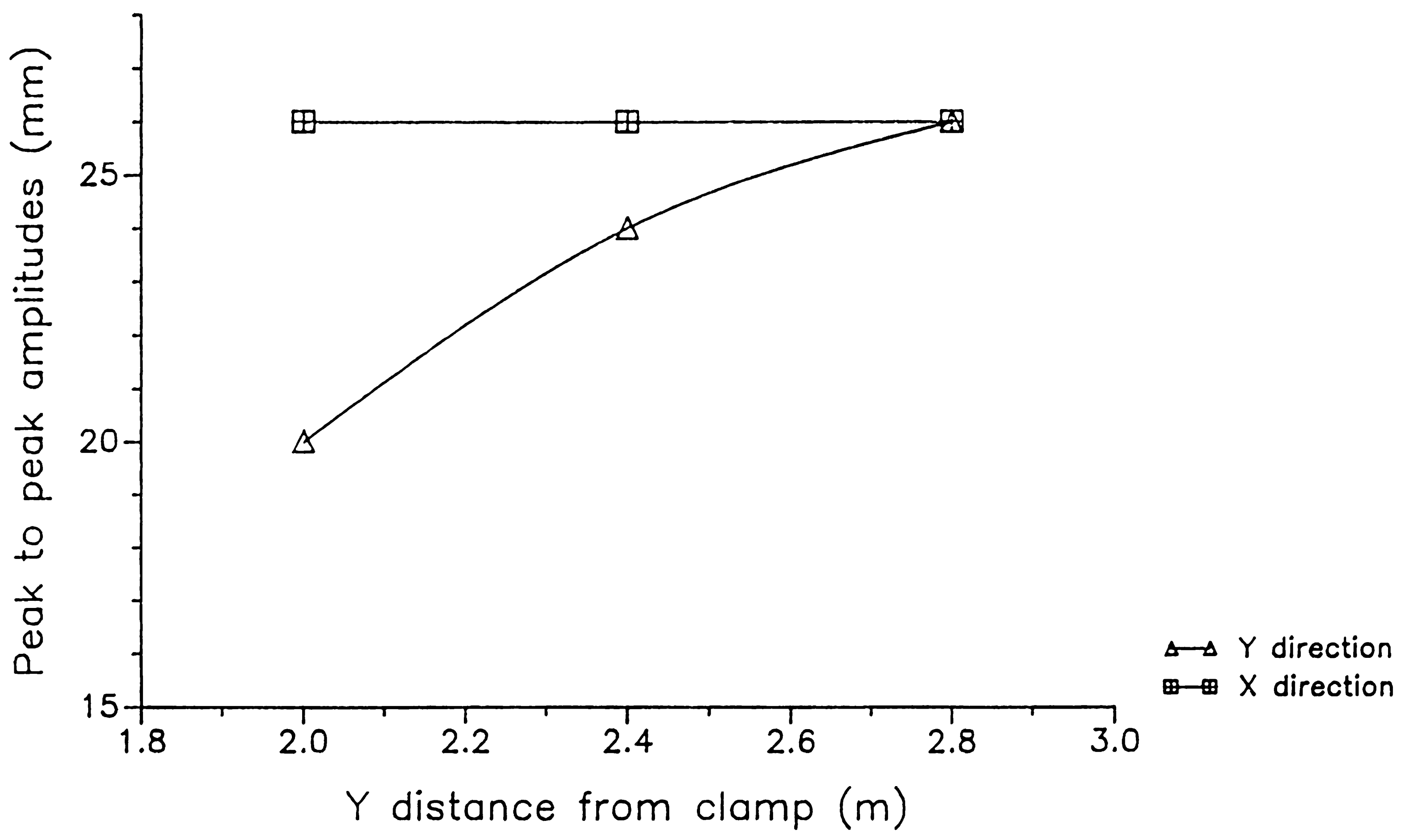

Figure 4.18— Variation of the position of the tail weight
Free shake

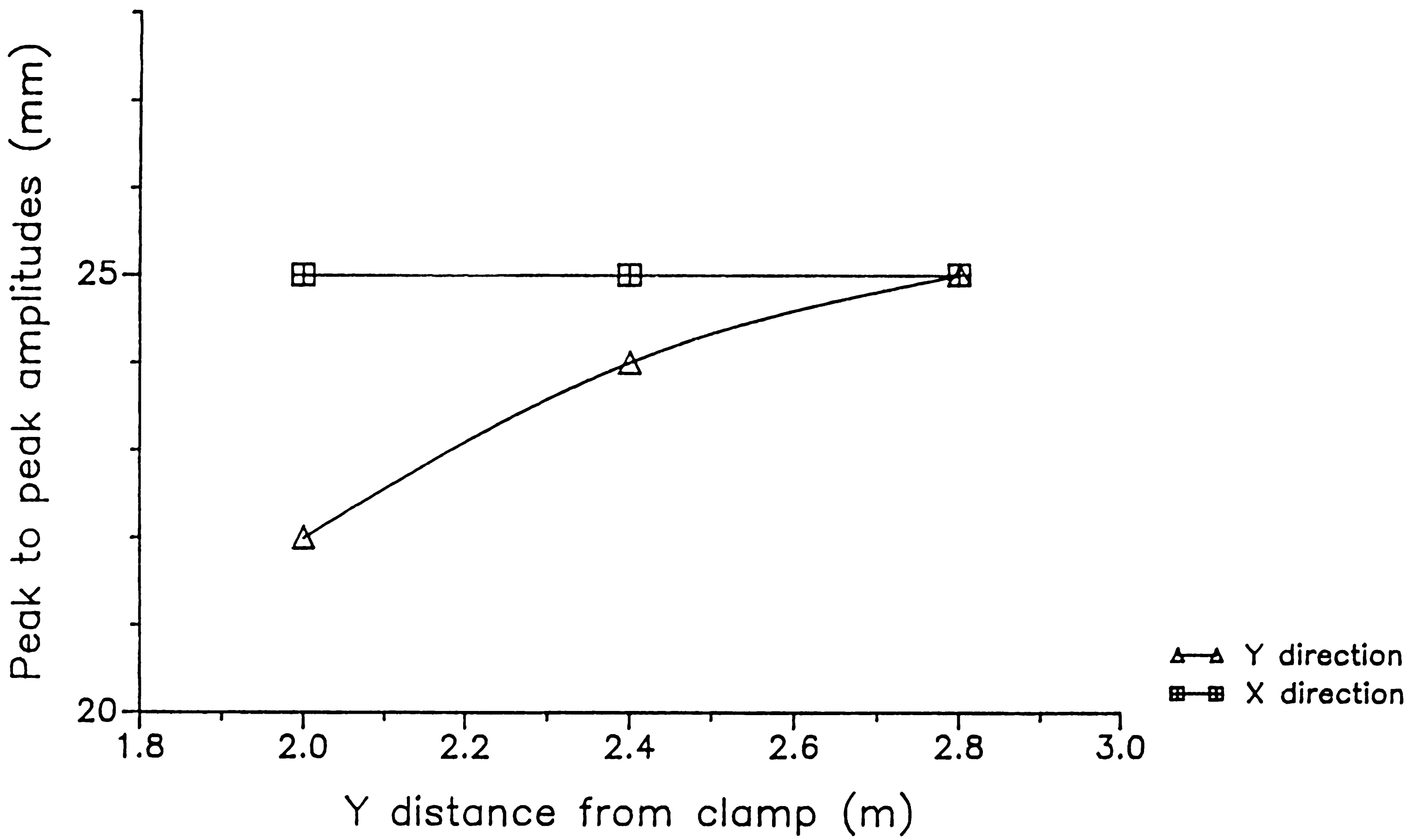

Figure 4.19— Variation of the position of the tail weight
Small tree shake

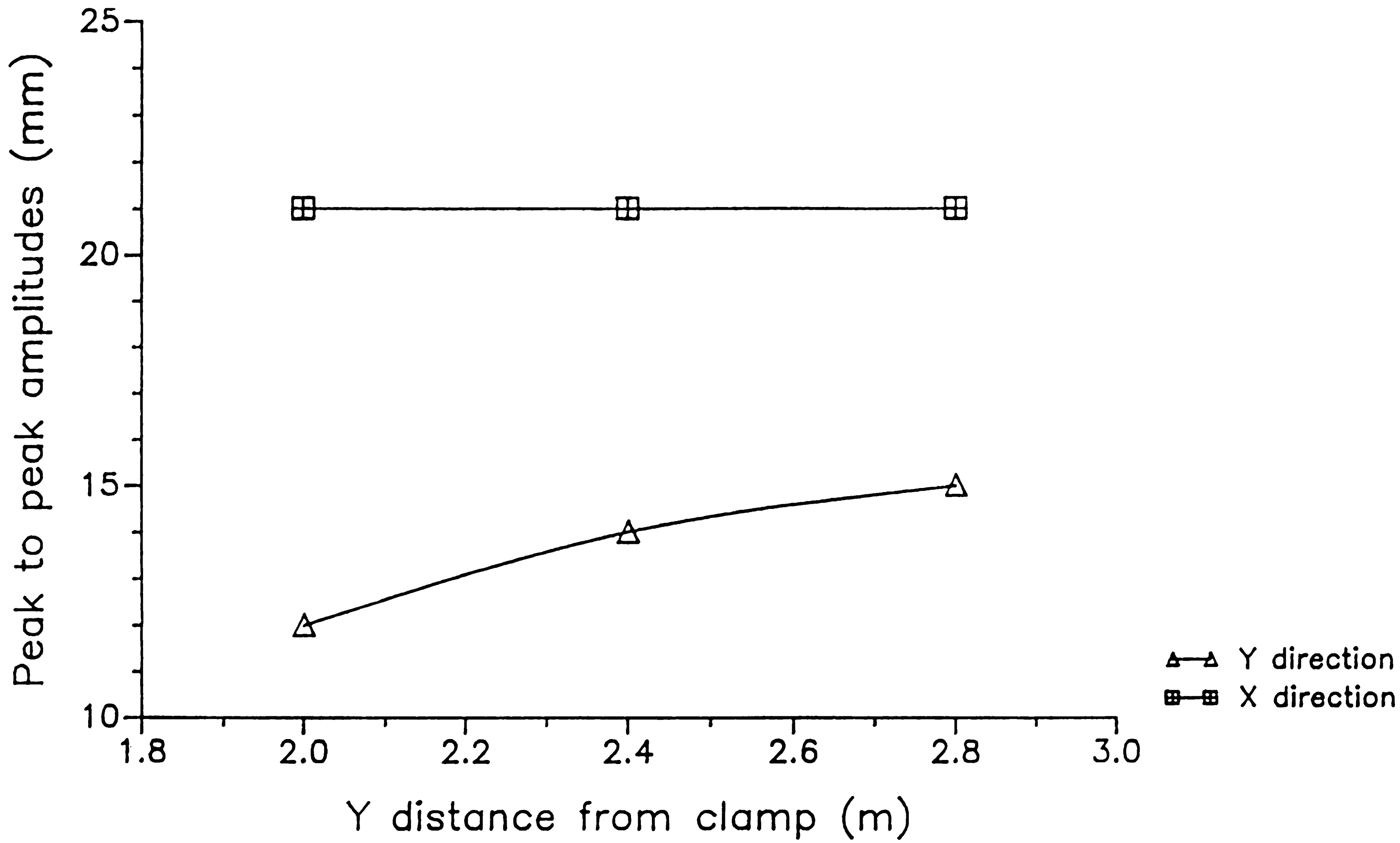

Figure 4.20— Variation of the position of the tail weight
Large tree shake

4.7 - Evaluation of the results

Although displacements from the variable eccentricity shaker experimental tests (obtained by Esch in the fall of 1987, presented in Appendix B) were higher than the ones displayed by the ADAMS model, the simulation results were in qualitative agreement with the actual shaker results.

General shaker dynamic behavior is illustrated in Figures 4.21 to 4.24. Figure 4.21 shows a close-up view of the mass housing for a short period after engagement. Figure 4.22 is a top view of the shaker housing with masses in motion for about 0.5 seconds of steady state simulation time. Figure 4.23 shows the trace of the center of mass of the eccentrics and the center of tree at the start of a steady state shake cycle. A complete steady state shake cycle is illustrated in Figure 4.24, while tracing corner points of the shaker housing, tree center, and the center of rotation of the eccentrics. The graphic illustrations of the model behavior are in agreement with expected actual shaker behavior which gives confidence to the model as a tool to predict overall shaker behavior.

The tests of the shaker showed a fairly uniform shake in the x and y direction of about 40 mm during free shake at a 10 Hz operating frequency. In tree shake tests, however, the y amplitudes recorded were higher than amplitudes in the x direction. This is attributed to a larger shaker tail weight than initially estimated for model input. Also, the tests were conducted in fall when trees had lost a substantial amount of their leaves, resulting in a lower system damping and increasing the possibility of resonant excitations. Leaves count for a large portion of tree damping due to air drag. The damping data used for modeling had been gathered in the summer months when trees had a full load of leaves.

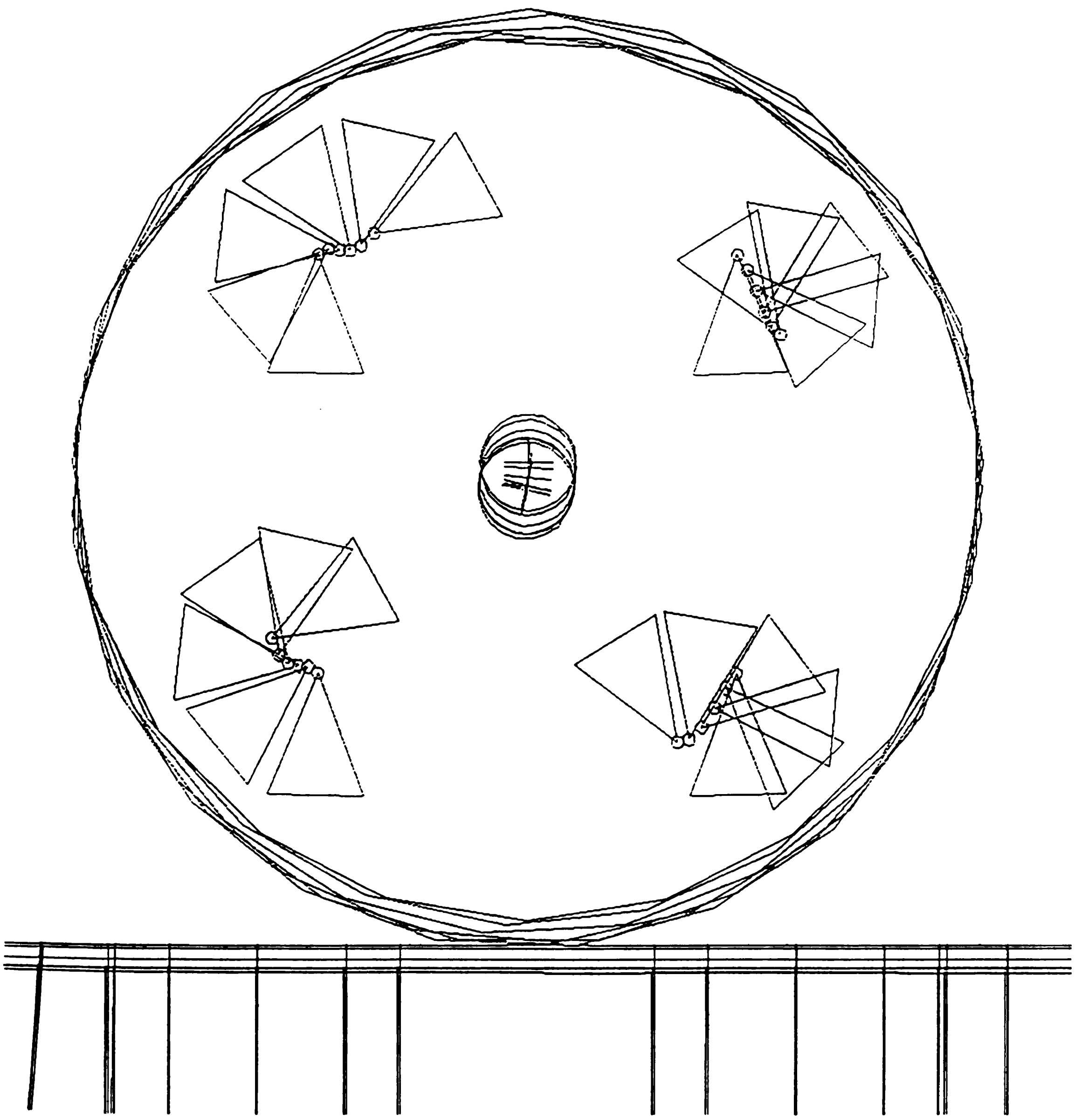

Figure 4.21 - Close-up top view of the model mass housing in motion

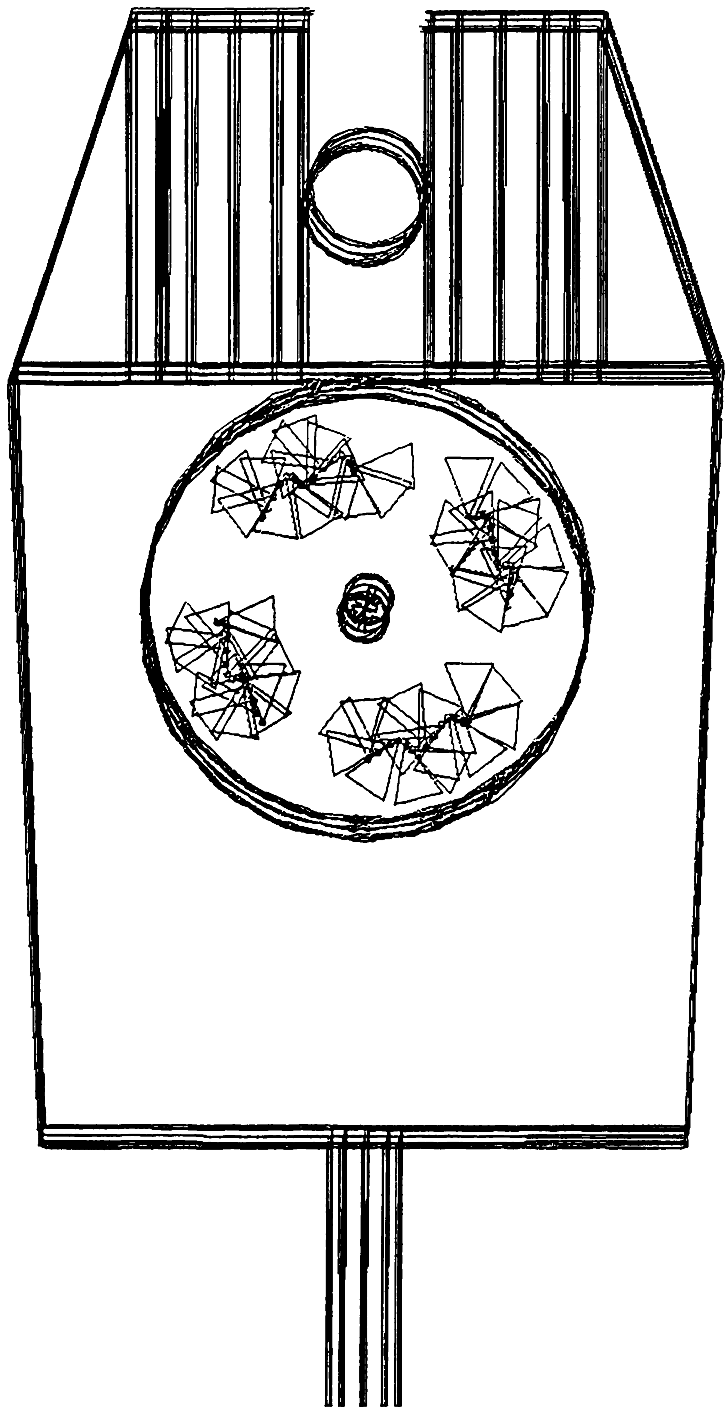

Figure 4.22 - Close-up top view of the model shaker housing in steady state motion

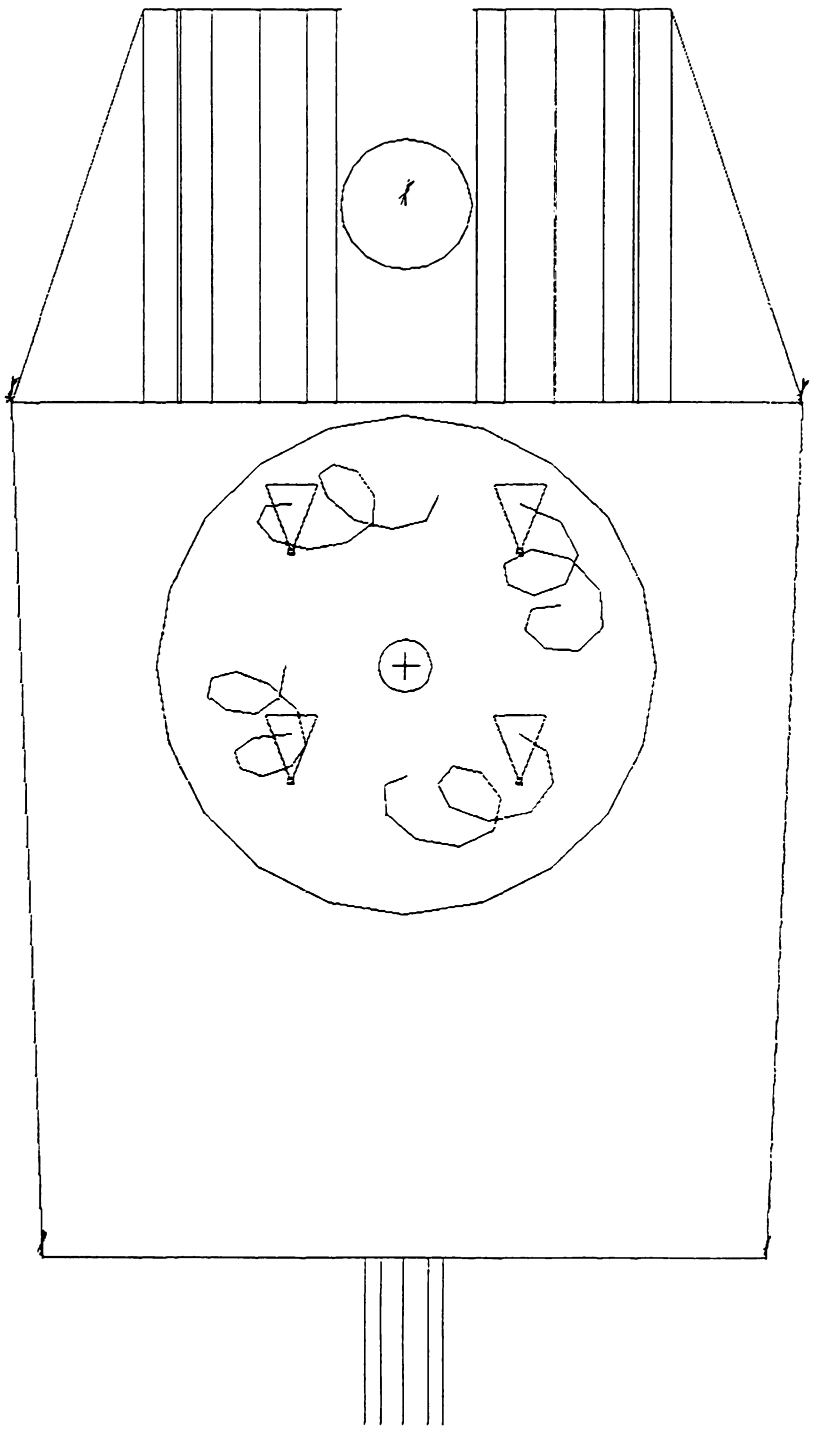

Figure 4.23 - Trace of center of mass of model eccentrics and tree center at start of a steady state shake cycle

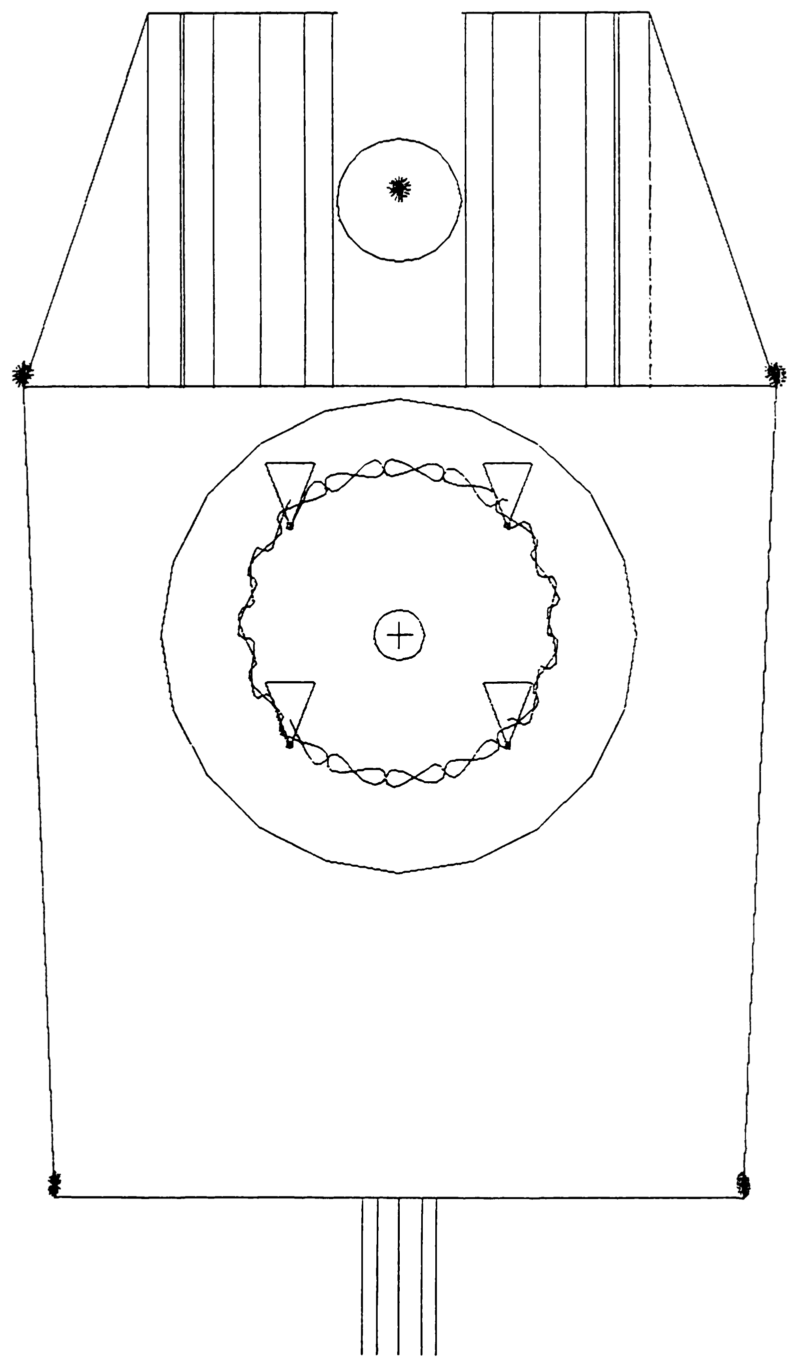

Figure 4.24 - Trace of model shaker housing corner points, tree center, and center of rotation of the eccentrics for a full cycle

The variations among the simulated and experimental results can also be attributed to the rigid body formulation of the shaker mechanism by ADAMS. The actual shaker structure is not as perfectly rigid as theoretically assumed by the model. This is specifically true in the case of the aluminum tubing which connects the tail weight to the shaker. The relative elasticity (compared to a rigid member) allows nonlinear vibrations within the tube, caused by reaction forces from the tail weight, that could very well be responsible for amplification of tree displacements in the y direction.

An overview of the this study leads to the following deductions about the variable eccentricity shaker's behavior:

1) Total mass of the shaker (excluding the mass of the eccentrics) effects tree shake amplitudes by absorbing a portion of the forces created by the rotating masses to overcome its own inertia. A relatively higher ratio of unbalance (eccentric) to shaker mass should result in a more effective transmission of shake to the tree. This ratio is, however, limited due to space limitations for eccentric masses and the weight of hardware used in shaker assembly and power transmission.

2) Eccentric mass rotating frequencies of 10 Hz and higher are above the natural frequency of the shaker and a shaker-small tree system. Therefore, for smaller trees, operating the shaker at the 10 Hz neighborhood should, for practical purposes, result in the same shake amplitudes when operating at the common (13-15 Hz) frequencies. For larger trees, a high natural frequency of the shaker-tree system (well over the common operating frequency), due to high tree stiffness, allows the increase or reduction of shake amplitude by varying the eccentric mass frequency.

3) The mass housing position on the long axis of the shaker, relative to the clamp point, has a substantial effect on the magnitude of displacements in

the y direction. A shorter distance between the mass housing and the clamp is needed for creating uniform shake amplitudes in the x and y direction in shaking larger trees. If the distance was to be minimized ,the shaker would be suitable for creating uniform amplitudes in large tree shakes, but would result in higher y amplitudes in small tree shakes. In this case decreasing resultant eccentricity would create the desired y amplitude, but would at the same time reduce x amplitudes, resulting in an ineffective shake in the x direction.

At this time, space limitations in the shaker housing prevent the mass housing from being moved any closer to the clamp.

4) The tail weight mass and its position relative to the clamp are interchangeable parameters for varying the y direction shake amplitudes. The variation of these parameters have the same type of effect as does the position of the mass housing. Increasing tail weight mass, or its distance to the clamp, does help in creating uniform x and y amplitudes in large tree shakes but, on the other hand, causes larger y amplitudes in small tree shakes. Adjustment of the tail weight position is a practical solution to tailor to different tree sizes.

In this study, only two tree diameters were considered while orchards consist of a variety of tree sizes, each having a different stiffness and damping. This would require more than one adjustment in the tail weight position during harvest.

A larger mass, or a longer distance from the clamp, of the tail weight also reduces shaker tail movement which results in less shear stress.

Chapter 5

Conclusions

1) The ADAMS model of the variable eccentricity shaker mechanism was successful in predicting its behavioral characteristics and its response to variations in the following parameters:

    Shaker housing mass

    Rotating frequency of the eccentric masses

    Position of the mass housing

    Tail weight mass

    Position of the tail weight

   Variations existed among the simulated and the experimental results of shaker operation that were attributed to the linearity and rigid body assumptions in modeling.

2) The variable shake force capability obtained by adjusting the phase angle

between two pair of counter-rotating eccentric masses is a successful method to achieve a wide range of shake amplitudes.

3) Unless the center of shake forces in both x and y direction is positioned at the center of the clamp, shakers will always create a non-uniform shake pattern. The sliding tail weight introduced in the variable eccentricity shaker does help in creating a uniform shake but, to achieve this, its position must be adjusted for different tree sizes.

4) Shaker housing mass should be minimized for a more effective transfer of inertia forces created by the eccentric masses.

Chapter 6

Recommendations

1) Field tests should be conducted in the harvest season to validate the the trends in shaker behavior presented in this study.

2) More field experimental tests are needed to determine suitable tail weight mass and position for a uniform shake in all directions on several common tree sizes.

3) At present, the tube connecting the tail weight to the shaker is too weak and does not support the tail weight as rigidly as desired. It should be replaced with a stronger member to allow positioning of the tail weight at further distances from the shaker.

4) A mechanism should be designed to allow the sliding of the tail weight in the field. This would lead to a quicker adjustment to achieve a uniform shake for different tree sizes in the orchard.

5) The existing ADAMS model of the shaker should be used in conjunction

with more accurate tree and shaker physical properties to support experimental results of recommendation one.

Appendix A

ADAMS Code of The Model

Shaker (2-D)

```
        RUN    ON    ADAMS !!:!!:!   ( DYNAMIC PROBLEM )
                                     ( SHAKER WITH FOUR MASSES )

                      ( PART IDENTIFICATION )

PART/1,GROUND
MARKER/101,QP=850,600,250
MARKER/102,QP=850,600,-250
MARKER/103,QP=3100,600,600
MARKER/104,QP=3100,600,-600
MARKER/105,QP=3700,300,0
MARKER/106,QP=822,300,0,REULER=0,270D,0
MARKER/107,QP=4200,300,0
MARKER/108,QP=3700,300,500

   !!!! EXTRA GROUND FOR DAMPER SUPPORT!!
MARKER/109,QP=850,300,750
MARKER/110,QP=1350,300,250
MARKER/111,QP=850,300,-750
MARKER/112,QP=1350,300,-250
MARKER/113,QP=3100,300,1100
MARKER/114,QP=3600,300,600
MARKER/115,QP=3100,300,-1100
MARKER/116,QP=3600,300,-600
MARKER/117,QP=2300,300,550
MARKER/118,QP=1800,300,1050
MARKER/119,QP=2300,300,-550
MARKER/120,QP=1800,300,-1050

   !!!! TUBE !!!!

PART/2,MASS=22,CM=203,IM=203,IP=0,6E6,0
,QG=0,300,0,REULER=0,0,0
MARKER/201,QP=0,0,0,REULER=90D,90D,0
MARKER/202,QP=822,0,0,REULER=90D,90D,0
MARKER/203,QP=900,0,0
MARKER/204,QP=1800,0,0


   !!!! BLOCK MASS   !!!!

PART/3,MASS=180,CM=300,IM=300
,IP=10E6,10E6,6E6,QG=822,300,0
MARKER/300,QP=0,0,0,REULER=90D,90D,0
MARKER/301,QP=28,0,-250
MARKER/302,QP=0,0,0,REULER=0,270D,0
MARKER/303,QP=-222,125,450
MARKER/304,QP=-222,125,-450
MARKER/305,QP=278,125,-225
MARKER/306,QP=278,125,225
MARKER/307,QP=278,-125,225
MARKER/308,QP=278,-125,-225
MARKER/309,QP=-222,-125,-450
MARKER/310,QP=-222,-125,450
MARKER/311,QP=28,0,250
MARKER/312,QP=278,0,0,REULER=90D,90D,0
MARKER/313,QP=-222,0,0,REULER=90D,90D,0

   !!!! SHAKER  !!!!

PART/4,MASS=405,CM=403,IM=403,IP=55E6,198E6,154E6
,QG=1800,300,0
MARKER/401,QP=0,0,0                                 TUBE
```

```
MARKER/402,QP=900,0,0,REULER=0,270D,0          MASS HOUSING
MARKER/403,QP=1300,0,0              CLAMP
MARKER/404,QP=1900,0,0              TREE
MARKER/405,QP=1300,150,-600         HANGERS -->
MARKER/406,QP=1300,150,600
MARKER/407,QP=0,150,-550
MARKER/408,QP=0,150,550
MARKER/409,QP=1900,150,-400
MARKER/410,QP=1300,-150,-600
MARKER/411,QP=1300,-150,600
MARKER/412,QP=1900,150,400
MARKER/413,QP=0,-150,-550
MARKER/414,QP=0,-150,550
MARKER/415,QP=1300,150,-400
MARKER/416,QP=1300,150,400
MARKER/417,QP=1900,-150,400
MARKER/418,QP=1300,-150,400
MARKER/419,QP=1900,-150,-400
MARKER/420,QP=1300,-150,-400
MARKER/421,QP=1300,150,-350
MARKER/422,QP=1300,-150,-350
MARKER/423,QP=1900,150,-350
MARKER/424,QP=1900,-150,-350
MARKER/425,QP=1300,150,350
MARKER/426,QP=1300,-150,350
MARKER/427,QP=1900,150,350
MARKER/428,QP=1900,-150,350
MARKER/429,QP=1300,0,-225,REULER=90D,90D,0
MARKER/430,QP=1300,0,225,REULER=90D,90D,0
MARKER/431,QP=1600,-150,0,REULER=0,270D,0

   !!!! MASS HOUSING  !!!!!

PART/5,MASS=1,CM=504,IP=0,0,0
,QG=2700,300,0
MARKER/500,QP=175,0,175,REULER=0,270D,0          M1
MARKER/501,QP=175,0,-175,REULER=0,270D,0         M2
MARKER/502,QP=-175,0,175,REULER=0,270D,0         M3
MARKER/503,QP=-175,0,-175,REULER=0,270D,0        M4
MARKER/504,QP=0,0,0,REULER=0,270D,0              SHAKER
MARKER/505,QP=20,0,0
MARKER/506,QP=-20,0,0
MARKER/507,QP=0,0,20
MARKER/508,QP=0,0,-20
MARKER/509,QP=0,-150,0,REULER=0,270D,0

       !!! MASS1 !!!

PART/6,MASS=21.6,CM=602,IP=0,0,0
,QG=2875,300,175,REULER=0,270D,0
MARKER/601,QP=0,0,0
MARKER/602,QP=70,0,0
MARKER/603,QP=100,40,0
MARKER/604,QP=100,-40,0
MARKER/605,QP=0,0,50
MARKER/606,QP=100,40,50
MARKER/607,QP=100,-40,50

   !!!! MASS2   !!!!

PART/7,MASS=21.6,CM=702,IM=702,IP=0,0,0
,QG=2875,300,-175,REULER=0,270D,0
MARKER/701,QP=0,0,0
MARKER/702,QP=70,0,0
MARKER/703,QP=100,40,0
MARKER/704,QP=100,-40,0
```

```
MARKER/705,QP=0,0,50
MARKER/706,QP=100,40,50
MARKER/707,QP=100,-40,50

   !!!! MASS3   !!!!

PART/8,MASS=21.6,CM=802,IP=0,0,0
,QG=2525,300,175,REULER=0,270D,180D
MARKER/801,QP=0,0,0
MARKER/802,QP=70,0,0
MARKER/803,QP=100,40,0
MARKER/804,QP=100,-40,0
MARKER/805,QP=0,0,50
MARKER/806,QP=100,40,50
MARKER/807,QP=100,-40,50

   !!!! MASS4   !!!!

PART/9,MASS=21.6,CM=902,IP=0,0,0
,QG=2525,300,-175,REULER=0,270D,180D
MARKER/901,QP=0,0,0
MARKER/902,QP=70,0,0
MARKER/903,QP=100,40,0
MARKER/904,QP=100,-40,0
MARKER/905,QP=0,0,50
MARKER/906,QP=100,40,50
MARKER/907,QP=100,-40,50

          ( JOINT IDENTIFICATION )

JOINT/11,I=302,J=106,PLANAR


         !! BLOCK-TUBE !!

JOINT/99,I=202,J=300,TRANS

         !! TUBE-SHAKER !!

JPRIM/101,I=204,J=401,ATPOINT
JPRIM/102,I=204,J=401,ORIENTATION

         !! SHAKER-HOUSING !!

JOINT/110,I=402,J=504,REV

         !! HOUSING-MASSES !!

JOINT/111,I=500,J=601,REV
JOINT/112,I=501,J=701,REV
JOINT/113,I=502,J=801,REV
JOINT/114,I=503,J=901,REV

               ( MOTIONS, & SPDP'S )

               ( MASS ASSEMBLY @ 50 RPM )
MOTION/1,JOINT=110,ROTATIONAL,FUNCTION=POLY(TIME,0,0,300D)

               ( MASSES COUNTER-ROTATE @ 800 RPM )

MOTION/2,JOINT=111,ROTATIONAL,FUNCTION=POLY(TIME,0,0,4800D)

MOTION/3,JOINT=113,ROTATIONAL,FUNCTION=POLY(TIME,0,0,4800D)

MOTION/4,JOINT=112,ROT,FU=POLY(TIME,0,0,-4800D)
MOTION/5,JOINT=114,ROT,FU=POLY(TIME,0,0,-4800D)
```

```
        COUPLER/1,JOINTS=112,111,SCALES=1,1
        COUPLER/2,JOINTS=114,113,SCALES=1,1

    !!! TREE STIFFNESS !!.

!! SPRINGDAMPER/1,I=107,J=404,TRANS,C=300,K=500
!! SPRINGDAMPER/2,I=108,J=404,TRANS,C=300,K=500
SPRINGDAMPER/3,I=109,J=311,TRANS,C=10,K=34,L=500              (10.88)
SPRINGDAMPER/4,I=110,J=311,TRANS,C=0.5,K=2.75,L=500
SPRINGDAMPER/5,I=111,J=301,TRANS,C=10,K=34,L=500
SPRINGDAMPER/6,I=112,J=301,TRANS,C=0.5,K=2.75,L=500
SPRINGDAMPER/7,I=113,J=406,TRANS,C=1,K=5.0,L=500               (17.6)
SPRINGDAMPER/8,I=114,J=406,TRANS,C=1,K=5.0,L=500
SPRINGDAMPER/9,I=115,J=405,TRANS,C=1,K=5.0,L=500
SPRINGDAMPER/10,I=116,J=405,TRANS,C=1,K=5.0,L=500
!! SPRINGDAMPER/11,I=117,J=408,TRANS,C=4.05,K=17.6,L=500
!! SPRINGDAMPER/12,I=118,J=408,TRANS,C=4.05,K=17.6,L=500
!! SPRINGDAMPER/13,I=119,J=407,TRANS,C=4.05,K=17.6,L=500
!! SPRINGDAMPER/14,I=120,J=407,TRANS,C=4.05,K=17.6,L=500

        ( OUTPUT REQUESTS )

REQUEST/1,DISPLACEMENTS,I=404,J=105
REQUEST/2,DISPLACEMENTS,I=300,J=106

        ( GRAPHICS )

GRAPHICS/1,OUT=303,304,305,306,303,310,309,304,309,308
,305,308,307,306,307,310

GRAPHICS/2,OUT=407,408,406,405,407,413,414,408,414,411
,406,411,410,405,410,413

GRAPHICS/3,CYL,CM=201,L=1800,RAD=62,SIDES=10

GRAPHICS/4,CIRCLE,CM=504,RAD=380

GRAPHICS/5,OUT=601,603,604,601,605,606,603,606,607,604,607,605
GRAPHICS/6,OUT=701,703,704,701,705,706,703,706,707,704,707,705
GRAPHICS/7,OUT=801,803,804,801,805,806,803,806,807,804,807,805
GRAPHICS/8,OUT=901,903,904,901,905,906,903,906,907,904,907,905
GRAPHICS/9,OUT=505,506
GRAPHICS/10,OUT=507,508
GRAPHICS/11,OUT=405,409,415,420,419,409,419,410,405,421,423
GRAPHICS/12,OUT=406,412,416,418,417,412,417,411
GRAPHICS/13,OUT=421,422,424,419,424,423,409
GRAPHICS/14,OUT=425,426,428,417,428,427,412,427,425
GRAPHICS/15,CYL,CM=429,L=600,RAD=125,SIDES=5
GRAPHICS/16,CYL,CM=430,L=600,RAD=125,SIDES=5
GRAPHICS/17,CYL,CM=431,L=300,RAD=100,SIDES=10
GRAPHICS/18,CYL,CM=509,L=300,RAD=40,SIDES=10

GRAPHICS/19,CIRCLE,CM=312,RAD=100
GRAPHICS/20,CIRCLE,CM=313,RAD=100

GRAPHICS/21,CYL,CM=601,L=50,RAD=5
GRAPHICS/22,CYL,CM=701,L=50,RAD=5
GRAPHICS/23,CYL,CM=801,L=50,RAD=5
GRAPHICS/24,CYL,CM=901,L=50,RAD=5

            (MUST MULT. BY 25 BEFORE USE)
      GRAPHICS/69,SPDP,I=105,J=402,DA=0.2,DB=0.3,DC=0.3
      ,LA=0.3,LB=0.3,LC=0.35,LD=0.35,COILS=6

      GRAPHICS/79,SPDP,I=106,J=402,DA=0.2,DB=0.3,DC=0.3
      ,LA=0.3,LB=0.3,LC=0.35,LD=0.35,COILS=6
```

```
( SYSTEM & CONTROL PARAMETERS )

ACCGRAV/GC=1000,JGRAV=-9807

!!      DEBUG/DUMP,EPRINT,VERBOSE,DOF

OUTPUT/REQSAVE,GRSAVE,FIXED,TELETYPE

END
```

Appendix B

Experimental Shaker Data

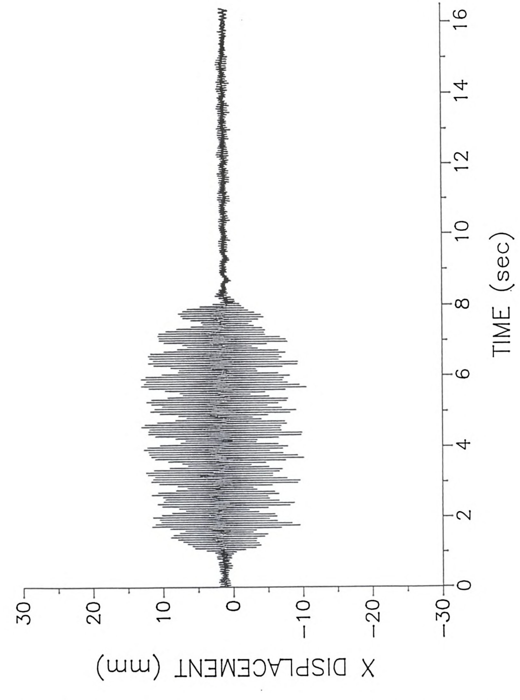

Figure B.1 - Experimental shaker X displacement at 15 Hz (150 mm tree)

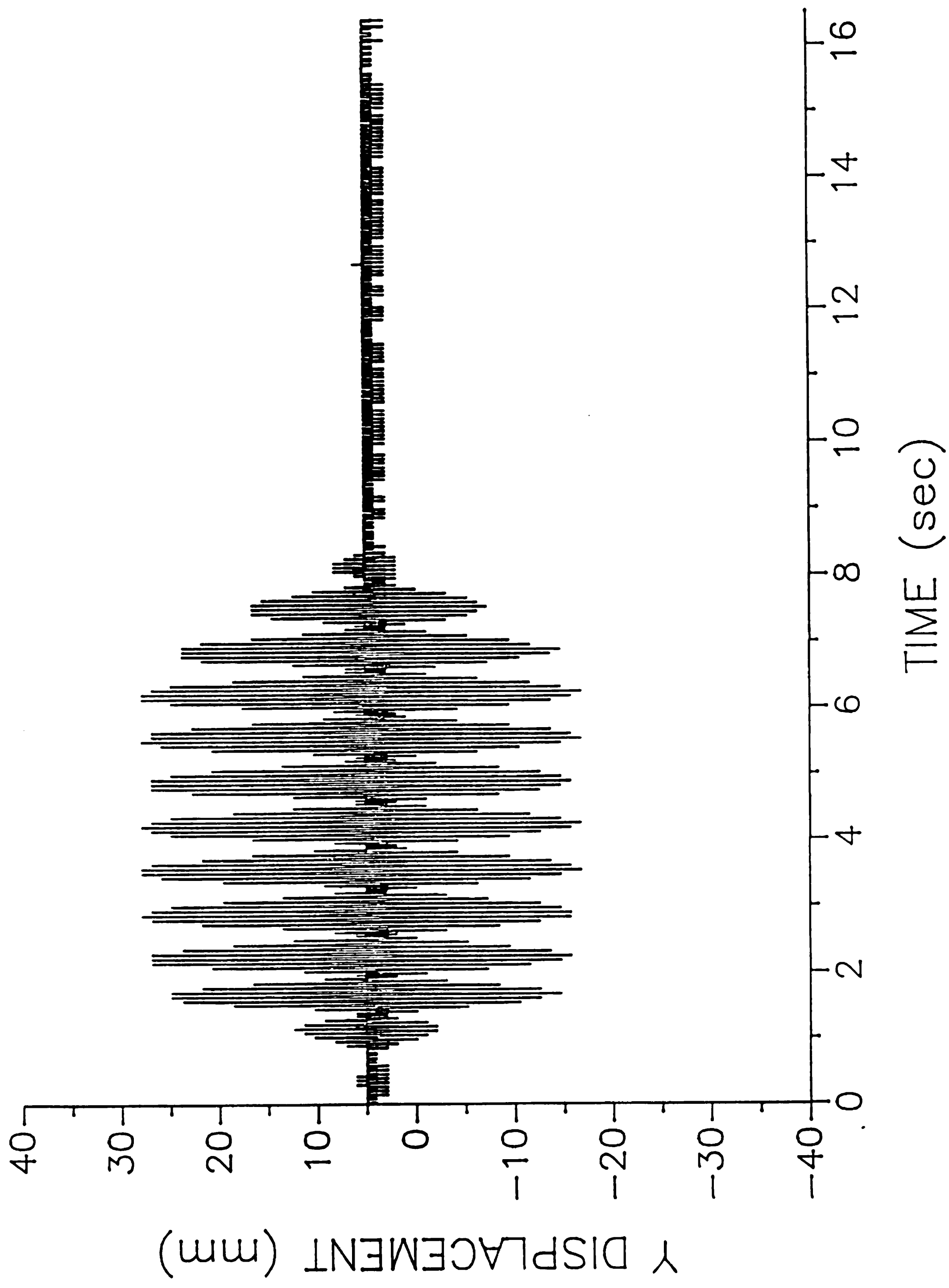

Figure B.2 - Experimental shaker Y displacement at 15 Hz (150 mm tree)

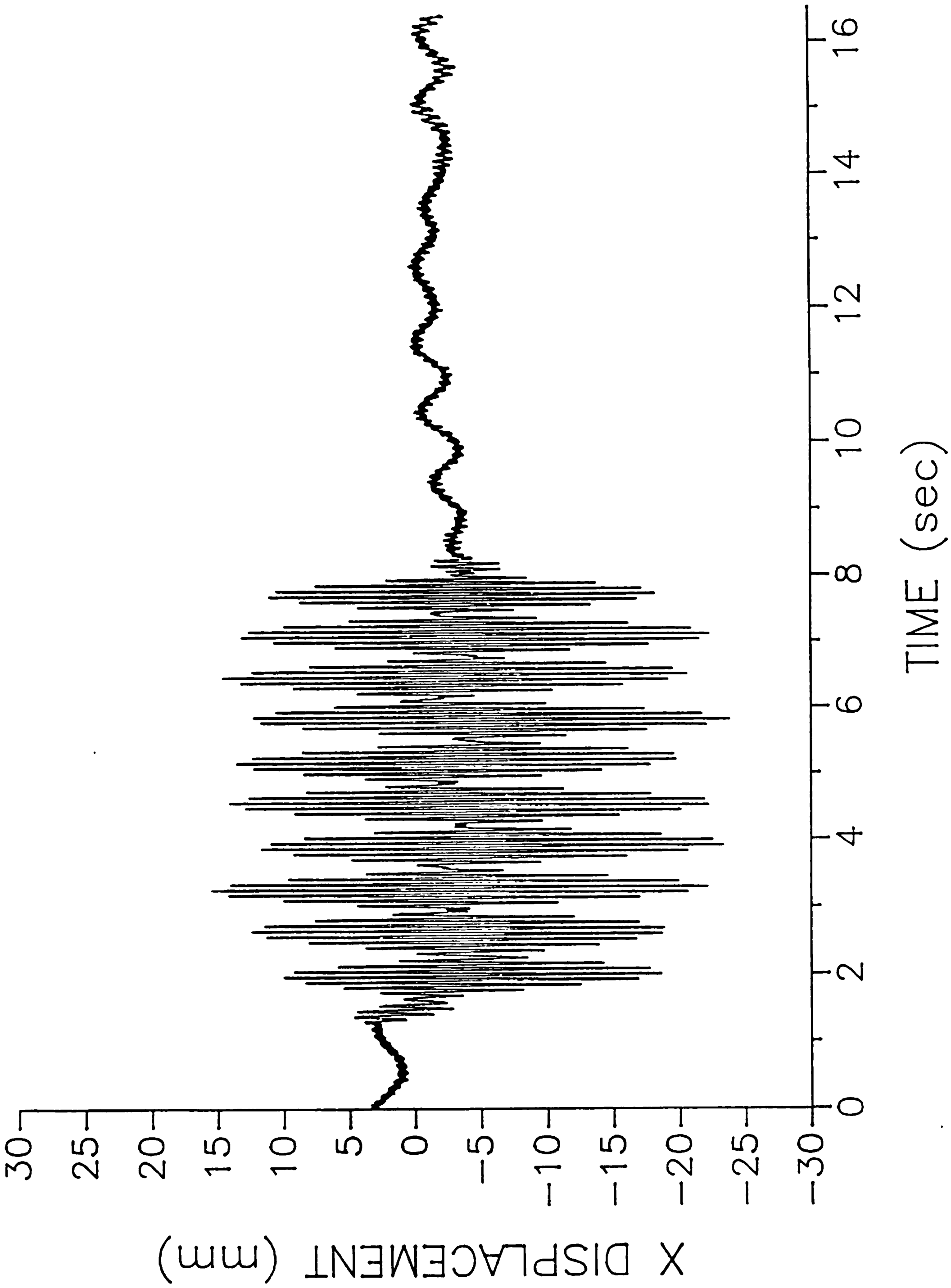

Figure B.3 - Experimental shaker X displacement (Free shake)

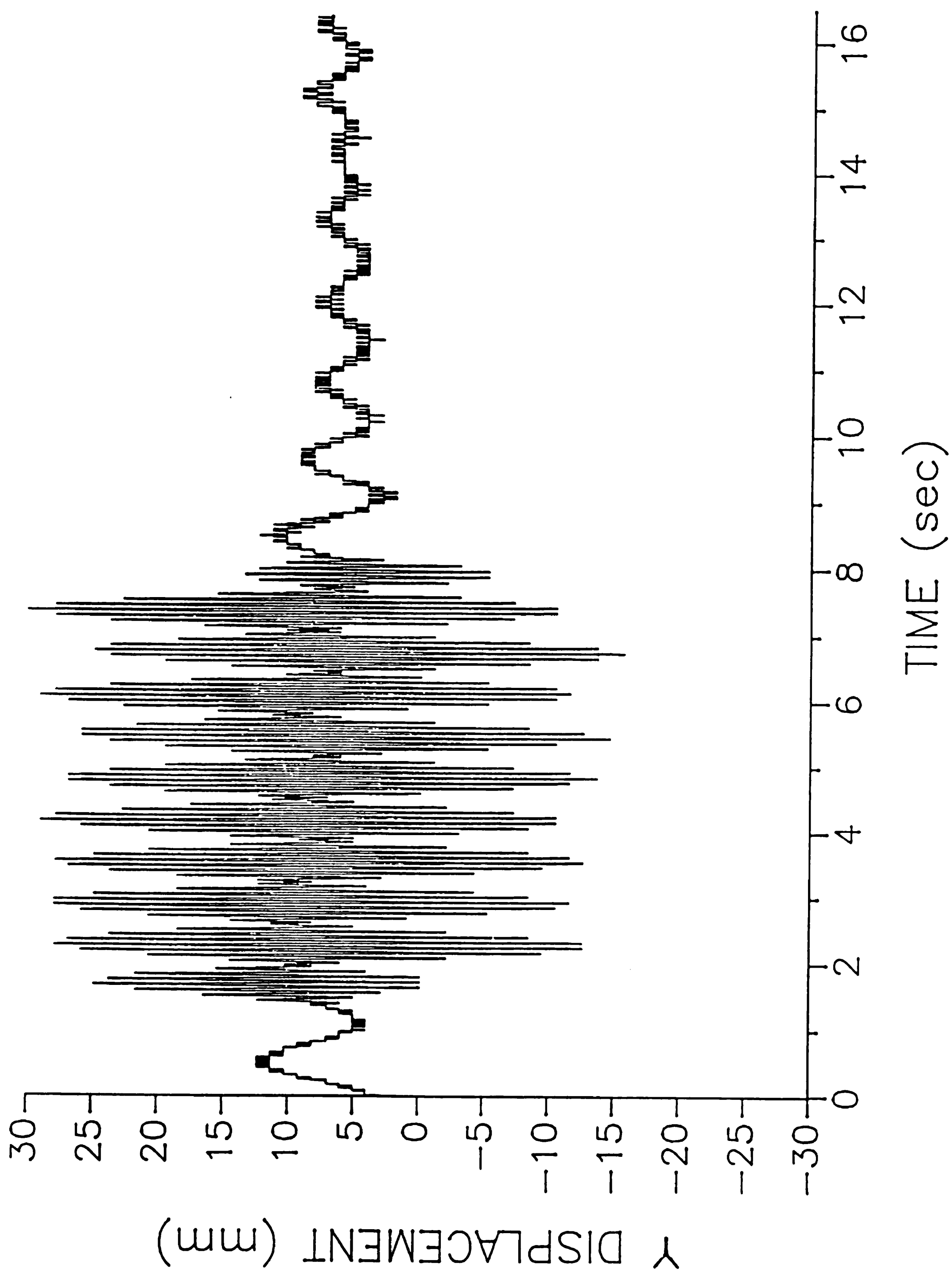

Figure B.4 - Experimental shaker Y displacement (Free shake)

Appendix C

Single Degree of Freedom Models

Simple oscillators were modeled using ADAMS, IMP, and a Fortran program of the equations of motion. The results of ADAMS and IMP followed the Fortran model results, as well as each other's, quite closely. The accurate performance of the simple models indicate an initial confidence in both ADAMS and IMP for further, more complex modeling of the shaker.

$$F = mew^2$$
$$M = 1.0 \text{ kg}$$

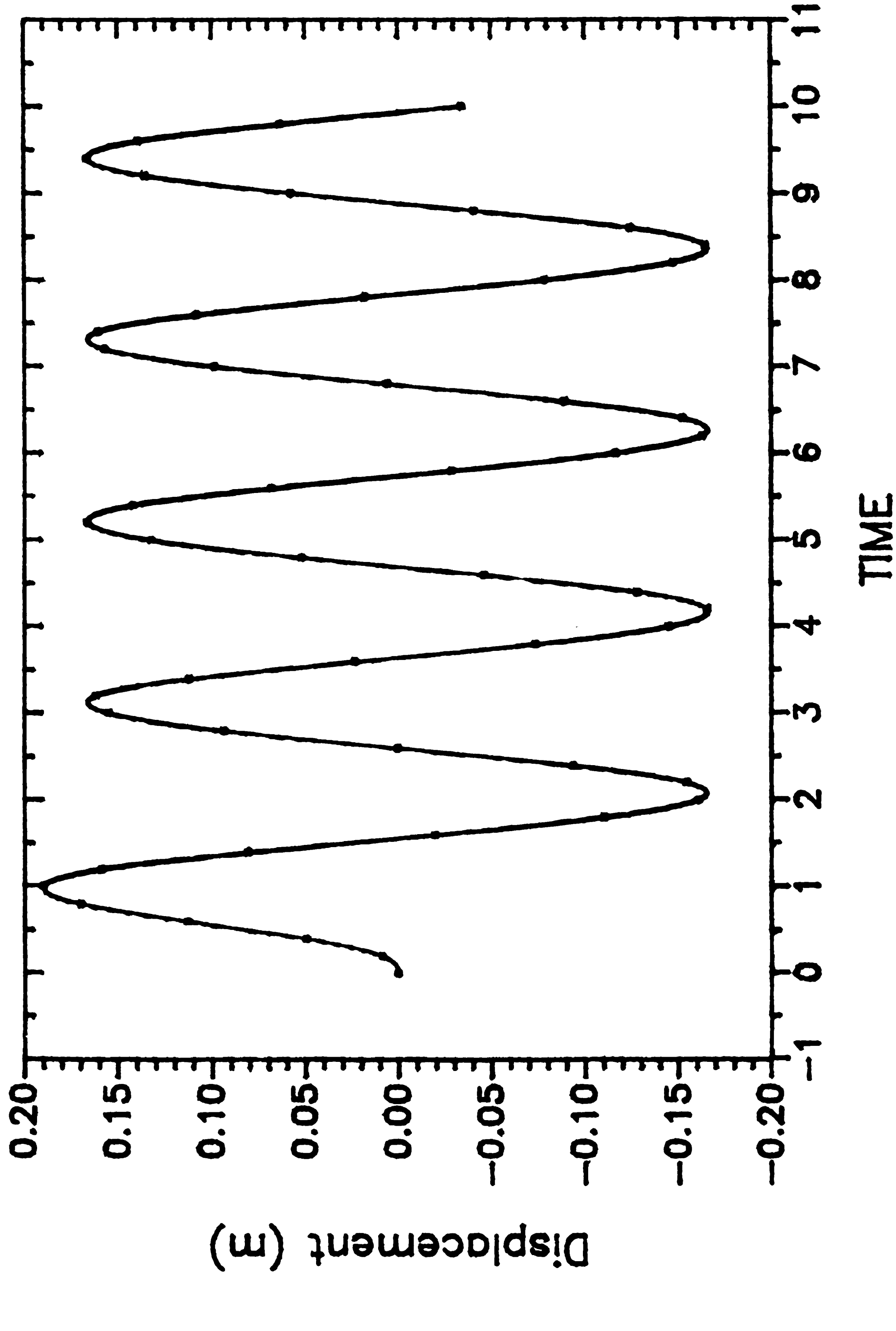

C.1 - Fortran Model
F=3,W=3
k=10,c=6

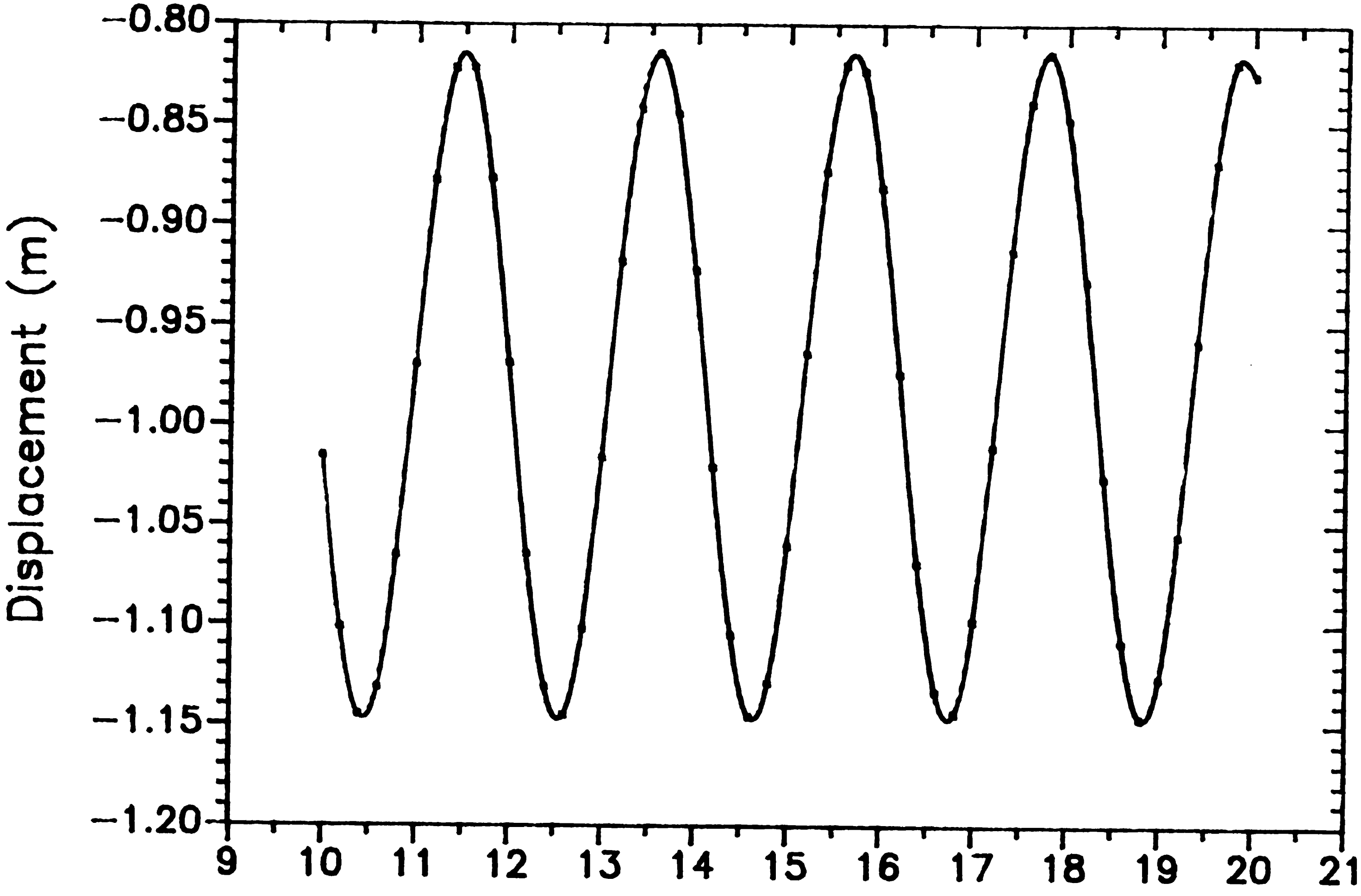

C.2 - ADAMS Model
F=3.0,W=3.0
k=10,c=6

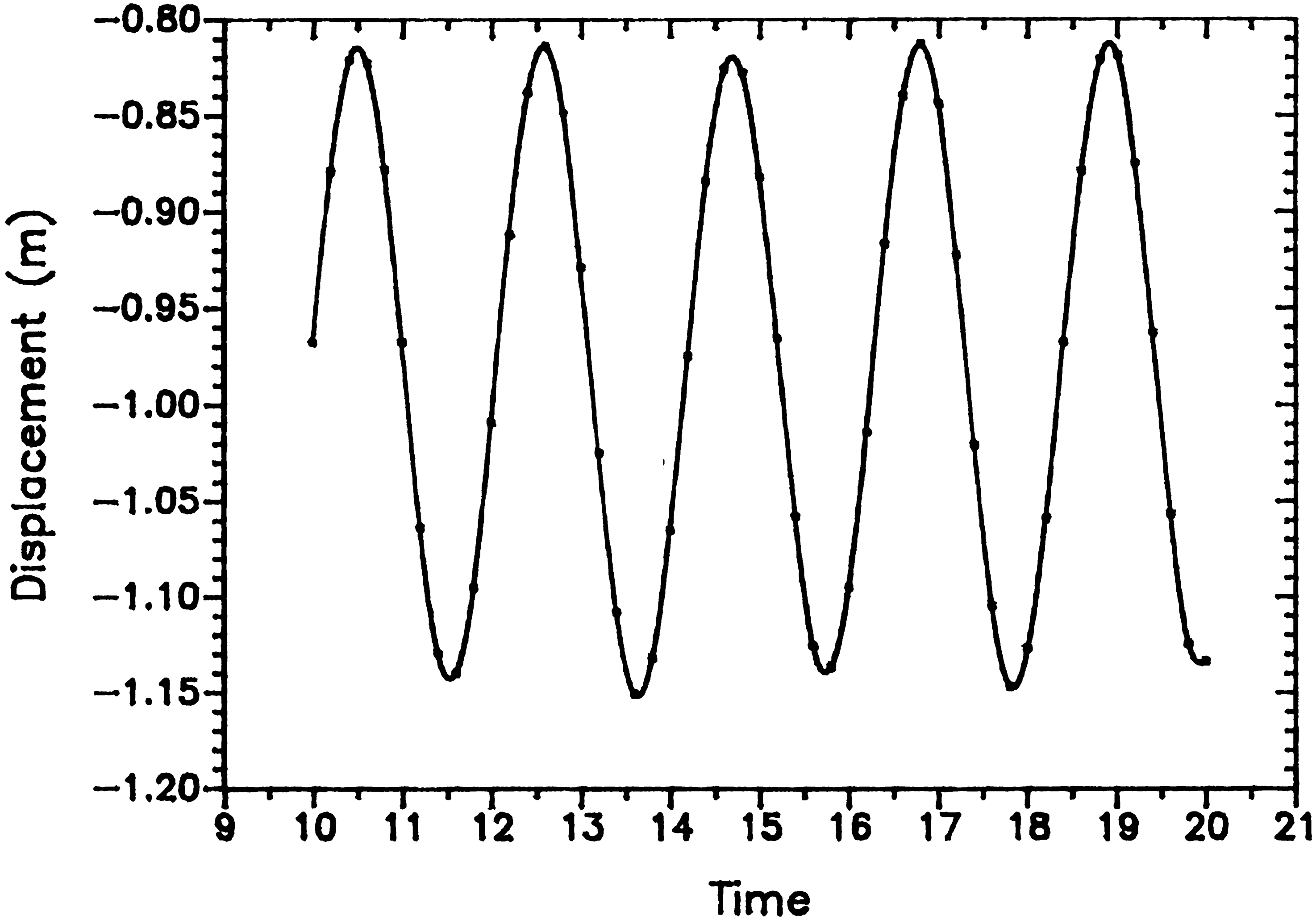

C.3 - IMP Model
F=3.0,W=3.0
k=10,c=6

```
      PROGRAM ROTMASS   (FORTRAN)
C
C
C
C
C
      REAL A,B,D,E,F,G,PHI,PHI1
      REAL W,K,WN,C,CCR,X1,N,N1,T,P
      REAL MASS,RMASS,XNUM,XDEN,ZETA
      REAL TERM1,TERM2,TERM3,TERM4
      REAL X(50)
      OPEN(UNIT=1,FILE='DISP.DAT',STATUS='NEW')
C
C
      PRINT*,'ENTER SPRING STIFFNESS :'
      READ*,K
C
      MASS =1
      RMASS=0.2
      WN   = SQRT(K/MASS)
      CCR  = 2*MASS*WN
      PRINT*,'WN,CCR'
      PRINT*,WN,CCR
C
      PRINT*,'ENTER SPEED OF ROTOR (RAD/SEC):'
      READ*,W
C
      PRINT*,'ENTER DAMPING COEFFICIENT :'
      READ*,C
C
      PRINT*,'ENTER SIMULATION TIME (SEC.):'
      READ*,T
C
      PRINT*,'ENTER NUMBER OF OUTPUTS DESIRED:'
      READ*,N1
C
      E    =1
      ZETA = C/CCR
      A    = C*W
      B    = K-MASS*W*W
      PHI  = ATAN(A/B)
      H    = SIN(PHI)
      D    = COS(PHI)
      F    = RMASS*E*W*W
      G    = SQRT(1-ZETA*ZETA)
      PHI1 = ATAN(G/(ZETA-(W/(WN*TAN(PHI)))))
      X1   = (F*H)/(SIN(PHI1)*SQRT(B*B+A*A))
      N    = T/N1
C
C
      I=0
      DO 10 P=0,T,N
        I=I+1
        X(I)  = 0
        TERM1 = (SIN(W*P-PHI))*F
        TERM2 = SQRT(B*B+A*A)
        TERM3 = SIN(PHI1+G*WN*P)
        TERM4 = EXP(-ZETA*WN*P)
        X(I)  = (X1*TERM4*TERM3)+(TERM1/TERM2)
        WRITE(1,*),P,X(I)
10    CONTINUE
      END
```

UNBALANCED ROTOR (ADAMS)

```
PART/1,GROUND
MARKER/101,QP=0,0,0,REULER=180D,90D,90D
MARKER/102,QP=-0.1,0.1,0
MARKER/103,QP=0.1,0.1,0
MARKER/104,QP=0,0.1,0


PART/2,MASS=1,CM=201,QG=0,-1,0
,IP=0,0,2E-5,REULER=180D,90D,90D
MARKER/201,QP=0,0,0
MARKER/202,QP=0,0,0
MARKER/203,QP=0,-0.05,0
MARKER/204,QP=0,-0.05,0.05
MARKER/205,QP=0,0.05,0.05
MARKER/206,QP=0,0.05,0

JOINT/11,I=201,J=101,TRANS

GRAPHICS/1,OUT=102,103
GRAPHICS/2,OUT=203,204,205,206,203

SFORCE/1,I=201,J=101,TRANSLATIONAL,ACTIONONLY
,FUNCTION=SHF(TIME,0,3,3,0,0)
           SHF: F=A*SIN(WX-PHI) F-THIRD,W-FOURTH
FORCE/44,I=201,J=104,GFORCE,C=6,K=10,L=1

REQUEST/1,DISPLACEMENT,I=201,J=101

ACCGRAV/GC=1,JGRAV=-9.81
ANALYSIS/ERR=10E-5
EXECUTION/END=20,STEPS=100
OUTPUT/REQSAVE,GRSAVE
END
```

```
SYSTEM=SPDP (IMP)

REMARK: JOINT DEFINITION


PRISM(BASE,WHT)=PRJ
DATA PRISM(PRJ)=0,0,0;0,5,0;0,0,1

REMARK: GRAPHICS


POINT(WHT)=P101,P102,P103,P104,P101
DATA POINT(P101,ABS)=-0.5,-0.5,0
DATA POINT(P102,ABS)=-0.5,0.5,0
DATA POINT(P103,ABS)=0.5,0.5,0
DATA POINT(P104,ABS)=0.5,-0.5,0

POINT(WHT)=P105
DATA POINT(P105,ABS)=0,0,0

POINT(BASE)=P106,P107
DATA POINT(P106,ABS)=-1,1,0
DATA POINT(P107,ABS)=1,1,0

POINT(BASE)=P108
DATA POINT(P108,ABS)=0,1,0

POINT(BASE)=P110
DATA POINT(P110,ABS)=0,-1,0

SPRING(P108,P105)=SP
DAMPER(P108,P105)=DP
DATA SPRING(SP)=10,1
DATA DAMPER(DP)=6

VALUE(F)=3*SIN(3*TIME)
FORCE(P105/P108,P105)=PUSH
DATA FORCE(PUSH)=F

UNIT MASS=1.0

DATA MASS(WHT,PRJ)=1;0,0,0

DATA INERTIA(WHT,PRJ)=2E-5,0,0,0,0,0


DATA GRAVITY=0,-9.81,0

FIND DYNAMICS

ZERO SPRING=0.00000001
remark ZERO ZERO=0.0000001
ZERO POSITION=0.0000001
ZERO INERTIA=0.0000001
DATA TIME=20,0.0001,0.2

LIST position(PRJ)

RETURN
```

LIST OF REFERENCES

LIST OF REFERENCES

ADAMS User's Manual, Version 5.2. 1987. Mechanical Dynamics Inc., Ann Arbor, MI.

Adrain, P. A. and R. B. Fridley. 1963. Shaker Clamp Design as Related to Allowable Stresses of The Tree Bark.
ASAE Paper No. 63-121. American Society of Agricultural Engineers, St. Joseph, MI 49085.

Adrian, P. A. and R. B. Fridley, 1965. Dynamics and Design Criteria of Inertia-Type Tree Shakers.
Transactions of ASAE 8(1):12-14

Adrain, P. A., R. B. Fridley, and Coby Lorenzen. 1962. Forced Vibration of a Tree Limb.
ASAE Paper No. 62-154. American Society of Agricultural Engineers, St. Joseph, MI 49085.

Affeldt, H. A. 1987. Spectral Analysis for Optimal Design of a Variable Eccentricity Trunk Shaker Harvester System.

Ph.D. Dissertation. Michigan State University, E. Lansing, MI 48824.

Affeldt, H. A., G. K. Brown, J. B. Gerrish, and C. J. Radcliffe. 1984. Microcomputer Detection of Dynamic Displacements within Trunk Shaker Pads.

ASAE Paper No. 84-1067. American Society of Agricultural Engineers, St. Joseph, MI 49085.

Al-Soboh, G. 1986. A Simulation Study of the Displacement Behavior of a Trunk Shaker System during Cherry Harvest.

Ph.D. Dissertation. Michigan State University, E. Lansing, MI 48824.

Brown, G. K., J. R. Frahm, R. L. Ledebuhr, and B. F. Cargill. 1982. Bark Damage when Trunk Shaking Cherry Trees.

ASAE Paper No. 82-1557. American Society of Agricultural Engineers, St. Joseph, MI 49085.

Brown, G. K., J. R. Frahm, L. J. Segerlind, and B. F. Cargill. 1986. Bark Strength and Shaker Pads vs Cherry Bark Damage During Harvesting.

Transactions of ASAE 30(5):1266-1271

Brown, G. K., L. J. Segerlind, P. L. Richey. 1984. Bark Stress Caused By Trunk Shaker Displacements.

ASAE Paper No. 84-1066. American Society of Agricultural Engineers, St. Joseph, MI 49085.

Burton, C. L., N. L. Schulte-Pason, G. K. Brown, and D. E. Marshal. 1986. Influence of Mechanical Harvesting on Cherry Tree Decline.

ASAE Paper No. 86-1559. American Society of Agricultural Engineers, St. Joseph, MI 49085.

Cargill, B. F., G. K. Brown, and M. J. Bukovac. 1982. Factors Affecting Bark Damage to Cherry Trees by Harvesting Machines.

Michigan State University, CES, AIES Bulletin No. 471.

Cook, J. R. and R. H. Rand. 1969. Vibratory Fruit Harvesting: A Linear Theory of Fruit Stem Dynamics.

Journal of Agricultural Engineering Research 14(3):195-209.

DeVay, J. E., W. H. English, F. L. Lukezic, and H. J. O'Reilly. 1960. Mallet Wound Canker of Almond Trees.

California Agriculture 14(8):8-9.

DeVay, J. E., F. L. Lukezic, W. H. English, W. J. Moller, and B. W. Parkinson. 1965. Ceratocystic Canker of Stone Fruit Trees.

California Agriculture 19(10):2-4.

Diener, R. G., J. H. Levin, and R. T. Wittenberger. 1969. Relation of Frequency and Length of Shaker Stroke to the Mechanical Harvesting of Apples.

ARS 42-148. U.S. Department of Agriculture.

Esch, T. A. 1987. Personal Communications.

Ph.D. Graduate Student in Agricultural Engineering. Michigan State University, E. Lansing, MI 48824.

Frahm, J. R., G. K. Brown, and L. J. Segerlind. 1983. Mechanical Properties of Trunk Shaker Pads.

ASAE Paper No. 83-1078. American Society of Agricultural Engineers, St. Joseph, MI 49085.

Frahm, J. R., L. J. Segerlind, G. K. Brown, and J. R. Clemens. 1984. Instrumentation for Bark Strength and Shaker Pad Pressure Determination.

ASAE Paper No. 84-1569. American Society of Agricultural Engineers, St. Joseph, MI 49085.

Fridley, R. B., G. K. Brown, and P. A. Adrian. 1970. Strength Characteristics of Fruit Tree Bark.

Higardia 40(8):205-223.

Gould, R. D. and J. E. Richter. 1971. Variable Inertia weight for Tree Shaker.

U.S. Patent No. 3,564,825.

Halderson, J. L. 1966. Fundamental Factors in Mechanical Cherry Harvesting.

Transactions of ASAE 9(5):681-684.

Lenker, D. H. and S. L. Hedden. 1968. Optimum Shaking Action for Citrus Fruit Harvesting.

Transactions of ASAE 11(3):347-349.

Michigan Department of Agriculture. 1987.

Michigan Agricultural Statistics. P.O. Box 20008, Lansing, MI 48901.

O'Brien, M., B. F. Cargill, and R. B. Fridley. 1983. Principles and Practices for Harvesting and Handling Fruits and Nuts.

AVI Publishing Co., Inc. Westport, CT.

Timm, E. J. and G. K. Brown. 1985. Minimizing Shear Force Transmission in Trunk Shaker Pads.

ASAE Paper No. 85-1563. American Society of Agricultural Engineers, St. Joseph, MI 49085.

Upadhyaya, S. K., J. R. Cooke, and R. H. Rand. 1981. Limb Impact Harvesting, Part I: Finite Element Analysis.

Transactions of ASAE 24(4):856-863.

U.S. Department of Agriculture. 1987. U.S. Agricultural Statistics.

Yung, C. and R. B. Fridley. 1975. Simulation of Vibration of Whole Tree Systems Using Finite Elements.

Transactions of ASAE 18(3):475-481.